

Doctor's thesis
-- doctor philosophiae (dr. phil.) --
on

*The locus coeruleus:
The central relay between neuronal network
activation and sympathetic responses in
cognitive control*

presented to the council of the *Fakultät für Sozial- und
Verhaltenswissenschaften der Friedrich-Schiller-Universität Jena*

by **Ms. Stefanie Köhler (M.Sc.-Psych.)**

born on 24.06.1988 in Meerane

Reviewers:

- 1. Prof. Dr. Thomas Weiß**
- 2. Prof. Dr. Stefan Schweinberger**
- 3. Prof. Dr. Karl-Jürgen Bär**

Date of the oral exam: 06.06.2019

SUMMARY

The ability of humans to integrate different body processes is most important for survival. The neuro-visceral integration model suggests that both cognitions and emotions are regulated by superior brain systems also involved in the regulation of autonomic function. Therefore, cognitive performance and affective processing is closely linked to autonomic responses. In order to improve the understanding of human behavior and associated dysfunctions, we need to acquire a better understanding of the interplay between the central nervous system (CNS) and peripheral autonomic nervous system (ANS) in cognitive control.

A pivotal role of the noradrenergic neurotransmitter system in cognitive control has been suggested. In the present thesis, functional fMRI was used to expand our knowledge of the brain – body interaction in cognitive control with the locus coeruleus (LC), which is the main production site of noradrenaline in the brain, as central relay nucleus.

Broad functional connections of the LC to cortical and subcortical regions predominantly involved in executive function were found. The paramount importance of the LC in cognitive control was emphasized by an increase of its activation proportional to the increase of cognitive load. In patients with schizophrenia, this relation was absent indicating a deficient role of the LC-noradrenergic system. Furthermore, LC BOLD activation was associated with pupillary dilation which supports the interpretation of the LC playing a pivotal role in controlling sympathetic autonomic function.

With these findings, I was able to link the cognitive control network to the sympathetic nervous system with the LC as central relay nucleus. Thus, the present thesis contributes to an extension of the current state-of-the-art in neuropsychology.

ZUSAMMENFASSUNG

Die Fähigkeit des menschlichen Körpers verschiedenste Prozesse zu integrieren garantiert das Überleben. Das Neuroviszerale Integrationsmodell geht davon aus, dass Kognitionen sowie Emotionen von übergeordneten kortikalen Netzwerken reguliert werden, die ebenfalls für die Regulation unseres autonomen Nervensystems zuständig sind. Demzufolge sind die kognitive Leistungsfähigkeit sowie affektive Verarbeitungsprozesse sehr eng mit Reaktionen des sympathischen und parasympathischen Nervensystems assoziiert. Das bessere Verständnis der Interaktion zwischen dem zentralen und peripher autonomen Nervensystem ist essentiell, um menschliches Verhalten sowie daraus resultierende Dysfunktionen einordnen und behandeln zu können.

In Zusammenhang mit kognitiven Kontrollprozessen hebt die aktuelle Studienlage zunehmend die besondere Rolle des Neurotransmitters Noradrenalin hervor. Mittels funktioneller Magnetresonanztomografie wurde in der vorliegenden Dissertation eine Erweiterung des Verständnisses der wechselseitigen Beziehung zwischen dem zentralen und autonomen Nervensystem während kognitiver Kontrollprozesse untersucht. Der Locus coeruleus (LC), der den Hauptlieferanten von Noradrenalin im Gehirn darstellt, wurde als zentrale Umschaltstruktur angenommen.

Weit verzweigte funktionelle Konnektivitäten des LC zu kortikalen und subkortikalen Strukturen des kognitiven Kontrollnetzwerks konnten identifiziert werden. Die enorme Wichtigkeit des LC bei der Bearbeitung kognitiver Aufgaben wurde durch den proportionalen Anstieg dessen Aktivierung mit kognitiver Anstrengung bestärkt. Bei an Schizophrenie erkrankten Patienten wurde dieser Zusammenhang nicht gefunden. Dies weist auf eine abnorme Funktionsweise des noradrenergen Hirnstammkerns bei diesem Störungsbild hin. Ein weiterer wichtiger Befund war die Korrelation von LC BOLD Aktivierung und

Pupillenweite. Dies bestärkt die Interpretation, dass der LC eine zentrale Rolle in der Kontrolle des sympathischen Nervensystems einnimmt.

Mit der vorliegenden Dissertation war es möglich das kognitive Kontrollnetzwerk mit dem sympathischen Nervensystem zu verlinken, wobei der Locus coeruleus eine zentrale Umschaltstelle darstellt. Ein wichtiger Beitrag zu den aktuellen Kenntnissen der Neuropsychologie konnte geleistet werden.

TABLE OF CONTENT

Summary.....	3
Zusammenfassung.....	4
1. Basic concepts and theoretical background.....	8
1.1 Cognitive control in humans	8
1.2 The human nervous system	9
1.3 Involvement of the central nervous system in cognitive control	10
1.4 Involvement of noradrenaline in cognitive control.....	11
1.5 Cognitive control deficits in psychiatric disorders	11
1.6 Interplay of the central and autonomic nervous system in cognitive control.....	12
1.7 The pivotal role of brain – body interactions.....	14
1.7.1 The relationship between the central and autonomic nervous system.....	14
1.7.2 The neuro-visceral integration model	15
1.7.3 Findings supporting the brain – body interaction.....	16
1.7.4 Brain - body interaction in patients with schizophrenia	17
1.8 Research motivation.....	18
1.9 Primary goal of the present thesis.....	19
2. Thematic classification of the Studies.....	20
2.1 Study 1.....	20
2.2 Study 2.....	21
2.3 Study 3.....	22
2.4 Study 4.....	24
3. Discussion.....	25
3.1 Main results.....	25
3.2 LC as a link between the cognitive control network and sympathetic nervous system	26
3.1.1 Study one	26
3.1.2 Study two	27
3.1.3 Study three	28
3.1.4 Study four	29
3.3 General Discussion	29
4 Summary and Conclusion	32
4. Studies.....	34
REFERENCES	82
Appendix A.....	94

Appendix B..... 95
Appendix C..... 98

1. BASIC CONCEPTS AND THEORETICAL BACKGROUND

*"...if anger makes the hand rise in order to strike,
the will can ordinarily restrain it;
if fear incites the legs to flee,
the will can stop them..."*
(Descartes, 1989; p. 44)

1.1 COGNITIVE CONTROL IN HUMANS

Human behavior is not deterministic. It can be adapted given even subtle environmental changes, which is indispensable for everyday psychological functioning and psychological health. Consequently, the impact of *cognitive control* is omnipresent, but the nature of this concept is hard to grasp. The term cognitive control relates to a number of operations that enable the cognitive system to successfully pursue specific cognitive tasks, such as response inhibition or inhibiting impulsive actions, maintaining and manipulating goal-related information or stopping and overriding pre-potent response tendencies (Bari & Robbins, 2013; Botvinick, Braver, Barch, Carter, & Cohen, 2001; Logan, 1985; Posner & Snyder, 1975; Verbruggen & Logan, 2008). Previous research often defined cognitive control as a function of task performance. For instance, the conflict monitoring theory (Botvinick et al., 2001) claims that specific brain structures, in particular the ACC, respond to the occurrence of conflict. It can be tested with tasks such as the Stroop Color-Word task (Stroop, 1935). The Stroop effect is one of the most popular phenomena in all of cognitive sciences and was first reported by John Ridley Stroop (Stroop, 1935). In its basic form, the task is to name the color in which a word is printed, ignoring the word itself. To display the color word in a mismatched ink color (incongruent condition) results in slow and error-prone responding. The performance cost in the incongruent condition relative to the congruent condition is called Stroop effect or Stroop interference effect. Another theory is the error-likelihood model (Brown & Braver, 2005) which implies, that the ACC response to a given task condition will

be proportional to the perceived likelihood of an error in that condition. This theory is explored by studies applying, for example, Stop-Signal and Go/No-Go tasks. The Go/No-Go paradigm is a cognitive task which aims at determining the ability of an individual to inhibit a response considered inappropriate. Participants are required to either respond or withhold a pre-potent response depending on whether a Go stimulus or a No-Go stimulus is presented (Verbruggen & Logan, 2008). In the Go/No-Go task, the pre-potent response tendency is typically established by the very fast presentation of the Go stimuli. Thus, response inhibition refers to the ability to override the tendency towards automatic but inappropriate responses and interference control to the ability to select relevant information from amidst irrelevant information. Both functions have been grouped together in theoretical models of cognitive control and linked to prefrontal cortex function (Aron & Poldrack, 2006; N. P. Friedman & Miyake, 2004; Miller & Cohen, 2001). However, pre-potent response inhibition and interference control are separable facets of inhibition (Friedman and Miyake, 2004). In sum, various models are designed to capture functions considered to be most relevant to cognitive control, such as *response inhibition*.

1.2 THE HUMAN NERVOUS SYSTEM

The human nervous system consists of different parts. The *central nervous system* (CNS) integrates sensory input, coordinates conscious/unconscious information and consists of the brain, brainstem and spinal cord. The *peripheral nervous system* conveys information from and to the CNS. The *autonomic nervous system* (ANS), as a part of the peripheral nervous system, is essential to maintain the internal milieu of the human body and to adapt the homeostasis to changing environmental demands (Schmidt & Thews, 1983). The ANS regulates, for instance, the respiratory, cardiac, vasomotor, and endocrine system to adjust behavior to motor, emotional or cognitive challenges (Critchley et al., 2005; J. F. Thayer & Lane, 2000). Primary centers of autonomic regulation are located in the *brainstem*, which

connects the forebrain with the spinal cord and acts as a main information relay between central and peripheral nervous system. It receives sensory input from throughout the body via ascending pathways, such as the spinothalamic tract (e.g. temperature sensation) and the dorsal column (e.g. pressure sensation). Motor output from brainstem nuclei travels via descending tracts and the spinal cord to the peripheral nervous system. The brainstem has a central role in autonomic regulation, pain perception, awareness, alertness, and consciousness. Basal reflexes such as swallowing, vomiting, coughing, and sneezing are mainly coordinated at the brainstem level.

1.3 INVOLVEMENT OF THE CENTRAL NERVOUS SYSTEM IN COGNITIVE CONTROL

On the neural level, cognitive control is characterized by a dynamic interplay between prefrontal, posterior parietal and subcortical structures (Miller & Cohen, 2001). The lateral prefrontal cortex (PFC), consisting of the dorsolateral and ventrolateral prefrontal cortex (DLPFC, VLPFC), the dorsal anterior cingulate cortex (dACC), the parietal cortex and the thalamus, are regarded as central nodes of this cognitive control network (Mansouri, Tanaka, & Buckley, 2009). A successful inhibition of pre-potent motor responses depends on fronto-striatal loops including the inferior frontal gyrus, the (pre-) supplementary motor area (SMA), the striatum and brainstem nuclei (Alexander & Crutcher, 1990; Aron & Poldrack, 2006; Jentsch & Taylor, 1999; Simmonds, Pekar, & Mostofsky, 2008). Deficits in the dorsomedial prefrontal cortex (DMPFC) were found to be responsible for impaired performances in response inhibition tasks (Godefroy, Lhullier, & Rousseaux, 1996). Patients with lesions including the (pre-)SMA and subdivisions of the anterior cingulate cortex (ACC) showed prolonged reaction times and increased error-rates (Picton et al., 2007; Stuss, Binns, Murphy, & Alexander, 2002).

1.4 INVOLVEMENT OF NORADRENALINE IN COGNITIVE CONTROL

A pivotal role of the noradrenergic neurotransmitter system in cognitive control can be assumed. The *locus coeruleus* (LC) is the main production site of noradrenaline in the brain. In their review, Aston-Jones and Cohen (2005) emphasized the specific role of the LC in cognitive flexibility. The authors proposed that enhanced LC activity produces a temporally specific release of noradrenaline, which increases the gain of specific task-associated cortical networks and optimizes task appropriate behavior. Besides, the noradrenergic neurotransmitter system seems to be critically involved in inhibiting an already initiated response (Eagle, Bari, & Robbins, 2008; Robbins & Arnsten, 2009). Thus, a decisive role of the noradrenergic neurotransmitter systems in successful and unsuccessful response inhibition can be assumed (Claassen et al., 2017; Eagle, Tufft, Goodchild, & Robbins, 2007; Kohno et al., 2016).

1.5 COGNITIVE CONTROL DEFICITS IN PSYCHIATRIC DISORDERS

Spontaneous and rash behavior is characteristic for impulsive individuals and might frequently result in behavioral failures. Some psychiatric disorders (e.g., attention deficit hyperactivity disorder; Brewer & Potenza, 2008) are characterized by elevated impulsivity or diminished behavioral flexibility. It was assumed that impulsivity might arise due to deficient inhibitory processes (Bari & Robbins, 2013).

Schizophrenia is a serious debilitating disorder going along with immense cognitive dysfunctions. Growing evidence for abnormal cognitive task activation in the PFC, thalamus, striatum and cerebellum was reported in patients suffering from schizophrenia (Callicott et al., 2000; Koch et al., 2010; Schlosser et al., 2008; Wagner et al., 2013). Schizophrenia is a severe psychiatric disorder characterized by a multitude of symptoms affecting a variety of emotional and cognitive domains. For instance, Wagner et al. (2015) observed decreased neural activation in a predominantly right lateralized fronto-striato-thalamic network in

patients during execution of the Stroop task. Ettinger et al. (2017) focused on two facets of inhibition: pre-potent response inhibition and interference control in patients with schizophrenia. Interestingly, they found robust performance impairments in the Stroop task and in the Go/No-Go paradigm. Patients with schizophrenia showed longer response times in the Stroop task, especially in the incongruent condition, as well as prolonged reaction times in the Go/No-Go task, which was, however, independent of condition. This suggests a general performance deficit which is not specific to inhibitory control. Nevertheless, exact pathomechanisms of schizophrenia are still not fully understood and need further investigation. The LC-noradrenaline system was implied to be most important in cognitive control but was rarely investigated in schizophrenia.

1.6 INTERPLAY OF THE CENTRAL AND AUTONOMIC NERVOUS SYSTEM IN COGNITIVE CONTROL

The brainstem, as a relay and processing station between the spinal cord, cerebellum and neocortex, contains vital nodes of various functional systems. A growing number of studies investigated the role of different cortical and subcortical brain regions involved in autonomic control. Important brain regions associated with ANS regulation are the ACC, insula, amygdala, SMA, prefrontal cortices and the midbrain (Beissner, Meissner, Bar, & Napadow, 2013).

Accumulating research has revealed the close interrelationship between the autonomic state and cognition. The internal state determines the way we react to the environment (Critchley, 2009). In a study by Urai, Braun, and Donner (2017), the link between decision uncertainty and its arousal-dependent modulation was emphasized. They found that an increase in pupil-linked arousal boosts the tendencies of individuals to alternate their choice on the subsequent trial. Therefore, decision uncertainty seems to drive rapid changes in the pupil-linked arousal state, which shapes ongoing behavior. Thus, assessing the activity of the autonomic nervous

system is indicative of an individual's functional state and behavior highlighting peripheral indicators of autonomic function as an important addendum to research in neurosciences (Samuels & Szabadi, 2008; Urai et al., 2017).

It is likely that manipulating the physiological state, for instance by painful stimulation, produces consistent changes in LC activity, affecting arousal, autonomic function and cognitive control (Aston-Jones, Rajkowski, & Cohen, 1999; Lapid & Morilak, 2006; Samuels & Szabadi, 2008). LC neuron loss in aging resulted in decreases in arousal, a reduced activity of the sympathetic nervous system and cognitive function (Wilson et al., 2013). In sum, the LC seems to be critically involved in controlling the regulation of arousal, autonomic function and, thus, cognitive control. There may be separate populations of LC neurons associated with sympatho-excitatory and parasympathetic-inhibitory effects (Mather et al., 2017; Samuels & Szabadi, 2008).

Skin conductance (SC) is an important autonomic measure of psychophysiology research as it reflects sympathetic neural responses. The SC level has been proposed to indicate mental efforts (Jacobs et al., 1994; Kohlisch & Schaefer, 1996; Mehler, Reimer, Coughlin, & Dusek, 2009; Reimer & Mehler, 2011). M'Hamed, Sequeira, and Roy (1993) proposed a crucial influence of the reticular formation, a brainstem network including the LC, on SC. Yamamoto, Arai, and Nakayama (1990) showed that lesions to noradrenergic fiber bundles in cats abolish skin conductance responses (SCR) and spontaneous fluctuation of SC. Neuroimaging studies reported that BOLD changes and metabolism in regions congruent to LC are related to spontaneous SC fluctuations at rest (Patterson, Ungerleider, & Bandettini, 2002).

Some studies already suggested a close interaction between the peripheral ANS and the CNS in response inhibition and error processing (Critchley et al., 2003; Hajcak, McDonald, & Simons, 2003; Hofmann, Friese, & Strack, 2009; Zhang et al., 2012; Zhang et al., 2015). For instance, previous research showed enhanced SCRs to errors in impulsive individuals (Zhang

et al., 2012; Zhang et al., 2015). Hajcak et al. (2003) applied electroencephalography and a modified Stroop task and found a fronto-centrally negative deflection in the ERP signal as well as an elevation in SCR in error trials. SCR is suggested to be closely related to dACC activity (Critchley, Mathias, & Dolan, 2001; Nagai, Critchley, Featherstone, Trimble, & Dolan, 2004; Zhang et al., 2014) and is used as an indirect measure of cognitive effort. For instance, healthy subjects were found to show increases in SCR prior decision making (Bechara, Damasio, Tranel, & Damasio, 1997) and the magnitude of ACC activity strongly reflected the degree of anticipatory arousal indexed by SCR (Critchley et al., 2001). Mehler et al. (2009) reported that SCR changes indicate cognitive workload already before the appearance of a clear decline in performance. Moreover, Zhang et al. (2012) applied a Stop-Signal Task and found that fluctuations in SCR during Go trials which followed another Go trial are driven by participants' effort in negotiating between speed and accuracy. In contrast, changes in SCR during trials following a Stop signal are in response to an antecedent response conflict. Thus, there is some evidence that the physiological state might influence successful response inhibition, behavioral monitoring and, might already hold predictive information for performance accuracy.

1.7 THE PIVOTAL ROLE OF BRAIN – BODY INTERACTIONS

1.7.1 THE RELATIONSHIP BETWEEN THE CENTRAL AND AUTONOMIC NERVOUS SYSTEM

Investigators have identified functional units within the central nervous system that support goal-directed behavior and adaptability (J. F. Thayer, Ahs, Fredrikson, Sollers, & Wager, 2012). One such entity is the central autonomic network (CAN; Benarroch, 1993). Functionally, this network is an integrated component of an internal regulatory system through which the brain controls visceromotor, neuroendocrine, and behavioral responses which are critical for goal-directed behavior. Structurally, the CAN includes, for instance, the ACC, insular, orbitofrontal, and ventromedial prefrontal cortices, the amygdala, nuclei of the

hypothalamus, periaqueductal gray, the nucleus ambiguus, the ventrolateral medulla, the ventromedial medulla, and the medullary tegmental field. These components are reciprocally interconnected such that information flows bidirectional between lower and higher levels of the CNS. The primary output of the CAN is mediated through sympathetic and parasympathetic neurons. Sensory information from periphery (e.g., pressure receptors) is fed back to the CAN. The central regulation system of most target organs is organized in a widely antagonistic action of the sympathetic and parasympathetic branch of the ANS (e.g. the heart, pupil, gastrointestinal tract).

Sweat glands of humans are predominantly innervated by sudomotor nerves from the sympathetic chain (Shields, MacDowell, Fairchild, & Campbell, 1987). Excitatory and inhibitory influences on the sympathetic nervous system are distributed in various parts of the brain and therefore the neural mechanisms and pathways involved in the central control of SC are numerous and complex (Boucsein, 1992). Central SC control involves, for instance, the frontal cortex, the premotor cortex, the hypothalamus, the limbic system as well as different brainstem nuclei. Knowledge of the central control of human SC has increased dramatically with advances in neuroimaging technology. Researchers were able to examine the relationship between patterns of brain activation and simultaneously recorded SC (e.g., Critchley, Elliott, Mathias, & Dolan, 2000; Nagai et al., 2004). In sum, activation of brain areas involved in evaluating stimulus significance, particularly the vmPFC, ACC and right inferior parietal region, were found to be associated with elicitation of SC responses.

1.7.2 THE NEURO-VISCERAL INTEGRATION MODEL

The ability of humans to integrate different body processes is characterized by the neuro-visceral integration model (Lane et al., 2009; J. F. Thayer & Lane, 2000), which suggests that both cognitions and emotions are regulated by superior brain systems also involved in the regulation of autonomic function. Moreover, a link between executive function and frontal as

well as midbrain areas that regulate the vagal control of the heart is assumed (J. F. Thayer et al., 2012; J. F. Thayer & Brosschot, 2005; J. F. Thayer & Lane, 2000, 2009). The model was first applied in the context of emotion regulation (Thayer & Lane, 2000) and proposed that affective regulation requires selective attention to motivationally or affectively relevant stimuli and the inhibition of attention to irrelevant stimuli. Therefore, from a neuro-visceral perspective, attentional and affective regulations work together in the process of self-regulation and goal-directed behaviors. The neuro-visceral integration model can also be extended to focus on attentional and cognitive processes in the absence of affective dimensions. The examination of this aspect of the model has been primarily based on high frequency heart rate variability (HF-HRV) which is a marker of parasympathetic activity. HF-HRV is supposed to reflect frontal – midbrain – vagal control and relates to cognitive function. For instance, resting HF-HRV was related to working memory, sustained attention, mental flexibility and inhibitory control (Thayer et al., 2009).

1.7.3 FINDINGS SUPPORTING THE BRAIN – BODY INTERACTION

A recent study by Nikolin, Boonstra, Loo, and Martin (2017) showed that measures of HRV present potential indices for cortico-subcortical circuitry following activation of the PFC both during vagally dominated periods of resting-state activity and sympatho-adrenal mediated task-related activity. This network is shared for cognitive processes as well as regulation of cardiovascular control via changes to sympatho-vagal tone. It can be assessed using HRV in conjunction with more standardized behavioral outcomes. A HF-HRV measure was able to detect increased vagal activity both during rest and task performance. Additionally, power in the LF band was found to correlate with changes in cognitive functioning, indicating an association between PFC activity and the sympathetic branch of the ANS.

Sympatho-excitatory subcortical threat circuits are under tonic inhibitory control by the PFC (Amat et al., 2005). For example, the amygdala, which has outputs to autonomic, endocrine,

and other physiological regulation systems, and becomes active during threat and uncertainty, is under tonic inhibitory control via GABAergic mediated projections from the PFC (Davidson, 2000; Julian F. Thayer, 2006). Thus the default response to uncertainty, novelty and threat is the sympatho-excitatory preparation for action. From an evolutionary perspective this represents a system that errs on the side of caution when in doubt prepare for the worst - thus maximizing survival and adaptive responses (LeDoux, 1996). However, in normal, modern life this response has to be perpetually inhibited and this inhibition is achieved via top-down modulation from the PFC. Thus, under conditions of uncertainty and threat the PFC is deactivated. This hypoactive state is associated with disinhibition of sympatho-excitatory circuits that are essential for energy mobilization. However, when this state is prolonged it dramatically wears and tears on the system which is characterized as allostatic load (McEwen, 1998).

1.7.4 BRAIN - BODY INTERACTION IN PATIENTS WITH SCHIZOPHRENIA

Schizophrenia is a multifaceted neuropsychiatric disorder that is characterized by delusions, hallucinations, passivity, disordered thought, disorganized behavior and cognitive deficits. Its pathophysiology is highly complex (Northoff, 2015; van Os & Kapur, 2009). Schizophrenia is associated with autonomic dysfunctions, prefrontal hypoactivity and a lack of inhibitory neural processes as reflected, for instance, in poor habituation to novel neutral stimuli, a pre-attentive bias for threat information, deficits in working memory and executive function as well as poor affective information processing and regulation (Bär et al., 2005; Waford & Lewine, 2010). For instance, Mathewson, Jetha, Goldberg, and Schmidt (2012) found patients to exhibit faster resting heart rates than healthy controls. Moreover, patients performed worse on a task thought to index aspects of higher order thinking, including abstract concept formation, set-shifting and inhibitory control (Wisconsin Card Sorting Test). Within the patient group, relatively better task performance was associated with slower resting heart rate,

suggesting that inefficient executive and autonomic functioning in schizophrenia may be linked. Clamor et al. (2015) showed a relationship between low HRV and the ability to successfully regulate emotions in participants with psychosis. The findings support the assumption that regulative mechanisms such as emotion regulation are an important link between low HRV, an index of impaired prefrontal inhibitory control, and the increased subjective stress and cortisol level in psychosis. Proper functioning of inhibitory processes is essential to the preservation of the integrity of the system and therefore is vital to health.

1.8 RESEARCH MOTIVATION

In order to improve our understanding of human behavior and associated dysfunctions, we need to acquire a better understanding of the interplay between the peripheral ANS and CNS in cognitive control and response inhibition focusing on the definite involvement of the LC-noradrenergic neurotransmitter system.

Despite of the long-lasting interest and multitude of research efforts to fully understand the concept of cognitive control in all its complexity, its exact characteristics are still a matter of debate. In the *first study*, the main focus was to identify the involvement of the LC in cognitive control during the Stroop task in healthy subjects. Further, dysfunctions within the noradrenergic neurotransmitter system are considered to play a central role in psychiatric diseases, such as schizophrenia. Thus, the *second study* sought to investigate the putatively aberrant activation patterns of the noradrenergic LC in patients with schizophrenia during the Stroop task. In our *third study*, we assessed physiological indices of cognitive effort to investigate the link to activation patterns of the LC in the Stroop task. To expand our understanding of neural correlates of cognitive control, we aimed to investigate indices of successful/unsuccessful response inhibition, paying particular attention to the interplay between the brainstem as well as peripheral markers in the *fourth study*.

1.9 PRIMARY GOAL OF THE PRESENT THESIS

The neuro-visceral integration model was previously extended to focus on cognitive processes. However, the model mainly focused on HRV which is principally a marker of parasympathetic activity without looking at the crucial involvement of central brainstem structures.

The assumption of the present thesis is that the sympathetic branch of the peripheral ANS is activated by the LC-noradrenergic system. Sympathetic activity is suggested to be closely related to dACC activity and is used as an indirect measure of cognitive effort. The present thesis aims at broadening the view of the brain – body interaction by focusing on the involvement of the LC in cognitive control in relation to neuronal networks and the sympathetic branch of the ANS (**Figure 1**).

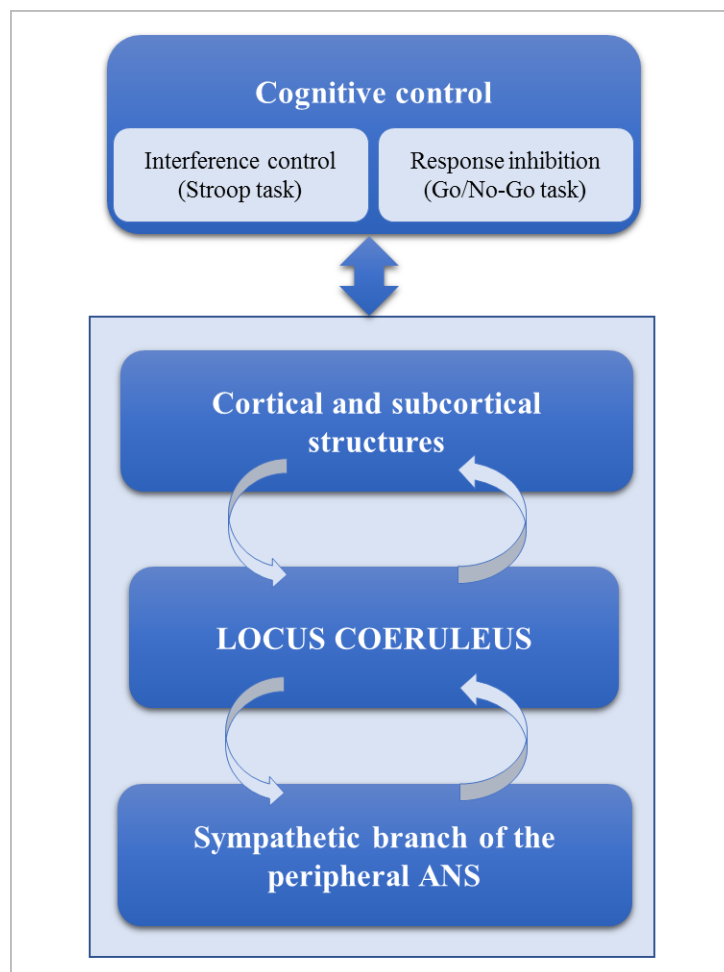


Figure 1. *Assumption of the present thesis: The locus coeruleus as central relay nucleus regarding the interplay between cortical and subcortical structures and the sympathetic branch of the peripheral autonomic*

nervous system in different domains of cognitive control. Cognitive tasks are proposed to address cortical and subcortical structures, the LC-noradrenergic system as well as on the sympathetic branch of the ANS. This in turn impacts on cognitive performance. I also suppose that the LC-noradrenergic system activates the sympathetic branch of the ANS and plays a key role in functional neuronal network organization. Thus, the close interrelation between cortical and subcortical structures and the sympathetic nervous system is assumed to be mediated by the LC-noradrenergic system.

2. THEMATIC CLASSIFICATION OF THE STUDIES

2.1 STUDY 1

Several lines of evidence suggest that the lateral PFC, the dorsal ACC, the parietal cortex, and the thalamus are central cortical nodes in a network underlying cognitive control. However, the role of the LC in cognitive control is still elusive and has rarely been addressed by functional magnetic resonance imaging (fMRI). Therefore, we aimed at identifying functional activation patterns and functional connectivity characteristics of the LC during the Stroop task (Stroop, 1935). Based on the theory of Corbetta, Patel, and Shulman (2008), we expected changes in the functional connectivity of the LC with the dorsal fronto-cingulo-parietal network during an increased demand of cognitive control. We hypothesized differential activation patterns in the LC with respect to the degree of cognitive control in healthy subjects.

Forty-five healthy subjects (age $M = 27.5$ years, $SD = 7.8$ years; range 18-56 years; 26 females) were investigated using fMRI and the Stroop task. In detail, the manual version of the Stroop task was presented in an event-related design that consisted of two conditions: a congruent and an incongruent condition. In the congruent condition, color words were presented in the color denoted by the corresponding word (e.g. the word “red” shown in red); in the incongruent condition, color words were displayed in one of three colors not denoted by the word (e.g. the word “green” shown in red). Two possible answers (color words in black type) were presented below it. The subjects had to indicate the type color by pressing one of two buttons, which corresponded spatially to both possible answers. Correct answers were

counterbalanced on the right and left sides of the display. 18 congruent stimuli and 18 incongruent combinations of four color words “red”, “green”, yellow” and “blue” written in the German language and corresponding colors were presented in a pseudorandom sequence. No colors were repeated consecutively to avoid positive priming effects.

We observed significant BOLD activation in the LC during the Stroop interference condition (incongruent > congruent condition). Furthermore, the LC BOLD activation significantly correlated with the Stroop interference time. Interestingly, a significant linear decrease in BOLD activation during the experiment in the incongruent condition was mainly found in the fronto-cingulo-striatal network, but not in the LC. For the LC, a distinct functional connectivity pattern was observed to the dorsolateral and ventrolateral PFC. Moreover, the LC revealed significant functional connectivity to the dACC, parietal and occipital regions.

Thus, we showed for the first time that functional activation patterns in the LC are modulated by different demands of cognitive control. The pivotal role of the noradrenergic neurotransmitter system in cognitive control was demonstrated.

2.2 STUDY 2

In this study, we wanted to improve our understanding of specific mechanisms of the noradrenergic neurotransmitter system in a pathological condition. Research findings suggest that cognitive control functions as well as the underlying brain network are impaired in schizophrenia. Dysfunctions within the noradrenergic neurotransmitter system are considered to play a central role in the pathophysiology of schizophrenia.

We sought to investigate activation patterns of the LC in patients with schizophrenia during the Stroop task in the same task version as applied in the first study.

A total of 29 patients (age $M = 33.1$ years, $SD = 8.02$ years; range: 20-51 years; 10 females) meeting the DSM-IV criteria for schizophrenia were recruited from the inpatient service of the Department of Psychiatry and Psychotherapy of the University Hospital Jena. They were

matched for age and gender with 28 healthy subjects (age $M = 33.14$ years, $SD = 8.46$ years; range: 22-56 years; 10 females), who were recruited from the local community. Subjects with past or current neurological or psychiatric diseases according to M.I.N.I (Sheehan et al., 1998) and/or first-degree relatives with Axis I psychiatric disorders were excluded from the study. Finally, 28 medicated patients and 27 healthy controls were investigated. An important finding was comparable LC BOLD activations in patients and healthy controls. However, in controls, LC BOLD activation was significantly correlated with the Stroop interference time, but not in patients.

A methodological limitation of our first two studies was the image acquisition technique. Considering the spatial extent of brainstem nuclei, functional MR imaging requires highly precise approaches (Beissner & Baudrexel, 2014; Beissner, Schumann, Brunn, Eisentrager, & Bar, 2014). To gain more confidence in the definite location of small nuclei, we prospected for more sophisticated structural and functional imaging techniques. Moreover, due to the presence of nearby major arteries and cerebrospinal fluid filled spaces located adjacent to the brainstem, the signal-to-noise ratio was demonstrated to benefit dramatically from physiological noise correction (Brooks, Faull, Pattinson, & Jenkinson, 2013).

2.3 STUDY 3

In this study, we wanted to validate the activation pattern revealed by our previous analyses using high-resolution fMRI, advanced brainstem co-registration techniques and physiological noise correction in order to precisely identify brainstem regions involved in cognitive control during the Stroop task. Importantly, pupil size and skin conductance were acquired as physiological indices of cognitive demand. We hypothesized that the LC is involved in the generation of physiological responses to the task.

Fourteen healthy subjects (age $M = 27$ years, $SD = 7$ years, 9 females) participated in this study. Three subjects were excluded due to inadequate quality of the eyetracker signal. Thus, eleven subjects were analyzed (age $M = 28$ years, $SD = 7$ years, 4 females).

Interestingly, we found that pupil size but not skin conductance might be an indicator of cognitive control. The pupillary Stroop effect correlated to the Stroop interference effect of reaction times. Pupillary reactions to congruent and incongruent stimuli habituated over time. Our main finding shows activation of the noradrenergic LC being positively correlated with the strength of pupillary responses. Skin conductance responses (SCR) were not different between both task conditions and were neither related to reaction time nor to trial number.

The anatomical position of the LC cluster being activated proportionally to pupillary responses ($x=-2$, $y=-36$, $z=-18$) corresponds to the LC coordinates that we extracted in our first study ($x=-2$, $y=-30$, $z=-26$). Murphy, O'Connell, O'Sullivan, Robertson, and Balsters (2014) reported a widely extended cluster related to pupillary responses in an oddball task that included LC coordinates we reported in our study. The authors also mentioned the problem of extensive spatial smoothing when analyzing small nuclei close to tissue boundaries. Besides their main analysis, which applied a smoothing kernel of 6mm, they also reported results without smoothing. The more specific demarcation of the LC closely matches our localization of the upper LC ($x=0$, $y=-32$, $z=-20$, Murphy et al., 2014). This also supports our notion that precise spatial resolution is crucial when investigating brainstem and midbrain structures. In our current analysis, the spatial resolution of 1.4 mm is far more sensitive compared to previous investigations (Köhler, Bär, & Wagner, 2016; Murphy et al., 2014). Additionally, we prepared the acquired functional data by physiological noise correction involving cardiac and respiratory signals. By including the pupillary responses in our functional data analysis, we validated the location and functional role of the LC.

2.4 STUDY 4

To further expand our understanding of human behavior and its abnormalities, we aimed to investigate indices of successful/unsuccessful response inhibition paying particular attention to the interplay between the LC and peripheral markers.

A total of 35 healthy controls were recruited from the local community. Two subjects were excluded from the final analysis because they reported forgotten task instructions. Thus, the final sample comprised 33 subjects (age $M = 26.8$ years, $SD = 5.2$ years; range: 20 to 40 years; 17 females). We applied a Go/No-Go paradigm which is a commonly used task to measure the ability to inhibit a pre-potent response. The No-Go-signal, which triggers the inhibitory processes, is presented unexpectedly following a Go-signal, measuring the inhibition of a planned response (action restraint; Eagle et al., 2008).

In respect of the requirements regarding fMRI analyses, I have developed a modified version of the Go/No-Go task with longer inter-stimulus-intervals (ISI) to allow the hemodynamic response to return to baseline. At the beginning of the task, people saw the word 'READY' in white capital letters in the middle of a black screen. Then, 'READY' was replaced by a clay jug, in which water was dropping very fast representing our baseline measure and was supposed to create a pre-potent response tendency. After varying time intervals, a stimulus appeared which was either a Go or a No-Go trial. The Go stimuli are two kinds of transverse cracks either starting from the left-handed side or from the right-handed side of the jug. The No-Go stimuli are two kinds of vertical cracks either starting from the upper end or from the bottom end of the jug. Moreover, stimulus presentation onsets were jittered. All subjects were asked to indicate which type of crack was presented by pressing a button (with the right index finger) as fast as possible when a Go stimulus appeared or by restraining their response when a No-Go stimulus appeared. Immediately after stimulus presentation, water kept on dropping into the jug. To create a pre-potent response tendency, there were more Go stimuli (in ~74%

of cases) than No-Go stimuli (in ~26% of cases). In sum, our Go/No-Go experiment lasted for 11 minutes and 35 seconds comprising 81 Go and 21 No-Go stimuli.

High-resolution fMRI data were preprocessed by specialized brainstem normalization and corrected for respiratory signal and cardiac noise. Skin conductance was acquired simultaneously to link BOLD activation to autonomic responses.

Our main results characterize specific neural activation patterns during successful and unsuccessful response inhibition especially comprising the anterior cingulate as well as the medial and lateral PFC. Most remarkably, specific neural activation patterns (i.e., dACC) as well as accompanying autonomic indices (i.e., skin conductance response) were identified to hold predictive information on an individual's performance. Thus, autonomic indices and specific neural activation patterns may contain valuable information to predict task performance. However, no BOLD activations were found in the LC during successful/unsuccessful response inhibition.

3. DISCUSSION

3.1 MAIN RESULTS

The Stroop interference contrast exhibited clear BOLD activations in the cognitive control network and the LC in healthy subjects as well as in patients suffering from schizophrenia. In healthy controls, the LC showed functional connectivities to this network and was correlated to performance, i.e., response time. In patients, no such correlation with performance was found. LC BOLD activation did not decline over time as was the case in structures of the cognitive control network. Pupillary but no skin conductance responses (SCR) were sensitive to the level of cognitive demand. Moreover, the LC was correlated with responses of the pupil, but not with SCR. In the Go/No-Go paradigm the cognitive control network was also

activated during successful response inhibition. However, no LC BOLD activations were found.

3.2 LC AS A LINK BETWEEN THE COGNITIVE CONTROL NETWORK AND SYMPATHETIC NERVOUS SYSTEM

3.1.1 STUDY ONE

We detected functional connectivity patterns of the LC during the Stroop interference effect which is in accordance with known neuroanatomical projections of noradrenergic neurons. The frontal lobe and the cingulate cortex have been shown to contain the highest density of noradrenaline fibers of all neocortical areas (Fuxe, Hamberger, & Hokfelt, 1968). Accordingly, further analyses revealed that the DLPFC, VLPFC, dACC, the dorsal parietal lobe as well as visual and motor brain areas are functionally connected with the LC, indicating an important role of the LC in cognitive conflict resolution. Further support for this notion is provided by the significant correlation between LC BOLD activation and the Stroop interference time.

Tonic and phasic activity modes of LC neurons have been described previously (Aston-Jones & Bloom, 1981; Aston-Jones & Cohen, 2005). The LC-noradrenaline tonic signal regulates transitions between specific behavioral states, such as sleep or focused attention. The pattern of tonic activity follows the classical Yerkes-Dodson relationship between arousal and performance (Aston-Jones and Cohen, 2005). Phasic LC activity might provide a temporal attentional filter, which selectively facilitates behavioral responses to task-relevant features and optimizes task-appropriate behavior (Aston-Jones and Cohen, 2005). Prefrontal and anterior cingulate inputs were assumed to enable the transition between different tonic levels as well as to trigger the LC phasic response (Clayton, Rajkowski, Cohen, & Aston-Jones, 2004; Corbetta et al., 2008). Both excitatory as well as inhibitory influences from the PFC on LC have been described (Sara & Herve-Minvielle, 1995). With respect to this interaction, Sara and Bouret (2012) stated that the firing of frontal neurons due to an increased cognitive

demand “wake up” the LC, which in turn facilitates cortical processing. Thus, LC functioning is supposed to mediate activity and functional integration of the cognitive control network, including the frontal cortex, thalamus and posterior cortical regions, and to modulate dynamic plasticity of cognitive brain systems (Coull, Buchel, Friston, & Frith, 1999). Summarizing previous results and our findings, we assume that phasic LC signals facilitate cognitive conflict resolution and optimize behavioral responses to incongruent Stroop items by activating a specific task related brain network and further by amplifying task relevant features, as reflected by strong functional connectivity to the occipital, pre-/motor and superior parietal cortices. Moreover, the anatomical heterogeneity of the LC complex in the brainstem might indicate different parts of the LC being specifically contributing to distinct subcomponents of cognitive control processes. For instance, cognitive conflict monitoring/resolution are mainly based on the fronto-cingulate circuitry, and the inhibition of pre-potent motor responses (due to the motor version of the employed Stroop task in this study) is mainly based on the SMA/premotor/motor cortices. However, this interpretation warrants further studies to elucidate the contribution of specific LC nuclei to different cognitive control processes in more detail.

3.1.2 STUDY TWO

After having corroborated the role of the LC in cognitive control, we wanted to get a better understanding of its involvement in schizophrenia as a disease with strong cognitive impairments. Interestingly, a comparable LC activation magnitude was observed between patients and controls in both task conditions. This supports the important involvement of the LC in cognitive control. However, the positive correlation between the LC BOLD signal and the Stroop interference time found in healthy controls but not in patients might indicate altered LC functioning during conflict resolution in patients with schizophrenia. An abnormally working LC-NA system was supposed in schizophrenia (J. I. Friedman, Adler, &

Davis, 1999), which was related to the manifestation of cognitive deficits (Fields et al., 1988; van Kammen et al., 1989). However, only sparse empirical evidence exists to support this hypothesis (Lohr & Jeste, 1988; Shibata et al., 2008) and, thus, needs further investigations.

3.1.3 STUDY THREE

In this study, we extended our view and started to investigate the interplay between the central and peripheral autonomic nervous system in cognitive control with the brainstem as a binding link. We demonstrated an association of LC activation and pupillary responses during the Stroop task. The pupillary response was sensitive to different demands of cognitive control (Laeng, Orbo, Holmlund, & Miozzo, 2011; Rondeel, van Steenbergen, Holland, & van Knippenberg, 2015; Siegle, Steinhauer, & Thase, 2004). Most remarkably, the increase of reaction times in the cognitive more difficult incongruent Stroop task condition was correlated with the increase of pupil diameter responses (PDR). Surprisingly, skin conductance responses (SCR) were not different between both task conditions and were neither related to reaction times nor to trial number. Thus, SCR appears to be an unsuitable parameter to indicate the level of cognitive load. Stimuli might elicit multiple overlapping SCRs as well as an increase of the tonic level leading to a high inter- and intra-individual variability (Lim et al., 1997). Most probably, a large sample size is needed to uncover the potential relation of SCR and brainstem BOLD activations during cognitive control. However, PDR was strongly correlated with the activity of the LC in the incongruent Stroop condition. Thus, it seems conceivable that pupillary responses might reflect the phasic noradrenergic activation induced by cognitive control. Positive correlations between the BOLD response in the DLPFC and PDR provide further evidence for the selective engagement of the DLPFC in conflict resolution and generation of physiological responses (Corbetta et al., 2008).

In sum, the LC seems to be essentially involved in linking the CNS and peripheral ANS in cognitive control. However, skin conductance might not be a sensitive marker of this interaction and its significance needs further investigations.

3.1.4 STUDY FOUR

To generalize our findings, we broadened the concept of cognitive control and investigated the interplay between the central and autonomic nervous system in response inhibition using a Go/No-Go task. During response inhibition, no BOLD activations were found in the LC during successful response inhibition. This difference compared to study one might be due to the type of inhibitory control addressed. In the first study, we focused on a more cognitive domain of inhibitory control using the Stroop task. Therefore, two different domains of inhibitory control were investigated indicating that the LC is not as decisive in action restraint as in interference control (Nandam et al., 2013). However, specific neural activation patterns (i.e., dACC) as well as accompanying autonomic indices (i.e., SCR) were identified to hold predictive information on an individual's performance.

3.3 GENERAL DISCUSSION

The present thesis aimed at investigating the association of cortical and subcortical BOLD activations and sympathetic autonomic responses via the LC-noradrenergic system during a cognitive task. Two different paradigms were used to analyze this issue. The Stroop task is an established paradigm to measure cognitive, i.e., inhibitory control. The LC as well as cortical and subcortical structures of the cognitive control network were more activated with higher cognitive demand in the interference condition (incongruent > congruent). I hypothesized functional connectivities of the LC and higher order cortical/subcortical areas. The obtained results indicate that the lateral PFC, the dACC, dorsal parietal, visual and motor regions are connected with the LC (see **Figure 2**). This correlation pattern supports studies of functional

network organization reporting that the LC is part of the cognitive control network (Bär, 2016).

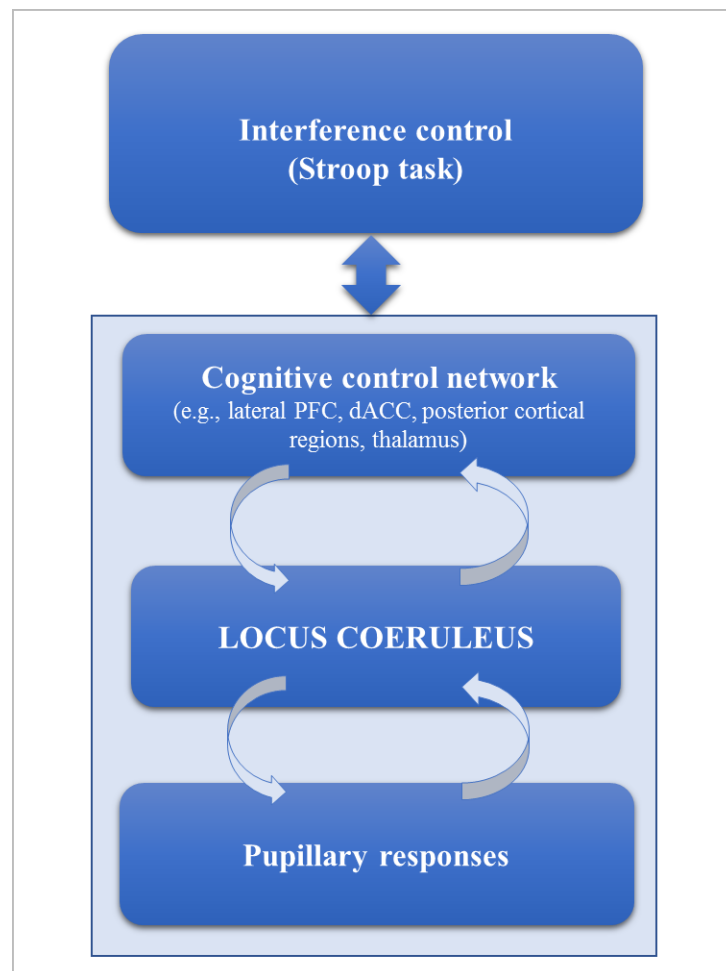


Figure 2. Findings of the present thesis: The locus coeruleus as central relay nucleus regarding the interplay between the cognitive control network and the sympathetic branch of the peripheral autonomic nervous system, i.e., pupillary responses, in interference control.

The present work revealed indications that the interaction of the LC and the cortex is more complex than a linear co-activation. Activations of key cortical structures such as the DLPFC, cingulate and motor areas declined over time due to learning effects. In contrast, no significant change of LC BOLD activation was detected over time. Different studies suggest a bidirectional connectivity of the LC to key regions of the cognitive control network. For instance, the PFC exerts both inhibitory and excitatory influence on the LC. In turn, the LC modulates the activity of cortical structures involved in cognitive control. Corbetta et al (2008) postulated that the LC acts as major switch between two subnetworks during cognitive

processing. The ventral fronto-parietal network detects salient stimuli whereas the dorsal fronto-parietal network directs attention and generates proper behavioral responses (Corbetta et al., 2008). The present results support a connection of the LC to both networks via the DLPFC, the VLPFC and parietal areas. Given that task events were randomized, the salience of congruent stimuli might have remained constant. Therefore, the activation of the VLPFC and LC showed no habituation. In contrast, attentional resources needed to respond adequately to the incongruent condition seem to have decreased due to a learning effect expressed as decline of BOLD activation of the DLPFC, parietal and motor areas. Moreover, the interference effect on response times correlated with LC activation in the interference contrast. Higher cognitive effort is associated with stronger LC activation. In sum, the LC-noradrenergic system plays a profound role in cognitive processing and exerts connections to important subnetworks of the cognitive control network.

Schizophrenia is a severe psychiatric disorder which is characterized by a multitude of symptoms affecting emotional and cognitive processing. Hypo- and hypervigilant states of the LC-noradrenergic system have been associated with impaired cognitive functioning in schizophrenia (Yamamoto & Hornykiewicz, 2004). Patients analyzed in this line of research showed higher reaction times in both task conditions. The interference effect on LC activation as well as response times was comparable in patients and controls. However, the linear correlation of both variables was present in controls only indicating that there is no association of performance and LC activation in the interference contrast in patients. Nevertheless, this contrast might not be sensitive enough to reveal cognitive impairment in patients as was suggested by prolonged response delays.

The model I aimed to investigate autonomic responses of the sympathetic branch likely to be related to LC activation during cognitive processing. Pupil diameter and skin conductance

showed significant reactions to the events of the Stroop task. Pupillary responses in the incongruent condition were higher than in the congruent condition. The interference effect of reaction times and the interference effect on pupillary responses were significantly correlated. The results corroborate that pupil dilation is indicative of cognitive effort. The LC was correlated to pupillary responses and was activated in the Stroop interference contrast. A strong co-variation of LC BOLD activation during task performance and pupil diameter was shown in electrophysiological and fMRI studies (see review by Eckstein et al 2017, Joshi et al 2016, Rajkowski et al 1994). The LC exerts noradrenergic excitatory influence over preganglionic sympathetic neurons innervating the pupil, sweat glands etc. Noradrenergic inhibitory impact from the LC on the parasympathetic Edinger-Westphal nucleus also modulates pupil size (Samuels & Szabadi 2008). It can be assumed that pupil dilation to task events was elicited by the inhibition of the parasympathetic and excitation of the sympathetic outflow to the pupillary muscles.

In the Go/No-Go paradigm, a facet of inhibitory control was addressed that is more focused on the motor component of cognitive control. Even in a relatively large sample, no contribution of the LC-noradrenergic system was detected during performance of this task. Therefore, I assume that the LC is less important when performing a more motor than cognitive domain of cognitive control.

4 SUMMARY AND CONCLUSION

The paramount importance of the LC in cognitive control was emphasized by an increase of its activation proportional to the increase of cognitive load. In patients with schizophrenia, this relation was absent indicating a deficient role of the LC-noradrenergic system. Broad functional connections of the LC to cortical and subcortical regions predominantly involved in executive function were also found. Furthermore, LC BOLD activation was associated with

pupillary dilation which supports the interpretation of the LC playing a pivotal role in controlling sympathetic autonomic function. For instance, the activation of the LC-noradrenergic system produces an increase in sympathetic activity by an inhibitory influence on preganglionic parasympathetic nuclei. The relation between the LC BOLD signal and pupillary response, which in turn indicates the amount of cognitive effort, strengthens the interpretation that LC activation depends on the level of cognitive load and determines the strength of autonomic responses. In the Go/No-Go task, which taps a more motor domain of cognitive control (i.e., response inhibition/impulse control), no LC BOLD activation was found. I conclude that the LC is crucially involved in tasks requiring a more cognitive domain of cognitive control.

With these findings, I was able to broaden the view of the brain – body interaction in cognitive control with the LC as central relay nucleus. LC was identified as a link between the cognitive control network and sympathetic nervous system. Thus, the present thesis contributes to an extension of the current state-of-the-art in neuropsychology.

4. STUDIES

STUDY 1

Title: **Differential involvement of brainstem noradrenergic and midbrain dopaminergic nuclei in cognitive control.**

Authors: Stefanie Köhler, Karl-Jürgen Bär, Gerd Wagner

Progress of the study: published in *Human Brain Mapping*

STUDY 2

Title: **Activation of brainstem and midbrain nuclei during cognitive control in medicated patients with schizophrenia.**

Authors: Stefanie Köhler, Gerd Wagner, Karl-Jürgen Bär

Progress of the study: published in *Human Brain Mapping*

STUDY 3

Title: **The use of physiological signals in brainstem/midbrain fMRI.**

Authors: Andy Schumann, Stefanie Köhler, Feliberto de la Cruz, Daniel Güllmar, Jürgen R. Reichenbach, Gerd Wagner, Karl-Jürgen Bär

Progress of the study: published in *Frontiers in Neuroscience*

STUDY 4

Title: **Towards response success prediction: An integrative approach using high-resolution fMRI and autonomic indices.**

Authors: Stefanie Köhler, Andy Schumann, Feliberto de la Cruz, Gerd Wagner, Karl-Jürgen Bär

Progress of the study: published in *Neuropsychologia*

Differential Involvement of Brainstem Noradrenergic and Midbrain Dopaminergic Nuclei in Cognitive Control

Stefanie Köhler, Karl-Jürgen Bär,* and Gerd Wagner

Department of Psychiatry and Psychotherapy, Psychiatric Brain and Body Research Group
Jena, University Hospital Jena, 07743, Germany

Abstract: Several lines of evidence suggest that the lateral prefrontal cortex (PFC), the dorsal anterior cingulate cortex (dACC), the parietal cortex, and the thalamus are central cortical nodes in a network underlying cognitive control. However, the role of catecholamine producing midbrain and brainstem structures has rarely been addressed by functional magnetic resonance imaging (fMRI). We hypothesized differential activation patterns in the ventral tegmental area (VTA)/substantia nigra (SN) and locus coeruleus (LC) with respect to the degree of cognitive control during a Stroop task in healthy subjects. Forty-five healthy subjects were investigated by the manual version of the Stroop task in an event-related fMRI design. We observed significant BOLD activation of both the SN/VTA and LC during the Stroop interference condition (incongruent vs. congruent condition). LC, but not SN/VTA activation significantly correlated with the Stroop interference. Interestingly, a significant linear decrease in BOLD activation during the incongruent condition during the experiment was mainly observed in the fronto-cingulo-striatal network, but not in SN/VTA and LC. Using psychophysiological (PPI) analyses, a significant functional connectivity during cognitive control was observed between SN/VTA and the nigrostriatal/mesolimbic dopaminergic system. For the LC, distinct functional connectivity pattern was observed mainly to the dorsolateral and ventrolateral PFC. Both regions revealed significant functional connectivity to the dACC, parietal and occipital regions. Thus, we demonstrate for the first time that functional activation patterns in the SN/VTA and the LC are modulated by different demands of cognitive control. In addition, these nuclei exhibit distinguishable functional connectivity patterns to cortical brain networks. *Hum Brain Mapp* 37:2305–2318, 2016. © 2016 Wiley Periodicals, Inc.

Key words: fMRI; cognitive control; locus coeruleus; ventral tegmental area; functional connectivity

Additional Supporting Information may be found in the online version of this article.

Contract grant sponsor: German Research Foundation; Contract grant number: DFG WA 3001/3-1.

Financial disclosures: All authors report no biomedical financial interests or potential conflicts of interest.

*Correspondence to: K.-J. Bär, Department of Psychiatry and Psychotherapy, University Hospital, Philosophenweg 3, 07743 Jena, Germany. E-mail: Karl-Juergen.Baer@med.uni-jena.de

Received for publication 11 September 2015; Revised 23 February 2016; Accepted 24 February 2016.

DOI: 10.1002/hbm.23173

Published online 11 March 2016 in Wiley Online Library (wileyonlinelibrary.com).

INTRODUCTION

The term “cognitive control” relates to a number of operations that enable the cognitive system to successfully pursue specific cognitive tasks, such as maintaining and manipulating goal-related information or inhibiting and overriding prepotent responses [Botvinick et al., 2001]. On the neural level, cognitive control is characterized by a dynamic interplay between prefrontal, posterior parietal and subcortical structures [Miller and Cohen, 2001]. The lateral prefrontal cortex (PFC), consisting of the dorsolateral and ventrolateral prefrontal cortex (DLPFC, VLPFC), the dorsal anterior cingulate cortex (dACC), the parietal cortex and the thalamus, are regarded as central nodes of this cognitive control network [Mansouri et al., 2009].

Dopamine-producing (DA) neurons are mainly located in the ventral tegmental area (VTA) and substantia nigra (SN) and are part of two proposed systems: the nigrostriatal and the mesolimbic dopaminergic system [Ungerstedt, 1971]. The nigrostriatal system originates from the SN and projects to thalamic nuclei, the caudate nucleus, and the putamen. The dorsal striatum receives strong input from the prefrontal as well as from premotor and posterior parietal brain regions [Haber et al., 2000; Parent, 1990]. This system is mainly associated with cognitive functions and motor outcomes [Alexander et al., 1986], in particular with cognitive flexibility and the development of stimulus-response (S-R) contingencies. The mesolimbic dopaminergic system arises from the VTA and the medial part of the SN. It has dense projections to the nucleus accumbens (NAc), but also to other limbic regions including the hippocampus, amygdala, and the medial PFC [Ikemoto, 2007]. The system contributes to reward-guided behavior and motivation. Haber [2003] provided substantial evidence for the close interaction between both dopaminergic systems, reflecting the DA-dependent interaction between motivational and cognitive processes. In addition, studies investigating cognitive control processes in subjects with abnormal DA transmission consistently reported an altered regional cerebral blood flow (rCBF) or BOLD activation in the fronto-cingulate network during the Stroop task [Bolla et al., 2004; Salo et al., 2009].

The locus coeruleus (LC) is a brainstem structure containing noradrenaline-producing neurons. Axon terminals of LC neurons are distributed throughout most cortical and subcortical areas. The frontal lobe and the cingulate cortex have been shown to contain the highest density of noradrenergic (NA) fibers of all neocortical areas [Fuxe et al., 1968], which enable the modulation of cognitive flexibility and executive functioning of this brain network [Foote et al., 1983; Sara and Bouret, 2012]. In their review, Aston-Jones and Cohen [2005] emphasize the specific role of the LC in cognitive flexibility. The authors propose that enhanced LC activity produces a temporally specific release of noradrenaline, which increases the gain of specific task-associated cortical networks and optimizes task-appropriate behavior. Several studies in rats provided

evidence for the important involvement of LC in cognitive flexibility [Devauges and Sara, 1990]. It was reported that attentional set shifting is mainly dependent on the NA system influencing the medial PFC, which corresponds to the ACC in humans [Tait et al., 2007]. Reducing LC activity in rats by a centrally acting alpha 2-adrenergic agonist clonidine negatively affects response time and accuracy in attentional and memory tasks [Mair et al., 2005].

The so-called “network reset” theory by Bouret and Sara [2005] suggests that the activation of the LC-NA system in response to a particular sensory event will produce or facilitate the dynamic reorganization of neural networks leading to new functional networks that regulate the adaptive behavioral output. Corbetta et al. [2008] has linked in more detail the LC-NA system to attention shifting and cognitive flexibility. The authors described two separate functional anatomical networks underlying attentional processing. First, the dorsal fronto-parietal network that contains the DLPFC and the dorsal parietal cortex as core regions. It is involved in directing attention and top-down modulation of expected stimuli as well as generating appropriate stimulus-response contingencies. Second, the ventral fronto-parietal network mainly consisting of the temporo-parietal junction, VLPFC and anterior insula, is responsible for the detection of behaviorally salient stimuli [Corbetta et al., 2008]. Depending on the incoming stimuli, signals from the LC influence adaptive state shifts between the ventral and dorsal fronto-parietal networks. Thus, changes in the activation pattern of the LC during transition from an exploratory to a task-focused state are accompanied by a deactivation of ventral and an activation of dorsal networks [Corbetta et al., 2008].

However, the role of LC in cognitive tasks has rarely been investigated in humans by means of functional neuroimaging. Coull et al. [1999] demonstrated that clonidine increases the effective connectivity from LC to parietal cortex during an attentional task using positron emission tomography scanning. Raizada and Poldrack [2008] observed a complexity-dependent covariation of the LC and VLPFC in an audiovisual task with unpredictably varying stimulus onset asynchrony [SOA], supporting the theory of Corbetta et al. [2008].

Thus, there is strong evidence for the notion that NA and DA produced in brainstem/midbrain nuclei are crucially involved in cognitive control processes by exerting a modulatory influence on fronto-cingulo-striatal and fronto-cingulo-parietal networks. However, according to our knowledge the activation dynamics as well as the task-dependent functional connectivity of these nuclei during a cognitive control task have not yet been investigated using functional magnetic resonance imaging (fMRI). Therefore, the main goal of this study was to elucidate functional activation patterns and functional connectivity of noradrenaline and DA producing areas as well as the dynamics of the BOLD activation changes during the Stroop Color-Word task [Stroop, 1935]. It is a well-established

experimental paradigm to measure cognitive and especially inhibitory control, which requires an inhibition of an overlearned, prepotent response tendency (reading the word), in favor of an unusual, less prepotent action (reading the ink). We assumed a significant functional connectivity of the DA nuclei with the fronto-cingulo-striatal network, which enhances its strength with increasing cognitive control. Based on the theory of Corbetta et al. [2008], we expect changes in the functional connectivity of the LC with the dorsal fronto-cingulo-parietal network during an increased demand of cognitive control.

MATERIALS AND METHODS

Subjects

Forty-seven subjects (age $M = 27.7$ years; $SD = 7.7$ years; range: 18–56 years; 28 females) participated in this study. They were recruited from the local community. Subjects with past or current neurological or psychiatric diseases according to M.I.N.I [Sheehan et al., 1998] and/or first-degree relatives with Axis I psychiatric disorders were excluded from the study. None of the study participants was taking any psychopharmacological medication.

Two subjects were excluded from the final analysis due to movement artifacts exceeding 3 mm or 3° rotation. Thus, 45 subjects were finally analyzed (age $M = 27.5$ years; $SD = 7.8$ years; range: 18–56 years; 26 females). All participants were German native speakers, right-handed according to the modified version of Annett's handedness inventory [Briggs and Nebes, 1975] and provided written informed consent prior to participating in the study. The study protocol was approved by the Ethics Committee of the University of Jena. All subjects were paid 8 Euro per hour for their participation.

Experimental Paradigm

The manual version of the Stroop Color-Word task was described in detail previously [Wagner et al., 2015]. In brief, the Stroop task consists of two conditions: a congruent and an incongruent condition. In the congruent condition, 18 color words are presented in the color denoted by the corresponding word; in the incongruent condition, 18 color words are displayed in one of three colors, which are not denoted by the word. This target stimulus was presented in the center of the display screen. Two possible answers (color words in black type) were presented in the lower visual field to minimize contextual memory demands. All subjects had to indicate as fast as possible the type of color by pressing one of two buttons (with right index or middle finger), which corresponded spatially to both possible answers. Correct answers were counterbalanced on the right and left sides of the display. Stimulus presentation time was 1500 ms with an interstimulus interval of 10.5 s. Additionally, a temporal jitter

was introduced to enhance the temporal resolution. The presentation of stimuli was varied relative to the onset of a scan in 12 steps for 182 ms. This jitter was shifted over the repetition time three times per condition.

MRI Parameters

Functional data were collected on a 3 T Siemens TIM Trio whole body system (Siemens, Erlangen, Germany) equipped with a 12-element receive-only head matrix coil. Head immobilization was done using head pads within the head coil. T_2^* -weighted images were obtained using a gradient-echo EPI sequence ($TR = 2700$ ms, $TE = 30$ ms, flip angle = 90°) with 48 contiguous transverse slices of 2.7 mm thickness and an interslice gap of 10% covering the entire brain and including the lower brainstem. Matrix size was 72×72 pixels with in-plane resolution of 2.67×2.67 mm². A series of 220 whole-brain volume sets were acquired in one session. High-resolution anatomical T_1 -weighted volume scans (MP-RAGE) were obtained in sagittal orientation ($TR = 2300$ ms, $TE = 3.03$ ms, $TI = 900$ ms, flip angle = 9°, $FOV = 256$ mm, matrix = 256×256 mm², number of sagittal slices = 192, acceleration factor (PAT) = 2, $TA = 5:21$ min) with an isotropic resolution of $1 \times 1 \times 1$ mm³.

Univariate Functional Data Analyses

For image processing and statistical analyses, we used the SPM8 software (<http://www.fil.ion.ucl.ac.uk/spm>). Data preprocessing and single-subject level analyses were identical to our previous studies [Wagner et al., 2015]. The first four images were discarded to obtain steady-state tissue magnetization. The remaining 216 images were corrected for differences in time acquisition by sinc interpolation, realigned at the first image. The coregistered anatomical images were segmented using the tissue probability maps of the ICBM template in SPM8. Functional images were then spatially normalised to the MNI space using spatial normalisation parameters estimated during the segmentation process. The whole-brain data were smoothed with a Gaussian filter of 6 mm FWHM and were high-pass filtered with a cutoff period of 128 s and corrected for serial correlations choosing AR(1).

Subsequently, data were analyzed voxelwise within the general linear model to calculate statistical parametric maps of t statistics for condition-specific effects. Individual movement parameters entered a fixed effects model at a single-subject level as covariates of no interest. A fixed-effects model at a single-subject level was performed to create images of parameter estimates, which were then entered into a second-level analysis. For the second level group comparison, we set up an ANOVA design with a within-subjects factor TASK (congruent and incongruent condition) and tested for the interference contrast incongruent vs. congruent condition. For the whole-brain

analyses, the statistical comparisons were thresholded on the voxel-level at $P < 0.001$ (uncorrected) and $P < 0.05$ FWE corrected at the cluster-level as recently recommended by Woo et al. [2014].

Due to the small size of brainstem nuclei and therefore smaller expected number of activated contiguous voxels, we additionally performed an ROI analysis in the brainstem using a mask image, which was created by means of the WFU PickAtlas (<http://fmri.wfubmc.edu/software/PickAtlas>) and comprised the midbrain and the upper brainstem. The statistical comparisons were thresholded on the voxel-level at $P < 0.001$ (uncorrected) and on a more liberal cluster-extent threshold, which corresponded to the number of expected voxels per cluster k_e .

fMRI Analysis of Brainstem/Cerebellum Using SUIT Toolbox

To improve the normalization procedure and to verify statistical results in the brainstem detected at the whole-brain level and in the ROI analysis, data were normalized to the spatially unbiased infra-tentorial template (SUIT, version 3.1) [Diedrichsen, 2006]. The SUIT toolbox provides a new high-resolution atlas template of the human brainstem and cerebellum, based on the anatomy of 20 young healthy individuals. Using the SUIT toolbox, we applied the following preprocessing steps: (i) segmentation of the whole-brain image, (ii) cropping of the image, retaining only the cerebellum and brainstem, (iii) normalization using the DARTEL engine [Ashburner, 2007] that uses gray and white matter segmentation maps produced during cerebellar isolation to generate a flowfield using Large Deformation Diffeomorphic Metric Mapping [Beg et al., 2005], (iv) reslicing to a voxel size of $2 \times 2 \times 2$ mm³, and (v) smoothing with Gaussian filter of 4 mm FWHM. After high-pass filtering (128 s) and correction for serial correlations [AR(1)], a fixed-effects model (the same as at the whole-brain level) at the single-subject level was set-up with preprocessed functional brainstem/cerebellum images to create images of parameter estimates for the subsequent random-effects group analyses (RFX). The statistical comparisons at the brainstem/cerebellum level were thresholded on the voxel-level at $P < 0.001$ (uncorrected) and corrected at the cluster-level according to the expected voxels per cluster.

Correlational Analysis

The significance of a relationship between Stroop interference score (response time difference between incongruent and congruent conditions) and neural activation during the incongruent vs. congruent condition contrast were investigated using the regression analysis. The statistical comparisons were thresholded on the voxel-level at $P < 0.001$ (uncorrected) and $P < 0.05$ FWE corrected at the cluster-level. Statistical comparisons based on the ROI

analysis in the brainstem were thresholded on the voxel-level at $P < 0.001$ (uncorrected) and on a more liberal cluster-extent threshold, which corresponded to the number of expected voxels per cluster k_e . For this purpose, we used the mask image of the brainstem, which was created by means of the WFU PickAtlas.

We further performed a regression analysis with the Stroop interference score using the images of parameter estimates (incongruent vs. congruent conditions) from the brainstem/cerebellum analysis as preprocessed with the SUIT toolbox in order to confer the results of the whole-brain analysis. The statistical comparisons on the brainstem level were thresholded on the voxel-level at $P < 0.001$ (uncorrected) and on the cluster-level according to the expected voxels per cluster.

Practice-Related Signal Changes in Neuronal Activation

To examine the signal course across time, we conducted a parametric modulation analysis, which modulates the amplitude of the predicted HRF. Based on the behavioral data, we modeled the linear signal decrease as a covariate of interest to investigate whether, and in which regions, the change in BOLD response in the incongruent Stroop condition followed the anticipated linear time course. In addition, we modeled the linear signal increase as a covariate of interest to test for potential signal increases. Voxel-by-voxel t-tests were individually computed for each subject on the first level. The contrast images derived from these analyses were then entered into the group-level one-sample t-tests, which were thresholded on the voxel-level at $P < 0.001$ (uncorrected) and FWE corrected at the cluster-level. Lowering the cluster-level threshold to a more liberal cluster-extent threshold, we tested for linear signal changes in the brainstem based on the ROI analysis as described above. We further examined the linear BOLD signal changes in the incongruent Stroop condition in the brainstem/cerebellum only, as preprocessed with the SUIT toolbox and applied a statistical threshold of $P < 0.001$ (uncorrected) on the voxel-level at and on the cluster-level according to the expected voxels per cluster.

Psychophysiological Interactions (PPI)

Based on our initial hypothesis and the results of the significant univariate analysis (incongruent vs. congruent contrast), a PPI analysis as implemented in SPM8 was used to further elucidate changes in the functional connectivity between the dopaminergic SN/VTA as well as the NA LC and the neural network during cognitive control. First, we created a mask image from the cluster of significant BOLD activation difference between the incongruent and congruent condition comprising the SN/VTA as well as LC. Then, the individual local maximum within this mask image was determined to build the individual ROI

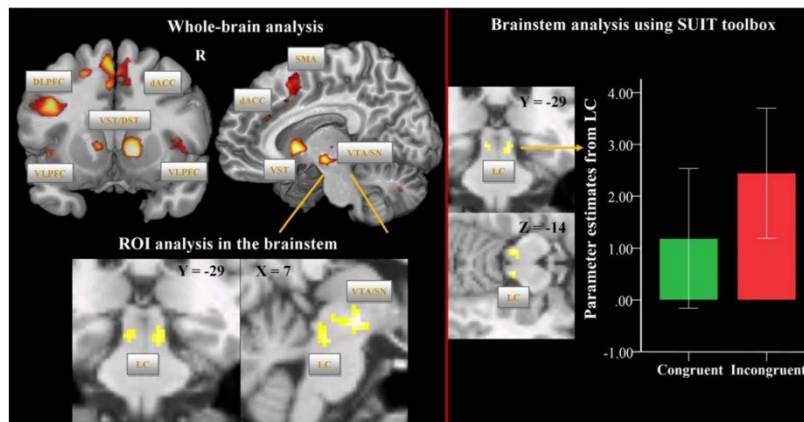


Figure 1.

Univariate fMRI analysis: incongruent vs. congruent Stroop task condition. On the upper left side, brain regions are depicted, which show increased BOLD signal during the incongruent vs. congruent condition at the whole-brain level (voxel-level: $P < 0.001$ uncorr., cluster-level: $P < 0.05$, FWE corr.). On the lower left side, BOLD activation differences (voxel-level: $P < 0.001$ uncorr., cluster-level: according to the number of expected voxels per cluster k_c) are illustrated based on the ROI analysis in the brainstem. The mask image was created using the WFU PickAtlas and comprised the midbrain and the upper brainstem. On the right side, brain regions are depicted, which show increased

BOLD signal during the incongruent vs. congruent conditions at the level of the brainstem/cerebellum as preprocessed with the SUIT toolbox and using 4 mm FWHM smoothing (voxel-level: $P < 0.001$ uncorr., cluster-level: according to the number of expected voxels per cluster k_c). The box plot shows the parameter estimates for the congruent and incongruent conditions as extracted from the LC cluster. Abbreviations: DLPFC, dorsolateral prefrontal cortex; VLPFC, ventrolateral prefrontal cortex; dACC, dorsal anterior cingulate cortex; SMA, supplementary motor area; VST, ventral striatum; DST, dorsal striatum; VTA/SN, ventral tegmental area/substantia nigra; LC, locus coeruleus.

of 3 mm radius sphere. In two subjects, we were not able to create an LC-ROI and to extract the time series. The averaged time series extracted from these ROIs from the contrast incongruent vs. baseline was adjusted for the effects of interest. An individual design matrix was created, with one regressor representing the activation time course in the SN/VTA and LC respectively, one regressor representing the time dependent change as a psychological variable of interest (incongruent vs. congruent Stroop condition from the design matrix), and a third regressor representing the element-by-element product of the previous two (the PPI term). The PPI analysis was individually computed for each subject and the contrast images derived from these analyses were then entered into the group-level one-sample t-test, which was thresholded on the voxel-level at $P < 0.001$ (uncorrected) and $P < 0.05$ FWE corrected at the cluster-level.

Behavioral Data Analysis

The behavioral analyses were performed by means of SPSS Statistics V22. Using the paired t-test the difference

in the response times between the incongruent and congruent Stroop conditions were tested for significance. Furthermore, potential differences in the response accuracy were analyzed using the Wilcoxon signed-rank test. Practice-related changes in response times were examined by means of linear regression analysis.

RESULTS

Behavioral Performance

Subjects responded significantly faster [$t(44) = 6.22$; $P < 0.001$] in the congruent than in the incongruent condition of the Stroop task, indicating a reliable induction of the Stroop interference effect [Stroop, 1935]. The averaged Stroop interference time, defined as difference in reaction time between incongruent and congruent condition, was $M = 250.82$ ms ($SD = 270.6$). In both conditions, high levels of accuracy were obtained: in the congruent condition 97.4% ($SD = 1.53$), and in the incongruent condition 92.3% ($SD = 1.71$). The nonparametric Wilcoxon test revealed a significant accuracy difference between congruent and

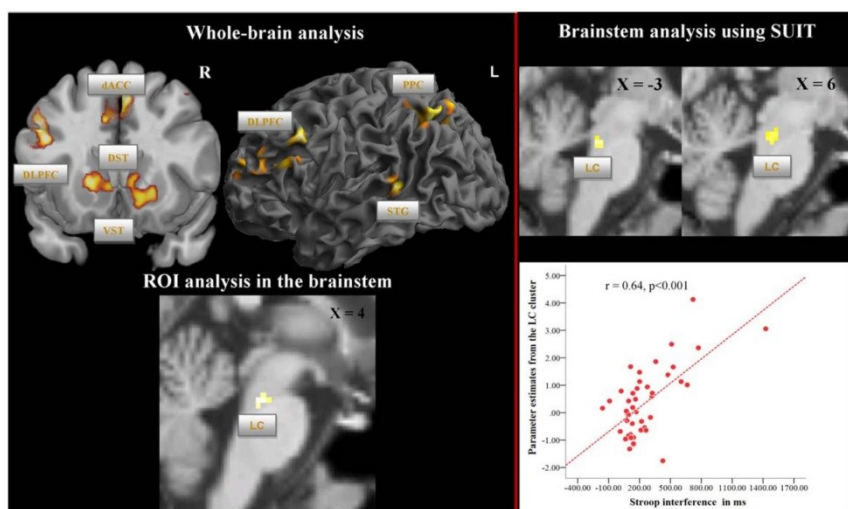


Figure 2.

Univariate fMRI analysis: correlation between Stroop interference time and BOLD activation in the contrast incongruent vs. congruent condition. On the upper left side, significant correlation between Stroop interference time (difference in response time between incongruent and congruent condition) and BOLD activation in the contrast incongruent vs. congruent condition is presented at the whole-brain level (voxel-level: $P < 0.001$ uncorr., cluster-level: $P < 0.05$, FWE corr.). On the lower left side, significant correlation between Stroop interference time and BOLD activation is presented based on the ROI analysis in the brainstem (voxel-level: $P < 0.001$ uncorr., cluster-level: according to the number of expected voxels per cluster k_c). On

the upper right side, significant correlation between Stroop interference time and BOLD activation is presented at the level of the brainstem/cerebellum as preprocessed with the SUIIT toolbox and using 4 mm FWHM smoothing (voxel-level $P < 0.001$: uncorr., cluster-level: according to the number of expected voxels per cluster k_c). In the right lower corner, the scatterplot of the significant positive correlation between parameter estimates from the LC cluster and Stroop interference time is depicted. Abbreviations: DLPFC, dorsolateral prefrontal cortex; dACC, dorsal anterior cingulate cortex; VST, ventral striatum; DST, dorsal striatum; STG, superior temporal gyrus; PPC, posterior parietal cortex; LC, locus coeruleus.

incongruent condition ($Z = -3.51$, $P = < 0.001$). The linear regression analysis revealed a significant linear decrease in RT in the whole group in the incongruent condition ($R^2 = 0.85$, $P < 0.001$).

Univariate fMRI Analyses

Incongruent vs. congruent Stroop conditions

Comparing the incongruent with the congruent condition, we detected increased, mainly left lateralized, BOLD activations especially in the VLPFC, DLPFC, dACC, SMA, mediadorsal thalamus, insula, the ventromedial head of the caudate, the NAc, and putamen as well as cerebellum (Fig. 1, Supporting Information Table S1). Similarly, the medial part of the midbrain comprising VTA and the medial portion of the SN showed increased BOLD activation patterns during incongruent vs. congruent condition

(voxel-level: $P < 0.001$ uncorr.; cluster-level: $P < 0.05$, FWE corrected, Fig. 1, left half).

As shown in Figure 1, based on the ROI analysis in the brainstem and using a more liberal cluster-extent threshold, which corresponded to the number of expected voxels per cluster k_c , we additionally detected a significant activation difference (voxel-level: $P < 0.001$ uncorr.) in two clusters in the brainstem, which most likely correspond to the left ($x = -4$, $y = -26$, $z = -16$, $t = 3.84$, $P < 0.001$, cluster size = 37) and right LC ($x = 8$, $y = -28$, $z = -16$, $t = 3.98$, $P < 0.001$, cluster size = 17), as identified from the known anatomical localization [Naidich et al., 2009; Nieuwenhuys, 1985].

Brainstem/cerebellum analysis using SUIIT toolbox: Incongruent vs. congruent Stroop conditions

Applying more sophisticated brainstem/cerebellum normalization and a smoothing filter of 4 mm FWHM, we

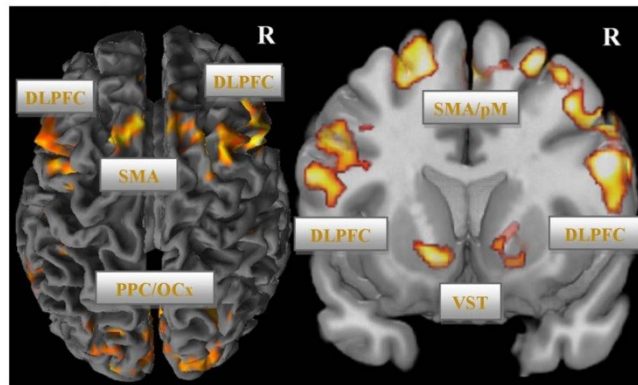


Figure 3. Practice-related BOLD signal decrease in the incongruent condition (voxel-level: $P < 0.001$ uncorr., cluster-level: $P < 0.05$, FWE corr.). Abbreviations: DLPFC, dorsolateral prefrontal cortex; dACC, dorsal anterior cingulate cortex; SMA, supplementary motor area; VST, ventral striatum; PPC, posterior parietal cortex; OCx, occipital cortex.

could confer the results of the whole-brain and ROI analyses. As illustrated in the Figure 1 (right half) and in the Supporting Information Figure S1 (unsmoothed data), we observed in the incongruent in contrast to congruent Stroop condition significantly increased BOLD signal in the left ($x = -6, y = -28, z = -13, t = 4.01, P < 0.001$, cluster size = 26) and right LC ($x = 8, y = -28, z = -15, t = 4.14, P < 0.001$, cluster size = 16).

Additionally, significantly increased BOLD activation in the incongruent vs. congruent condition was detected in

the clusters comprising VTA/SN ($x = 8, y = -18, z = -8, t = 3.83, P < 0.001$; cluster size = 40) as well as in the right ($x = 12, y = -70, z = -35, t = 4.69, P < 0.001$; cluster size = 99) and left cerebellum ($x = -14, y = -44, z = -29, t = 4.62, P < 0.001$; cluster size = 21).

Correlational analysis

As illustrated in Figure 2 (left half) and Supporting Information Table S2, a positive correlation between the

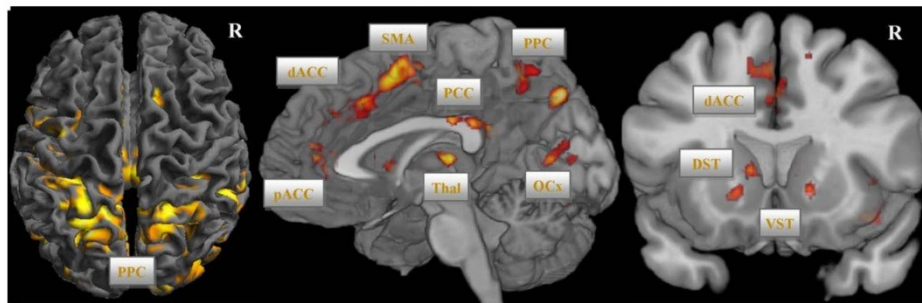


Figure 4. PPI analysis using VTA/SN as seed region (voxel-level $P < 0.001$ uncorr., cluster-level, $P < 0.05$, FWE corr.). Abbreviations: DLPFC, dorsolateral prefrontal cortex; dACC, dorsal anterior cingulate cortex; SMA, supplementary motor area; VST, ventral striatum; PCC, posterior cingulate cortex; PPC, posterior parietal cortex; OCx, occipital cortex

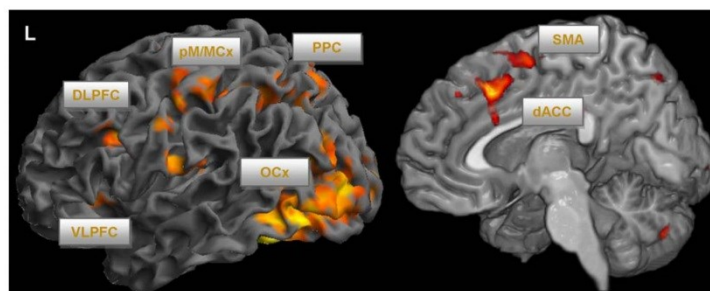


Figure 5.

PPI analysis using LC as seed region (voxel-level: $P < 0.001$ uncorr., cluster-level: $P < 0.05$, FWE corr.). Abbreviations: DLPFC, dorsolateral prefrontal cortex; VLPFC, ventrolateral prefrontal cortex; dACC, dorsal anterior cingulate cortex; SMA, supplementary motor area; pM/MCx, premotor/motor cortex; PPC, posterior parietal cortex; OCx, occipital cortex

RT interference scores and BOLD activation during the Stroop interference contrast (whole-brain analysis, incongruent vs. congruent condition; $P < 0.001$; cluster-level FWE corrected) was observed bilaterally in the DLPFC, bilaterally in the putamen and caudate, NAc, as well as in dACC extending to the SMA, in the left superior temporal gyrus (STG) and precuneus. Importantly, in the ROI analysis, a significant positive correlation (Fig. 2) was also found in the brainstem, presumably most likely corresponding to LC ($x = -2$, $y = -30$, $z = -26$, $t = 3.95$, $P < 0.001$; cluster size = 17), but not in the SN/VTA. The LC position was slightly different along the rostrocaudal axis in comparison to the contrast incongruent vs. congruent condition.

Brainstem/cerebellum analysis using SUIT toolbox: Correlational analysis

Using images of parameter estimates in the brainstem/cerebellum as preprocessed with the SUIT toolbox, we could confer the results of the regression analysis at the whole-brain level and based on the ROI analysis. We detected a significant positive correlation with the Stroop interference score (on the right side in Fig. 2 and Supporting Information Fig. S1) in a cluster comprising the left ($x = -2$, $y = -32$, $z = -23$, $t = 4.5$, $P < 0.001$) and right LC ($x = 6$, $y = -28$, $z = -21$, $t = 4.03$, $P < 0.001$; cluster size = 32), but not in the SN/VTA. Furthermore, a number of significant clusters were detected in the left and right cerebellum (Supporting Information Table S6).

Practice-related signal changes in neuronal activation over time

Group analysis of the linear signal decrease yielded significant results in several brain areas of the fronto-cingulo-striatal network, but not in the VTA/SN and LC in the

whole-brain as well as in the ROI analyses (see Fig. 3; Supporting Information Table S3). This activation decline was mainly present in VLPFC, DLPFC, dACC extending to pre-SMA, NAc, ventromedial caudatus, putamen as well as in the left STG, inferior parietal, and occipital cortex ($P < 0.001$; cluster-level FWE corrected). No significant linear BOLD activation increases were detectable.

Brainstem/cerebellum analysis using SUIT toolbox: Practice-related signal changes in neuronal activation over time

Investigating practice-related signal changes in the brainstem/cerebellum as preprocessed with the SUIT toolbox, we could confer the results at the whole-brain level and in the ROI analysis. We did not detect any significant linear BOLD signal changes in the LC and VTA/SN. Instead, a significant linear BOLD signal decrease was detected in the left ($x = -2$, $y = -76$, $z = -21$, $t = 4.44$, $P < 0.001$; cluster size = 45) and two clusters in the right ($x = 44$, $y = -58$, $z = -27$, $t = 4.35$, $P < 0.001$; cluster size = 79), ($x = 18$, $y = -76$, $z = -25$, $t = 4.6$, $P < 0.001$; cluster size = 26) cerebellum.

PPI Analysis

Substantia nigra/ventral tegmental area

A PPI analysis was performed to reveal brain regions interacting with the SN/VTA in the Stroop interference contrast (incongruent > congruent condition). As illustrated in Figure 4 and Supporting Information Table S4, using SN/VTA as seed region, a brain network mainly including NAc, ventral caudate, putamen, thalamus, perigenual ACC, and dACC extending to SMA, insula,

superior parietal lobe, and cerebellum ($P < 0.001$; cluster-level FWE corrected) was found.

Locus coeruleus

Using LC as seed region, differences in the functional connectivity with respect to the interference contrast were primarily observed in VLPFC, DLPFC, dACC/SMA, premotor cortex, occipital cortex, in the superior parietal lobe as well as in cerebellum ($P < 0.001$; cluster-level FWE corrected), which is illustrated in Figure 5 and Supporting Information Table S5.

DISCUSSION

In this study, we demonstrate for the first time that functional activation in the midbrain (SN/VTA) and brainstem (LC) is modulated by different demands of cognitive control and that these regions show distinguishable functional connectivity patterns to specific brain networks.

Substantia Nigra/Ventral Tegmental Area

The study showed that different cognitive demands modulate the functional connectivity between the medial SN/VTA, the nigrostriatal and the mesolimbic dopaminergic systems. This pattern of connectivity is highly consistent with known neuroanatomical projections from DA neurons and recent neuroimaging studies of dopaminergic resting state functional connectivity [Tomasi and Volkow, 2014]. The DA nigrostriatal pathway conveys information to the thalamus and the dorsal striatum, and further to neurocortical regions via direct (striato-nigral) and indirect pathways [Amalric and Koob, 1993]. The mesolimbic dopaminergic system arises from the VTA and the medial part of the SN and has dense projections to the NAc, but also to other limbic regions and the medial PFC, such as the observed functional connectivity to the perigenual ACC.

The concept of cortico-striatal loops is an influential model to comprehend the functional inter-relationships between the neocortex and the striatum [Alexander et al., 1986]. In this model, the so-called “sensorimotor loop” consists of the caudal and lateral aspects of the putamen, and receives input from primary and supplementary motor areas as well as from the somatosensory cortex. The putamen projects to the globus pallidus and SN, which in turn, send projections to the thalamus. Furthermore, thalamic projections to primary and supplementary motor areas close the circuit [Alexander and Crutcher, 1990; Grahn, et al., 2008]. Another loop, the “limbic loop” encompasses the ventromedial striatum, including NAc, and the ventral caudate, which receives input from the orbital and medial PFC [Haber et al., 2000; Kunishio and Haber, 1994]. A very close match between these anatomically and functionally defined loops and present results

are observable in our PPI analysis using SN/VTA as regions of interest.

Thus, it seems reasonable to conclude that the medial SN, dorsal striatum, thalamus, SMA, and dACC are mainly involved in detecting and resolving the “output” motor conflict, selecting the motor response as well as inhibiting prepotent motor responses, which arise when performing the manual version of the Stroop task. The close connection between the VTA, ventral striatum, and perigenual ACC gives rise to the assumption that the activation of this network might be additionally associated with goal-directed motivational processes, such as attributing an incentive value to selected goals [Mannella et al., 2013]. Previous research has demonstrated that the NAc is important for learning processes, which are associated with reward [O’Doherty et al., 2003, 2006]. Moreover, Tomasi and Volkow [2014] showed in an fMRI study that the temporal prediction of responses involved dopaminergic striato-cortical circuits. Interestingly, accurate responses that were rewarding per se activated the NAc stronger than inaccurate ones.

In this study, we found a linear decline of the RTs over time for the incongruent Stroop task condition. This was associated with a linear decrease in BOLD activation of the fronto-cingulo-striatal network, implying the diminished need of cognitive control over time due to adjustment. Similar results were reported in previous studies investigating practice-related effects on brain activation [Koch et al., 2006; Milham et al., 2003]. Furthermore, a linear BOLD activation decline was present in the ventral striatum, suggesting a decline in motivational processes over time. In contrast, despite this linear decline of the anatomically interconnected regions of the fronto-cingulo-striatal circuitry, no significant activation decline was observed in VTA/SN. This indicates a time invariant activation pattern and might be suggestive of an indirect influence on the brain network associated with cognitive control. The nonsignificant correlation with the Stroop interference time might add weight to this assumption.

Locus Coeruleus

The detected functional connectivity of LC during Stroop interference is in accordance with known neuroanatomical projections of NA neurons. The frontal lobe and the cingulate cortex have been shown to contain the highest density of NA fibers of all neocortical areas [Fuxe et al., 1968]. Accordingly, the PPI analysis revealed that the DLPFC and VLPFC, but also the dorsal parietal lobe, visual and motor brain areas are functionally connected with the LC activation pattern, indicating an important role of LC in cognitive conflict resolution. Further support for this notion is provided by the significant correlation between LC activation and Stroop interference time. Interestingly, no significant functional connectivity of LC with striatal regions was found in the PPI analysis.

Tonic and phasic activity modes of LC neurons have been described [Aston-Jones and Bloom, 1981; Aston-Jones and Cohen, 2005]. The LC-NA tonic signal regulates transitions between specific behavioral states, such as sleep or focused attention. The pattern of tonic activity follows the classical Yerkes-Dodson relationship between arousal and performance [Aston-Jones and Cohen, 2005].

Phasic LC activity might provide a temporal attentional filter, which selectively facilitates behavioral responses to task-relevant features and optimizes task-appropriate behavior [Aston-Jones and Cohen, 2005]. Prefrontal and anterior cingulate inputs were assumed to enable the transition between different tonic levels as well as to trigger the LC phasic response [Clayton et al., 2004; Corbetta et al., 2008]. Both excitatory as well as inhibitory influences from the PFC on LC have been described [Sara and Herve-Minvielle, 1995]. With respect to this interaction, Sara and Bouret [2012] stated that the firing of frontal neurons due to an increased cognitive demand “wake up” the LC, which in turn facilitates cortical processing. Thus, LC functioning is supposed to mediate activity and functional integration of the cognitive control network, including the frontal cortex, thalamus and posterior cortical regions, and to modulate dynamic plasticity of cognitive brain systems [Coull et al., 1999].

As described above, Corbetta et al. [2008] hypothesized that signals from the LC influence adaptive state shifts between the ventral and dorsal fronto-parietal networks. Supporting this theory, Hermans et al. [2011] provided strong evidence that noradrenalin is a key neuromodulator of the acute stress response, which is associated with state shifts in specific attentional control related networks.

In agreement with the theory proposed by Corbetta et al. [2008], we observed in the PPI analysis a significant functional connectivity of the LC as modulated by the cognitive control demand with the dorsal fronto-cingulo-parietal network. However, the precise temporal pattern in terms of a causal relationship between LC activity and the reorganization in the task-related dorsal and salience-related ventral fronto-parietal networks needs to be investigated in further studies using superior temporal and spatial resolution.

Summarizing previous results and our findings, we assume that the phasic LC signals facilitate cognitive conflict resolution and optimize behavioral responses to incongruent Stroop items by activating a specific task-related brain network and further by amplifying task-relevant features, as reflected by strong functional connectivity to the occipital, pre-/motor and superior parietal cortices.

Interestingly, whereas a strong linear decrease of BOLD activation was detected in the fronto-cingulo-striatal network as well as in the parietal and occipital regions, we did not observe such a linear decrease in activation regarding the LC. This finding indicates that despite the diminished need of cognitive control over time as reflected

in a significant linear decline of the RTs in the incongruent Stroop task condition, the activation of the LC did not significantly change over the course of the experiment.

The precise location of the LC is an important issue in this study. Previous studies have described seven NA cell groups (A1–A7) in rodents and primates [Dahlstroem and Fuxe, 1964; Schofield and Everitt, 1981], which are situated at the pontine and medullary tegmental level. Nieuwenhuys [1985] suggested that the cell groups A4 and A6 form the LC complex, whereas other authors suggested the cell groups A4–A7 [Pearson et al., 1983]. The LC proper was described as a bilateral, “tube-like,” pigmented nucleus [Fernandes et al., 2012; German et al., 1988]. It begins rostrally in the caudolateral part of the mesencephalic central gray, at the level of the inferior colliculus (A6), and extends caudally to a position in the lateral wall of the fourth ventricle (A4) [German, et al., 1988]. The LC measures ~16 mm long by 2 mm wide by 1.8 mm deep at the central zone [Fernandes, et al., 2012; German, et al., 1988]. The NA cell group A5, which is termed as nucleus subcoeruleus, extends ventrolaterally from the caudal pole of the LC (A4) [Bogerts, 1981]. The cell group A7 is situated in the rostral pons. This cell group connects the rostral part of the LC with the caudal poles of the dopaminergic SN and the VTA [Bogerts, 1981]. The relative ventral and rostral LC activation during the contrast incongruent vs. congruent condition most likely represents the A7 nucleus, whereas the more caudal position of the LC in the regression analysis might represent the nucleus subcoeruleus (A5 cell group).

Furthermore, LC coordinates in this study are in line with reported coordinates of previous fMRI studies. Minzenberg et al. [2008] used modafinil in healthy humans, a pharmacological agent, which increases synaptic NE and DA levels by inhibiting NA and DA transporters. Thereby the authors modulated the activation level of the LC while performing a cognitive control task, similarly to the Stroop task. Modafinil administration was associated with decreased task-independent, tonic LC activity, increased task-related LC and PFC activity, and enhanced LC-PFC functional connectivity.

Bearing in mind the isotropic resolution of 3.4 mm³ and a smoothing kernel of 8 mm used in the study by Minzenberg et al. [2008], the reported MNI coordinates of the LC based on the contrast modafinil challenge vs. placebo were coherent with the present position of LC in the incongruent vs. congruent contrast. In addition, Murphy et al. [2014] showed in a study combining pupillometry and fMRI a significant relationship between activation in the LC and pupil diameter in the resting state condition as well as during performance of an oddball task. Interestingly, the MNI coordinates of the LC during the oddball task overlapped with LC coordinates detected in the regression analysis of this study.

Using tract-tracing experiments in rats, Chandler et al. [2014] recently demonstrated that opposed to the

traditional view the LC exhibits functional differences depending on the terminal fields of LC neurons. The authors observed that LC neurons projecting to PFC in rats are more excitable and display higher spontaneous firing frequencies than those projecting to the motor cortex (2014). Furthermore, this observation implies a potentially differential NA modulation of PFC-dependent executive functions and behavioral outcomes, depending on cortical/subcortical motor circuitry. This finding can potentially explain the slight differences in the LC activation along the rostrocaudal axis found in this study. Comparing the incongruent vs. congruent condition, we observed BOLD signal differences in a more rostral part of the LC complex (corresponding to A7 cell group), whereas the cluster of significant correlation between LC BOLD signal and reaction time differences between incongruent and congruent condition was situated more ventrally in the subceruleus and in the A6. Thus, this observation might be consistent with the notion that given the anatomical heterogeneity of the LC complex in the brainstem and therefore potential varying cortical/subcortical connectivity, different parts of the LC are specifically contributing to distinct subcomponents of cognitive control processes, such as cognitive conflict monitoring/resolution mainly based on the fronto-cingulate circuitry and inhibition of prepotent motor responses (due to the motor version of the employed Stroop task in this study) mainly based on the SMA/premotor/motor cortices. However, this interpretation warrants further studies to elucidate the contribution of specific LC nuclei to different cognitive control processes in more detail.

We did not observe a significant functional connectivity between the LC, SN/VTA, and striatal regions. Nevertheless, NA modulation of cognitive functioning is likely to depend on the cooperation of a distributed network of brain regions, acting together in a functionally integrated way, as observed in the overlapping functional connectivity between VTA/SN and LC with dACC, SMA, and parietal regions. Ventura et al. [2003] analyzed the effects of medial PFC noradrenaline depletion in mice and showed an absence of amphetamine-induced conditioned place preference as well as a reduced amphetamine-induced mesoaccumbens DA release. In different psychiatric disorders such as schizophrenia, major depression, attention-deficit/hyperactivity disorder (ADHD) or obsessive-compulsive disorder, poor inhibition-related processes were assumed to be associated with abnormal monoaminergic neurotransmission [Arnsten and Rubia, 2012; Nigg, 2001]. For example, methylphenidate (MPH) and atomoxetine (ATX) are often administered to treat ADHD in children or adolescents [Hazell et al., 2011]. MPH blocks DA transporters (DAT) in the striatum and noradrenaline transporters mainly in thalamic and frontal regions, enhancing thereby DA and NA neurotransmission [Hannestad et al., 2010; Volkow et al., 1998]. Moeller et al. [2014] found that the consumption of MPH enhanced the

Stroop task performance and modulated BOLD activation in prefrontal cortical areas. ATX also affects both catecholamines in the PFC and NA in the thalamus, LC, cerebellum, and striatum [Bymaster et al., 2002; Gallezot et al., 2011]. Chou et al. [2015] studied the effects of 12-weeks treatment with ATX and MPH in children with ADHD and found improved inhibitory control. In an fMRI-study of Cubillo et al. [2014], the authors found that ATX up-regulated and normalized right DLPFC underactivation in children suffering from ADHD during a working memory task, while MPH up-regulated left VLPFC activation. Furthermore, MPH was found to significantly normalize the fronto-striatal underactivation in ADHD patients during interference inhibition [Rubia et al., 2011]. Thus, ATX and MPH were suggested to enhance fronto-striatal activation leading to increased inhibitory control in patients with ADHD due to an increase of NA and dopaminergic neurotransmission. In addition, similar effects of ATX on response inhibition and fronto-striatal activation as well as connectivity were detected in patients with Parkinson's Disease [Ye et al., 2015], emphasizing the mutual role of NA- and DA-systems in regulating response inhibition. Our results of LC and VTA/SN activation as well as functional connectivity findings are well in line with these studies indicating a crucial role of both DA and NA neurotransmitter systems in inhibitory control.

Thus, the findings of this study may provide an interesting approach to investigate the putatively abnormal interaction between midbrain/brainstem nuclei and the cortical regions in different neurological and psychiatric disorders in the future.

A number of limitations in our study should be noted. The nuclei within brainstem and midbrain are small compared with the cortical regions activated during cognitive control, and are more susceptible to signal distortion and artifacts arising from local tissue interfaces and physiological noise. Therefore, further studies with increased spatial resolution are required to support our findings. In addition, the current study lacks additional behavioral measurements (e.g., pupillometry) which have recently been shown to specifically track LC activity [Joshi et al., 2016]. Moreover, to more precisely define the anatomical position of the LC, an additional acquisition of a high resolution brainstem structural image may be necessary in future studies. For example, using a T1-weighted Turbo Spin Echo (T1-TSE) imaging protocol by Sasaki et al. [2006] and Keren et al. [2009] successfully visualized the LC in the 3T scanner. The T1-TSE sequence allows identification of LC by means of a neuromelanin-sensitive contrast. Recently, Keren et al. [2015] provided a histological validation that the neuromelanin-related LC contrast in the T1 images corresponded to the shape and distribution of LC in post-mortem tissue samples. However, in contrast to structural imaging, functional imaging relies on blood-oxygen-level-dependent (BOLD) contrast as the basic principle for detecting neuronal activation. The spatial accuracy and

extension of the activation maps in specific brain regions, especially in the brainstem are heavily dependent on the vascular effect, which may introduce uncertainty with respect to real neuronal activation site. This might be one reason for the slight difference in the LC position between our (more ventrally located) as well as previous functional studies and the structural neuromelanin-sensitive T1-TSE MRI studies. Thus, to gain more confidence in the definite location of small brain stem nuclei, a combination of sophisticated structural and functional imaging techniques and simultaneous behavioral measurements is needed in the future.

In summary, our study represents the first direct demonstration of the functional integration of the noradrenergic producing LC and dopaminergic nuclei SN/VTA within the cognitive control network in the human brain. Since catecholaminergic neurotransmission is essential to neocortical and subcortical functions, and represents an important target for pharmacotherapy, our novel findings contribute to a comprehensive understanding of the functional organization of the human brain and, in particular, to the broader understanding of the importance of the DA as well as NA systems for executive functions with potentially far-reaching implications for pathophysiological conditions and psychopharmacology.

REFERENCES

- Alexander GE, Crutcher MD (1990): Functional architecture of basal ganglia circuits: neural substrates of parallel processing. *Trends Neurosci* 13:266–271.
- Alexander GE, DeLong MR, Strick PL (1986): Parallel organization of functionally segregated circuits linking basal ganglia and cortex. *Annu Rev Neurosci* 9:357–381.
- Amalric M, Koob GF (1993): Functionally selective neurochemical afferents and efferents of the mesocorticolimbic and nigrostriatal dopamine system. *Prog Brain Res* 99:209–226.
- Arnsten AF, Rubia K (2012): Neurobiological circuits regulating attention, cognitive control, motivation, and emotion: disruptions in neurodevelopmental psychiatric disorders. *J Am Acad Child Adolesc Psychiatry* 51:356–367.
- Ashburner J (2007): A fast diffeomorphic image registration algorithm. *Neuroimage* 38:95–113.
- Aston-Jones G, Bloom FE (1981): Activity of norepinephrine-containing locus coeruleus neurons in behaving rats anticipates fluctuations in the sleep-waking cycle. *J Neurosci* 1:876–886.
- Aston-Jones G, Cohen JD (2005): An integrative theory of locus coeruleus-norepinephrine function: adaptive gain and optimal performance. *Annu Rev Neurosci* 28:403–450.
- Beg MF, Miller MI, Trounev A, Younes L (2005): Computing large deformation metric mappings via geodesic flows of diffeomorphisms. *Int J Comput Vis* 61:139–157.
- Bogerts B (1981): A Brain-Stem Atlas of Catecholaminergic Neurons in Man, Using Melanin as a Natural Marker. *J Comp Neurol* 197:63–80.
- Bolla K, Ernst M, Kiehl K, Mouratidis M, Eldredh D, Contoreggi C, Matochik J, Kurian V, Cadet J, Kimes A, Funderburk F, London E (2004): Prefrontal cortical dysfunction in abstinent cocaine abusers. *J Neuropsychiatry Clin Neurosci* 16:456–464.
- Botvinick MM, Braver TS, Barch DM, Carter CS, Cohen JD (2001): Conflict monitoring and cognitive control. *Psychol Rev* 108:624–652.
- Bouret S, Sara SJ (2005): Network reset: A simplified overarching theory of locus coeruleus noradrenergic function. *Trends Neurosci* 28:574–582.
- Briggs GG, Nebes RD (1975): Patterns of hand preference in a student population. *Cortex* 11:230–238.
- Bymaster FP, Katner JS, Nelson DL, Hemrick-Luecke SK, Threlkeld PG, Heiligenstein JH, Morin SM, Gehlert DR, Perry KW (2002): Atomoxetine increases extracellular levels of norepinephrine and dopamine in prefrontal cortex of rat: A potential mechanism for efficacy in attention deficit/hyperactivity disorder. *Neuropsychopharmacology* 27:699–711.
- Chandler DJ, Gao WJ, Waterhouse BD (2014): Heterogeneous organization of the locus coeruleus projections to prefrontal and motor cortices. *Proc Natl Acad Sci U S A* 111:6816–6821.
- Chou TL, Chia S, Shang CY, Gau SS (2015): Differential therapeutic effects of 12-week treatment of atomoxetine and methylphenidate on drug-naïve children with attention deficit/hyperactivity disorder: A counting Stroop functional MRI study. *Eur Neuropsychopharmacol* 25:2300–2310.
- Clayton EC, Rajkowski J, Cohen JD, Aston-Jones G (2004): Phasic activation of monkey locus coeruleus neurons by simple decisions in a forced-choice task. *J Neurosci* 24:9914–9920.
- Corbetta M, Patel G, Shulman GL (2008): The reorienting system of the human brain: From environment to theory of mind. *Neuron* 58:306–324.
- Coull JT, Buchel C, Friston KJ, Frith CD (1999): Noradrenergically mediated plasticity in a human attentional neuronal network. *Neuroimage* 10:705–715.
- Cubillo A, Smith AB, Barret N, Giampietro V, Brammer M, Simmons A, Rubia K (2014): Drug-specific laterality effects on frontal lobe activation of atomoxetine and methylphenidate in attention deficit hyperactivity disorder boys during working memory. *Psychol Med* 44:633–646.
- Dahlstroem A, Fuxe K (1964): Evidence for the existence of monoamine-containing neurons in the central nervous system. I. Demonstration of Monoamines in the Cell Bodies of Brain Stem Neurons. *Acta Physiol Scand Suppl* 232(SUPPL):1–55.
- Devauges V, Sara SJ (1990): Activation of the noradrenergic system facilitates an attentional shift in the rat. *Behav Brain Res* 39:19–28.
- Diedrichsen J (2006): A spatially unbiased atlas template of the human cerebellum. *Neuroimage* 33:127–138.
- Fernandes P, Regala J, Correia F, Goncalves-Ferreira AJ (2012): The human locus coeruleus 3-D stereotactic anatomy. *SRA* 34:879–885.
- Foote SL, Bloom FE, Aston-Jones G (1983): Nucleus locus coeruleus: New evidence of anatomical and physiological specificity. *Physiol Rev* 63:844–914.
- Fuxe K, Hamberger B, Hokfelt T (1968): Distribution of noradrenergic nerve terminals in cortical areas of the rat. *Brain Res* 8:125–131.
- Gallezot JD, Weinzimmer D, Nabulsi N, Lin SF, Fowles K, Sandiego C, McCarthy TJ, Maguire RP, Carson RE, Ding YS (2011): Evaluation of [(11)C]MREB for assessment of occupancy of norepinephrine transporters: Studies with atomoxetine in non-human primates. *Neuroimage* 56:268–279.
- German DC, Walker BS, Manaye K, Smith WK, Woodward DJ, North AJ (1988): The human locus coeruleus: Computer reconstruction of cellular distribution. *J Neurosci* 8:1776–1788.

- Grahn JA, Parkinson JA, Owen AM (2008): The cognitive functions of the caudate nucleus. *Prog Neurobiol* 86:141–155.
- Haber SN (2003): The primate basal ganglia: parallel and integrative networks. *J Chem Neuroanat* 26:317–330.
- Haber SN, Fudge JL, McFarland NR (2000): Striatonigrostriatal pathways in primates form an ascending spiral from the shell to the dorsolateral striatum. *J Neurosci* 20:2369–2382.
- Hannestad J, Gallezot JD, Planeta-Wilson B, Lin SF, Williams WA, van Dyck CH, Malison RT, Carson RE, Ding YS (2010): Clinically relevant doses of methylphenidate significantly occupy norepinephrine transporters in humans in vivo. *Biol Psychiatry* 68:854–860.
- Hazell PL, Kohn MR, Dickson R, Walton RJ, Granger RE, Wyk GW (2011): Core ADHD symptom improvement with atomoxetine versus methylphenidate: A direct comparison meta-analysis. *J Attention Disord* 15:674–683.
- Hermans EJ, van Marle HJ, Ossewaarde L, Henckens MJ, Qin S, van Kesteren MT, Schoots VC, Cousijn H, Rijpkema M, Oostenveld R, Fernandez G (2011): Stress-related noradrenergic activity prompts large-scale neural network reconfiguration. *Science (New York)* 334:1151–1153.
- Ikemoto S (2007): Dopamine reward circuitry: Two projection systems from the ventral midbrain to the nucleus accumbens-olfactory tubercle complex. *Brain Res Rev* 56:27–78.
- Joshi S, Li Y, Kalwani RM, Gold JJ (2016): Relationships between Pupil Diameter and Neuronal Activity in the Locus Coeruleus, Colliculi, and Cingulate Cortex. *Neuron* 89:221–234.
- Keren NI, Lozar CT, Harris KC, Morgan PS, Eckert MA (2009): In vivo mapping of the human locus coeruleus. *Neuroimage* 47:1261–1267.
- Keren NI, Taheri S, Vazey EM, Morgan PS, Granholm AC, Aston-Jones GS, Eckert MA (2015): Histologic validation of locus coeruleus MRI contrast in post-mortem tissue. *Neuroimage* 113:235–245.
- Koch K, Wagner G, von Consbruch K, Nenadic I, Schultz C, Ehle C, Reichenbach J, Sauer H, Schlosser R (2006): Temporal changes in neural activation during practice of information retrieval from short-term memory: An fMRI study. *Brain Res* 1107:140–150.
- Kunishio K, Haber SN (1994): Primate cingulo-striatal projection: limbic striatal versus sensorimotor striatal input. *J Comp Neurol* 350:337–356.
- Mair RD, Zhang Y, Bailey KR, Toupin MM, Mair RG (2005): Effects of clonidine in the locus coeruleus on prefrontal- and hippocampal-dependent measures of attention and memory in the rat. *Psychopharmacology (Berl)* 181:280–288.
- Mannella F, Gurney K, Baldassarre G (2013): The nucleus accumbens as a nexus between values and goals in goal-directed behavior: A review and a new hypothesis. *Front Behav Neurosci* 7:135.
- Mansouri FA, Tanaka K, Buckley MJ (2009): Conflict-induced behavioural adjustment: A clue to the executive functions of the prefrontal cortex. *Nat Rev Neurosci* 10:141–152.
- Milham MP, Banich MT, Claus ED, Cohen NJ (2003): Practice-related effects demonstrate complementary roles of anterior cingulate and prefrontal cortices in attentional control. *Neuroimage* 18:483–493.
- Miller EK, Cohen JD (2001): An integrative theory of prefrontal cortex function. *Annu Rev Neurosci* 24:167–202.
- Minzenberg MJ, Watrous AJ, Yoon JH, Ursu S, Carter CS (2008): Modanfinil Shifts Human Locus Coeruleus to Low-Tonic, High-Phasic Activity During Functional MRI. *Science (New York)* 322:1700–1702.
- Moeller SJ, Honorio J, Tomasi D, Parvaz MA, Woicik PA, Volkow ND, Goldstein RZ (2014): Methylphenidate enhances executive function and optimizes prefrontal function in both health and cocaine addiction. *Cerebral Cortex (New York)* 24:643–653.
- Murphy PR, O'Connell RG, O'Sullivan M, Robertson IH, Balsters JH (2014): Pupil diameter covaries with BOLD activity in human locus coeruleus. *Hum Brain Mapp* 35:4140–4154.
- Naidich TP, Duvernoy HM, Delman BN, Sorensen AG, Kollias SS, Haacke EM (2009): *Duvernoy's Atlas of the Human Brain Stem and Cerebellum*. Wien: Springer.
- Nieuwenhuys R. (1985): *Chemoarchitecture of the brain*. Berlin: Springer.
- Nigg JT (2001): Is ADHD a disinhibitory disorder? *Psychol Bull* 127:571–598.
- O'Doherty JP, Dayan P, Friston K, Critchley H, Dolan RJ (2003): Temporal difference models and reward-related learning in the human brain. *Neuron* 38:329–337.
- O'Doherty JP, Buchanan TW, Seymour B, Dolan RJ (2006): Predictive neural coding of reward preference involves dissociable responses in human ventral midbrain and ventral striatum. *Neuron* 49:157–166.
- Parent A (1990): Extrinsic connections of the basal ganglia. *Trends Neurosci* 13:254–258.
- Pearson J, Goldstein M, Markey K, Brandeis L (1983): Human Brain-Stem Catecholamine Neuronal Anatomy as Indicated by Immunocytochemistry with Antibodies to Tyrosine-Hydroxylase. *Neuroscience* 8:3–32.
- Raizada RD, Poldrack RA (2008): Challenge-driven attention: Interacting frontal and brainstem systems. *Front Human Neurosci* 1:3.
- Rubia K, Halari R, Cubillo A, Smith AB, Mohammad AM, Brammer M, Taylor E (2011): Methylphenidate normalizes fronto-striatal underactivation during interference inhibition in medication-naïve boys with attention-deficit hyperactivity disorder. *Neuropsychopharmacology* 36:1575–1586.
- Salo R, Ursu S, Buonocore MH, Leamon MH, Carter C (2009): Impaired prefrontal cortical function and disrupted adaptive cognitive control in methamphetamine abusers: A functional magnetic resonance imaging study. *Biol Psychiatry* 65:706–709.
- Sara SJ, Bouret S (2012): Orienting and reorienting: the locus coeruleus mediates cognition through arousal. *Neuron* 76:130–141.
- Sara SJ, Herve-Minvielle A (1995): Inhibitory influence of frontal cortex on locus coeruleus neurons. *Proc Natl Acad Sci U S A* 92:6032–6036.
- Sasaki M, Shibata E, Tohyama K, Takahashi J, Otsuka K, Tsuchiya K, Takahashi S, Ehara S, Terayama Y, Sakai A (2006): Neuromelanin magnetic resonance imaging of locus coeruleus and substantia nigra in Parkinson's disease. *Neuroreport* 17:1215–1218.
- Schofield SPM, Everitt BJ (1981): The organization of catecholamine-containing neurons in the brain of the Rhesus-Monkey (*Macaca-Mulatta*). *J Anat* 132:391–418.
- Sheehan DV, Lecrubier Y, Sheehan KH, Amorim P, Janavs J, Weiller E, Hergueta T, Baker R, Dunbar GC (1998): The Mini-International Neuropsychiatric Interview (M.I.N.I.): the development and validation of a structured diagnostic psychiatric interview for DSM-IV and ICD-10. *J Clin Psychiatry* 59:22–33. quiz 34–57.
- Stroop JR (1935): Studies of interference in serial verbal reactions. *J Exp Psychol* 18:643–662.
- Tait DS, Brown VJ, Farovik A, Theobald DE, Dalley JW, Robbins TW (2007): Lesions of the dorsal noradrenergic bundle

- impair attentional set-shifting in the rat. *Eur J Neurosci* 25: 3719–3724.
- Tomasi D, Volkow ND (2014): Functional connectivity of substantia nigra and ventral tegmental area: Maturation during adolescence and effects of ADHD. *Cerebral cortex (New York)* 24: 935–944.
- Ungerstedt U (1971): Stereotaxic mapping of the monoamine pathways in the rat brain. *Acta Physiol Scand Suppl* 367:1–48.
- Ventura R, Cabib S, Alcaro A, Orsini C, Puglisi-Allegra S (2003): Norepinephrine in the prefrontal cortex is critical for amphetamine-induced reward and mesoaccumbens dopamine release. *J Neurosci* 23:1879–1885.
- Volkow ND, Wang GJ, Fowler JS, Gatley SJ, Logan J, Ding YS, Hitzemann R, Pappas N (1998): Dopamine transporter occupancies in the human brain induced by therapeutic doses of oral methylphenidate. *Am J Psychiatry* 155:1325–1331.
- Wagner G, De la Cruz F, Schachtzabel C, Gullmar D, Schultz CC, Schlosser RG, Bär KJ, Koch K (2015): Structural and functional dysconnectivity of the fronto-thalamic system in schizophrenia: A DCM-DTI study. *Cortex* 66:35–45.
- Woo CW, Krishnan A, Wager TD (2014): Cluster-extent based thresholding in fMRI analyses: pitfalls and recommendations. *Neuroimage* 91:412–419.
- Ye Z, Altena E, Nombela C, Housden CR, Maxwell H, Rittman T, Huddleston C, Rae CL, Regenthal R, Sahakian BJ, Barker RA, Robbins TW, Rowe JB (2015): Improving Response Inhibition in Parkinson's Disease with Atomoxetine. *Biol Psychiatry* 77: 740–748.



RESEARCH ARTICLE

Activation of brainstem and midbrain nuclei during cognitive control in medicated patients with schizophrenia

Stefanie Köhler | Gerd Wagner | Karl-Jürgen Bär

Psychiatric Brain and Body Research Group
Jena, Department of Psychiatry and
Psychotherapy, University Hospital Jena, Jena,
Germany

Correspondence

K.-J. Bär, Psychiatric Brain and Body Research
Group Jena, Department of Psychiatry and
Psychotherapy, University Hospital,
Philosophenweg 3, 07743 Jena, Germany.
Email: karl-juergen.baer@med.uni-jena.de

Abstract

Evidence suggests that cognitive control functions as well as the underlying brain network, anchored by the prefrontal cortex (PFC) and the dorsal anterior cingulate cortex (dACC), are dysfunctional in schizophrenia. Catecholamine producing midbrain and brainstem nuclei are densely connected with the PFC and dACC and exert profound contributions to cognitive control processes. Dysfunctions within the underlying neurotransmitter systems are considered to play a central role in the occurrence of various symptoms of schizophrenia. We sought to investigate the putatively abnormal activation pattern of the dopaminergic midbrain nuclei, that is, ventral tegmental area (VTA) and substantia nigra as well as that of the noradrenergic locus coeruleus (LC) in patients with schizophrenia during cognitive control. A total of 28 medicated patients and 27 healthy controls were investigated with the manual version of the Stroop task using event-related fMRI. The main finding was a reduced BOLD activation in the VTA during both Stroop task conditions in patients in comparison to controls, which correlated significantly with the degree of negative symptoms. We further detected a comparable LC activation in patients and healthy controls. However, in controls LC activation was significantly correlated with the Stroop interference time, which was not observed in patients. The finding of reduced VTA activation in schizophrenia patients lends further support to the assumed dysfunction of the DA system in schizophrenia. In addition, despite comparable LC activation, the nonsignificant correlation with the Stroop interference time might indicate altered LC functioning in schizophrenia and, thus, needs further investigations.

KEYWORDS

brainstem, cognitive demand, fMRI, schizophrenia, ventral tegmental area

1 | INTRODUCTION

Schizophrenia is a severe psychiatric disorder characterized by a multitude of symptoms affecting a variety of emotional and cognitive domains. Some symptoms have been linked to specific brain regions and networks (Goghari, Sponheim, & MacDonald 3rd., 2010).

There is growing evidence for abnormal cognitive task activation (Callicott et al., 2000; Koch et al., 2010; Schlosser et al., 2008; Wagner et al., 2013) in the prefrontal cortex (PFC), thalamus, striatum, and cerebellum in schizophrenia as well as for abnormal functional and effective connectivity between these regions (Sheffield & Barch, 2016; Wagner et al., 2015; Wang et al., 2014). These functional connectivity alterations

were often related to deficits in multiple cognitive domains, for example, executive functions (Repovs, Csemansky, & Barch, 2011; Su et al., 2013). Accordingly, the concept of schizophrenia as a disorder characterized by a disconnection within relevant parts of this network is gaining increasing acceptance (Andreasen, 1999).

Dopaminergic (DA) midbrain nuclei, that is, the ventral tegmental area (VTA) and substantia nigra (SN) and noradrenergic brainstem nuclei, situated in the locus coeruleus (LC), project across multiple cortical and subcortical regions, and exert profound contributions to a variety of cognitive, emotional, and behavioral processes (Aston-Jones & Waterhouse, 2016; Haber & Knutson, 2010).

In schizophrenia, abnormal dopaminergic neurotransmission was postulated based on the antipsychotic effect of conventional antipsychotic drugs and on the observation, that DA-transmission stimulating

Gerd Wagner and Karl-Jürgen Bär contributed equally.

substances induce schizophrenia-like symptoms (Howes & Kapur, 2009).

A dysfunction of the DA system is considered to play a central role in the occurrence of various symptoms of schizophrenia (Artiges et al., 2017). Regarding the cognitive deficits, Tanaka (2006) suggested that impaired working memory in schizophrenia is mainly due to abnormal mesocortical DA modulation. Slifstein et al. (2015) demonstrated using PET and an amphetamine paradigm a blunted dopamine release in the DLPFC and VTA/SN in schizophrenic patients. Dopamine release in the DLPFC was significantly related to fMRI activation in this region during a working memory task.

Neuromelanin-sensitive structural MRI studies detected abnormal signals in the VTA (Yamashita et al., 2016) and SN (Watanabe et al., 2014) of medicated patients with schizophrenia. These observations indicate the presence of altered DA products in the DA-synthesizing nuclei supporting the DA hypothesis of schizophrenia.

To date, very few studies investigated functional activation patterns in the VTA of patients with schizophrenia. For instance, Yoon et al. used fMRI and investigated medicated (2013) as well as antipsychotic-medication-naïve first-episode patients with schizophrenia (2014) and detected in both studies a hyperactive SN. This indicates an antipsychotic independent altered SN activation in schizophrenia during task performance. In another study, Rausch et al. (2014) detected reduced activation in the ventral striatum and VTA in medicated patients during probabilistic decision-making. However, the antidopaminergic activity of antipsychotic drugs was not correlated with the VTA activation.

With regard to the noradrenergic LC, Aston-Jones and Cohen (2005) emphasized its specific role in cognitive functions by increasing the gain of particular task-associated brain networks (Sara & Bouret, 2012). Corbetta, Patel, and Shulman (2008) have specifically linked the LC-NA system to attention set shifting and cognitive control.

Given the important role of the noradrenergic system in cognitive functions, it is surprising that the structure and function of the LC was rarely investigated in schizophrenia. Friedman, Adler, and Davis (1999) concluded that abnormal NA system functioning might be involved in the pathophysiology of schizophrenia, particularly in the manifestation of cognitive impairments. In addition, the NA hypothesis of schizophrenia was proposed. It suggests the presence of hypovigilant and hypervigilant states of the LC-NA system, with the former being associated with impaired cognitive functioning (Yamamoto & Hornykiewicz, 2004).

Fitzgerald (2014) provided some evidence in his review that abnormal NA signaling may play a prominent role in a specific subtype of schizophrenia, for example, paranoid subtype. However, to our knowledge, there is no published fMRI study, which investigated LC functioning in schizophrenia. The few neuromelanin-sensitive structural MRI studies reported negative results (Shibata et al., 2008; Watanabe et al., 2014).

In a recent study of our group (Köhler, Bär, & Wagner, 2016), we explicitly investigated functional activation patterns of the VTA and LC in healthy volunteers during the Stroop task, measuring cognitive control. We observed significant BOLD activation of both the VTA/SN and LC during the Stroop interference condition and a significant functional connectivity between VTA/SN and the nigrostriatal/

mesolimbic dopaminergic system as well as between LC and the dorsolateral/ventrolateral PFC. Moreover, we found a linear decrease in BOLD activation in the fronto-cingulo-striatal network, but not in the VTA/SN and LC, which implies the diminished need of cognitive control over time (see also Koch et al., 2006; Milham et al., 2003). Therefore, in light of previous findings and the relevance of these neurotransmitter systems for schizophrenia, the aim of the present study was to specifically investigate the functional activation patterns and dynamics during the Stroop task in the midbrain/brainstem nuclei in patients with schizophrenia using fMRI. We hypothesized an abnormal activation pattern of the dopaminergic VTA and the SN in patients with schizophrenia relative to healthy controls. Furthermore, given the important role of the LC-NA system in cognitive functioning (Arnsten & Rubia, 2012; Aston-Jones & Waterhouse, 2016) and the pronounced cognitive deficits in schizophrenia (Barch & Sheffield, 2014) as well as based on the findings of our recent study (Köhler, Bär, & Wagner, 2016), we additionally expected to find an abnormal activation pattern in the LC in patients with schizophrenia relative to healthy controls.

2 | MATERIALS AND METHODS

2.1 | Subjects

A total of 29 patients (age $M = 33.1$ years; $SD = 8.02$ years; range: 20–51 years; 10 females) meeting the DSM-IV criteria for schizophrenia were recruited from the inpatient service of the Department of Psychiatry and Psychotherapy of the University Hospital Jena. They were matched for age and gender with 28 healthy subjects (age $M = 33.14$ years; $SD = 8.46$ years; range: 22–56 years; 10 females), who were recruited from the local community. Subjects with past or current neurological or psychiatric diseases according to M.I.N.I (Sheehan et al., 1998) and/or first-degree relatives with Axis I psychiatric disorders were excluded from the study.

All patients received second generation antipsychotics (see Supporting Information Table S2). The antipsychotic treatment was quantified using chlorpromazine (CPZ) equivalents (Andreasen, Pressler, Nopoulos, Miller, & Ho, 2010). The mean CPZ equivalent was 259.1 mg/day, indicating intermediate dose ranges. Four patients were additionally treated with an SSRI. The patients' psychopathological status was assessed using the Scales of Assessment of Positive and Negative Symptoms (SAPS and SANS) and the Positive and Negative Syndrome Scale (PANSS). Patients' scores were $M = 42.92$ ($SD = 19.78$) on SANS and $M = 34.5$ ($SD = 31.5$) on SAPS. The mean age at onset of schizophrenia was 23.2 years ($SD = 8.0$). On average, patients had five episodes (range: 1–21). All subjects were German native speakers, right-handed according to the modified version of Annett's Handedness Inventory (Briggs & Nebes, 1975) and provided written informed consent prior to participating in the study. The study protocol was approved by the Ethics Committee of the University of Jena. All subjects were paid 8 Euro per hour for their participation.

2.2 | Experimental paradigm

The manual version of the Stroop task was applied (Wagner et al., 2006). In detail, the Stroop task was presented in an even-related design and consisted of two conditions: a congruent and an incongruent condition. In the congruent condition, color words were presented in the color denoted by the corresponding word (e.g., the word "red" shown in red); in the incongruent condition, color words were displayed in one of three colors not denoted by the word (e.g., the word "green" shown in red). This target stimulus was presented in the center of the display screen. Two possible answers (color words in black type) were presented below it (in the lower visual field) to minimize contextual memory demand. The subjects had to indicate the type color by pressing one of two buttons (with index or middle finger), which corresponded spatially to both possible answers. Correct answers were counterbalanced on the right and left sides of the display. 18 congruent stimuli and 18 incongruent combinations of four color words "red," "green," "yellow," and "blue" written in the German language and corresponding colors were presented in a pseudorandom sequence. No colors were repeated consecutively to avoid positive priming effects. Stimulus presentation time was 1,500 ms with an intertrial interval (ITI) of 10.5 s to allow the hemodynamic response to return to baseline. A fixation cross was shown on a blank screen during the ITI, which was defined as a resting baseline condition. Additionally, we introduced a temporal jitter to enhance the temporal resolution. The presentation of the stimuli was varied relative to the onset of a scan in 12 steps for 225 ms. This jitter was shifted over the repetition time (TR) three times. For the present study, we adopted the Stroop task, which uses button press response instead of vocalization (Zysset, Müller, Lohmann, & von Cramon, 2001). This particular paradigm design enabled a better control of performance in comparison to a vocal answer and minimized movement related artifacts associated with speaking from the inside of a scanner. The Stroop task was implemented using Presentation software (<http://nbs.neuro-bs.com/>) running on a PC which was connected to a video projector. The visual stimuli were projected on to a transparent screen inside of the scanner tunnel, which could be viewed by the subject through a mirror system mounted on the top of the MRI head coil. The subjects' responses were registered by an MRI-compatible fiber optic response device (Lightwave Medical Industries) with two buttons on a keypad for the right hand. Prior to the fMRI measurement all subjects practiced the Stroop task outside of the scanner.

2.3 | MRI parameters

Functional data were collected on a 3 T Siemens TIM Trio whole body system (Siemens, Erlangen, Germany) equipped with a 20-element receive-only head matrix coil. T_2^* -weighted images were obtained an ascending sequential slice order using a gradient-echo EPI sequence (TR = 2,700 ms, TE = 30 ms, flip angle = 90°) with 48 contiguous transverse slices of 2.7 mm thickness and with in-plane resolution of $2.67 \times 2.67 \text{ mm}^2$. A series of 220 whole-brain volume sets were acquired in one session. High-resolution anatomical T1-weighted images (MP-RAGE) were obtained with an isotropic resolution of $1 \times 1 \times 1 \text{ mm}^3$.

2.4 | Univariate functional data analyses

For image processing and statistical analyses, we used the SPM12 software (<http://www.fil.ion.ucl.ac.uk/spm>). Data preprocessing and single-subject level analyses were identical to that in our previous study (Wagner et al., 2015). After standard preprocessing steps, the whole-brain data were smoothed with a Gaussian filter of 6 mm FWHM and were high-pass filtered (128 s) and corrected for serial correlations.

We also tested for significant differences in the motion parameters by means of two parameters suggested in the study of Van Dijk et al. (2012). We compared the "Mean Motion" parameter, which represents the mean absolute displacement of each brain volume as compared to the previous volume and which was estimated from the translation parameters in the x, y, and z directions. The "Mean Motion" for the healthy control group was $M = 0.08 \text{ mm}$ ($SD = 0.05$) and for the schizophrenia group $M = 0.13 \text{ mm}$ ($SD = 0.13$). The between-group difference in this motion parameter was not significant ($p = .09$). We also tested for the significance of the difference in the mean scan-to-scan displacement in 3D space which was computed as the root-mean-square (RMS) of the translation parameters (displacement = square root [$x^2 + y^2 + z^2$]). The between-group difference in this motion parameter was also not significant ($M_{HC} = 0.43 \text{ mm}$ [$SD = 0.31$] vs. $M_{SZ} = 0.54 \text{ mm}$ [$SD = 0.70$], $p = .43$).

Subsequently, data were analyzed voxel-wise within the general linear model (GLM) to calculate statistical parametric maps of t statistics for condition-specific effects. A fixed-effects model at a single-subject level was set up to create images of parameter estimates from correct congruent and incongruent trials only as compared to the resting baseline condition. Individual movement parameters as well as the incorrect responses were included in this model as covariates of no interest. Subsequently, individual contrast images, that is, congruent vs. resting baseline condition as well as incongruent vs. resting baseline condition, were then entered into a second-level analysis. For the second-level group comparison we set up an ANOVA design with a between-subjects factor GROUP (patients vs. healthy controls) and a within-subjects factor TASK (congruent and incongruent condition). For the whole-brain analyses, the statistical comparisons were thresholded on the voxel-level at $p < .001$ (uncorrected) and $p < .05$ FDR corrected at the cluster-level taking into account the recent publication of Eklund, Nichols, and Knutsson (2016).

2.5 | fMRI analysis of brainstem/cerebellum using SUIT toolbox

To improve the normalization procedure regarding the brainstem, the cropped brainstem/cerebellum data were normalized using a DARTEL engine to the spatially unbiased infratentorial template (SUIT toolbox; Diedrichsen, 2006). We checked the normalization quality of the normalized images by creating a video of the concatenated images, and observed a very good alignment between subject-specific normalized images. Subsequently, we smoothed the data with a Gaussian filter of 4 mm FWHM. The SUIT toolbox provides a new high-resolution atlas template of the human brainstem and cerebellum, based on the anatomy of 20 young healthy individuals. After high-pass filtering and

correction for serial correlations, a fixed-effects model (the same as at the whole-brain level) at the single-subject level was set-up with pre-processed functional brainstem/cerebellum images to create images of parameter estimates for the subsequent random-effects group analyses (RFX).

For the statistical comparison (ANOVA) based on our initial hypotheses, that is, regarding the activation differences in the VTA/SN and LC between patients and controls, we used the small volume correction (SVC) method to account for the small size of the brainstem/mid-brain nuclei. The VTA/SN and LC were a priori anatomically defined as region-of-interests (ROIs). To obtain the anatomically most precise ROIs, the VTA was manually traced based on the available atlases of the human brainstem (Naidich et al., 2009) as reported in our previous study (Bär et al., 2016). The boundaries of the VTA were defined laterally adjacent to the substantia nigra, and medially adjacent to the interpeduncular fossa. The SN was defined by means of the WFU Pickatlas (<http://fmri.wfubmc.edu/software/pickatlas>). VTA and SN were combined to one mask image. Regarding the LC-ROI, we used the LC mask image in the MNI coordinate space based on Keren, Lozar, Harris, Morgan, and Eckert (2009), which represents the extent of peak LC signal distribution, obtained from a sample of 44 healthy adults using high-resolution T1-weighted Turbo Spin Echo MRI. The statistical significance was set to $p < .05$, FWE voxel-level corrected.

2.5.1 | Practice-related signal changes in neural activation

In order to examine group differences in the BOLD signal course across time, we conducted a parametric modulation analysis, which modulates the amplitude of the predicted HRF. Based on the behavioral data, we modeled the linear signal decrease for the incongruent Stroop condition. We focused on the incongruent condition, because we expected to find the largest changes in neural activation due to decreasing demand in cognitive control over the course of the experiment. The contrast images derived from the single-subject analyses were entered into the group-level one-sample *t*-tests, which were thresholded on the voxel-level at $p < .001$ (uncorrected) and FDR corrected at the cluster-level at the whole-brain level. For the brainstem/cerebellum analysis the small volume correction (SVC) approach was used.

2.6 | Correlational analysis

Using SPSS Statistics V22, we conducted Pearson's correlation analyses between parameter estimates from the masked and unmasked LC as well as VTA/SN, which were extracted and averaged from all voxels within the significant cluster, and behavioral performance scores, antipsychotics, as well as the severity of positive/negative symptoms and the total score of the PANSS. To account for the problem of multiple comparisons, we adjusted the statistical significance level using the false discovery rate (FDR) approach.

2.7 | Behavioral data analysis

The behavioral analyses were performed by means of SPSS Statistics V22 and ANOVA design. Potential differences in the response accuracy were analyzed using the Wilcoxon signed-rank test. Practice-related

changes in response times were examined by means of linear regression analysis.

3 | RESULTS

3.1 | Behavioral performance

One "outlier" control subject was removed from the statistical analysis due to the average reaction times deviating more than 4 standard deviations (SD) from the group mean. One patient was also removed due to missing responses in the incongruent Stroop condition. The final ANOVA analysis revealed a significant main effect of TASK ($F[1, 53] = 78.1, p < .001$) and of GROUP ($F[1, 53] = 5.15, p < .05$), indicating slower RTs in both conditions in schizophrenia patients. The GROUP \times TASK interaction was not significant ($F[1, 53] = 0.66, p = n.s.$).

Patients and controls obtained high levels of accuracy in both conditions (HC_{congruent} = 99%, HC_{incongruent} = 92%; SZ_{congruent} = 93%, SZ_{incongruent} = 86%). Using the nonparametric Mann-Whitney test, no significant accuracy differences between groups were found. Focusing on the cognitive control condition, the linear regression analysis revealed a significant linear decrease in RTs in patients ($R^2 = .27, F = 5.88, p < .05$), but not in healthy controls ($R^2 = .14, F = 2.65, p = n.s.$). The quadratic regression analysis was also significant and explained more variance than the linear one in patients ($R^2 = .33, F = 3.6, p = .05$), but not in controls.

3.2 | fMRI analyses

3.2.1 | Main effect of task

Comparing the incongruent with the congruent Stroop task condition in patients and controls together, we found increased, mainly left lateralized BOLD activations within the cognitive control network, that is, dACC, VLPFC, DLPFC, and thalamus, in the dorsal and ventral striatum, in the premotor and posterior parietal cortex as well as in the VTA and LC (Figure 1, Supporting Information Table S1; voxel-level: $p < .001$ uncorrected; cluster-level $p < .05$, FDR corrected).

Using the SUIIT preprocessed brainstem/cerebellum functional images and the LC as well as VTA/SN as anatomical mask images (SVC), a significantly increased BOLD activation was detected comparing the incongruent with the congruent condition in the right LC ($x = 8, y = -38, z = -33, t = 4.9, \text{cluster size} = 5, p < .05, \text{FWE voxel-level corr.}$; Figure 2). Additionally, the unmasked results are provided in the Supporting Information (see Figure S1-A).

3.2.2 | Main effect of group

Comparing healthy controls with patients, we found decreased fMRI activations in patients with schizophrenia, especially in the cognitive control network (Figure 1, Table 1; voxel-level: $p < .001$ uncorrected; cluster-level $p < .05$, FDR corrected).

Using the SUIIT preprocessed brainstem/cerebellum functional images and the LC as well as VTA/SN as anatomical mask images (SVC), a significantly decreased BOLD signal in patients relative to controls was detected in the VTA ($x = 2, y = -16, z = -11, t = 3.75$,

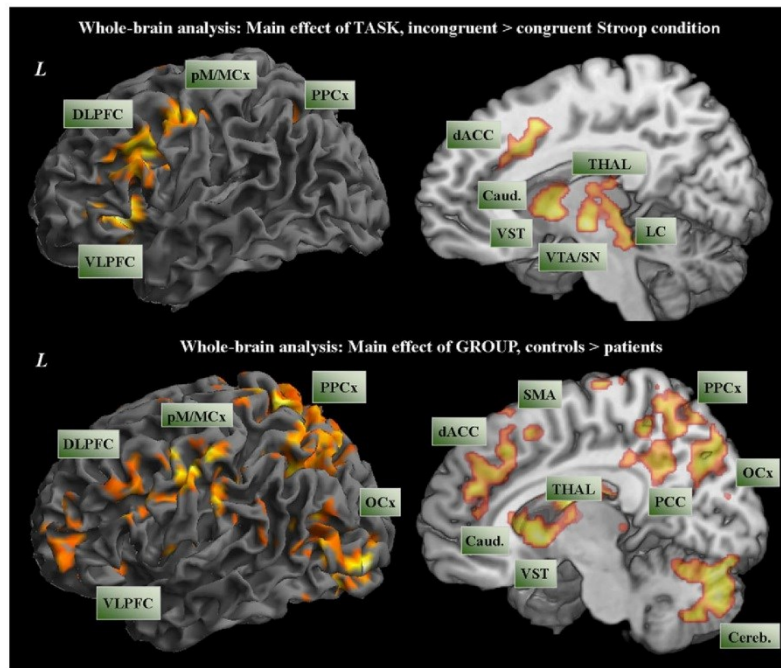


FIGURE 1 Whole-brain fMRI analysis: In the upper half of the figure the main effect of task (post hoc *t* test), that is, incongruent versus congruent Stroop task condition in the total group is illustrated (voxel-level $p < .001$ uncorr., cluster-level, $p < .05$, FDR corr.); in the lower half of the figure the main effect of group (post hoc *t* test), that is, healthy controls versus patients with schizophrenia is illustrated (voxel-level $p < .001$ uncorr., cluster-level, $p < .05$, FDR corr.). DLPFC = dorsolateral prefrontal cortex; VLPFC = ventrolateral prefrontal cortex; dACC = dorsal anterior cingulate cortex; PCC = posterior cingulate cortex; pM/MCx = premotor cortex/motor cortex; SMA = supplementary motor area; PPCx = posterior parietal cortex; OCx = occipital cortex; THAL = thalamus; Caud. = caudate nucleus; VST = ventral striatum; VTA/SN = ventral tegmental area/substantia nigra pars compacta; LC = locus coeruleus; Cereb. = cerebellum

cluster size = 10, $p < .05$, FWE voxel-level corr.; Figure 3). Additionally, the unmasked data are provided in the Supporting Information (see Figure S1-B).

3.2.3 | Group \times task interaction

We did not detect any significant voxels in the GROUP \times TASK interaction at the chosen threshold.

3.2.4 | Correlational analyses

We performed 16 correlations between estimates from the LC, VTA/SN, and behavioral performance scores, antipsychotic medication, as well as the severity of positive/negative symptoms (SAPS/SANS) and the total score of the PANSS. A significant positive correlation between parameter estimates from the LC in the interference (incongruent vs. congruent) condition and the Stroop interference time was observed in control subjects ($r = .57$, $p = .002$) but not in patients ($r = .00$, $p = \text{n.s.}$; see Figure 2). These correlation coefficients were significantly different from each other ($z = 2.27$, $p = .02$). We additionally tested for the effect of motion on the correlation between LC and Stroop interference time using a partial correlation analysis. We still found a significant correlation between parameter

estimates from the LC and the interference time in healthy controls, that is, "Mean Motion": $r = .568$; $p = .002$; mean scan-to-scan displacement in 3D space: $r = .581$; $p = .002$, but not in patients, that is, "Mean Motion": $r = .058$, $p = .776$; mean scan-to-scan displacement in 3D space: $r = .084$, $p = .678$.

Correlating VTA BOLD signal in the interference condition with clinical parameters, a significant negative association was found with the degree of negative symptoms (SANS; $r = -.43$, $p = .03$; see Figure 3). There was no significant correlation between parameter estimates from the VTA cluster and the degree of positive symptoms (SAPS).

Moreover, parameter estimates from the VTA and LC did not significantly correlate with the dose of antipsychotics, as quantified by chlorpromazine equivalents.

3.2.5 | Practice-related signal changes in neural activation

A significant BOLD signal decline in the incongruent condition was mainly detected in healthy subjects in the fronto-cingulo-striatal network (Figure 4, Table 2). In patients, a significant activation decline was detected in the left VLPFC, left insula and in the supplementary motor cortex (SMA) (Figure 4; Table 2).

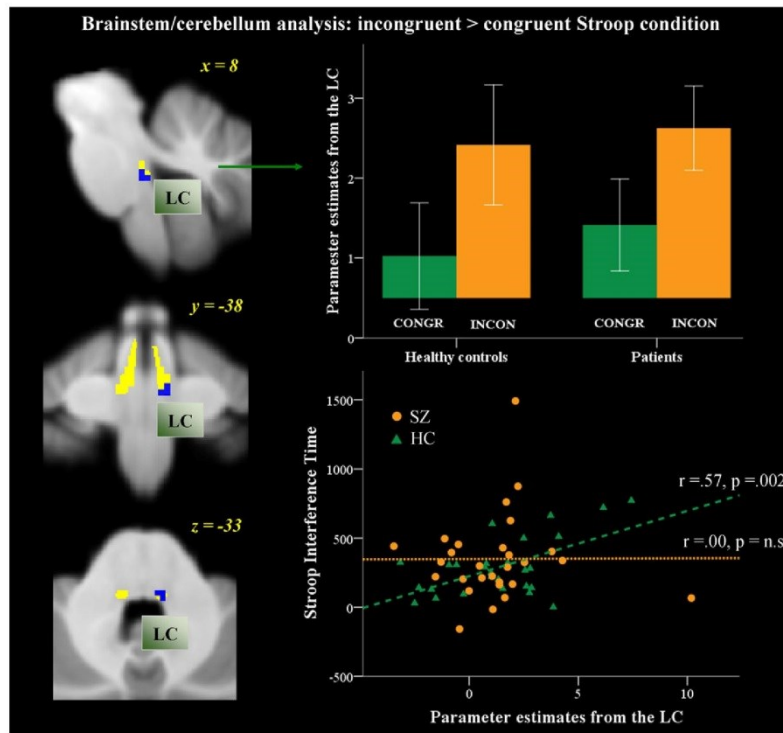


FIGURE 2 Brainstem/cerebellum fMRI analysis: On the left side of the figure the main effect of task (post hoc t test), that is, incongruent versus congruent Stroop task condition in the total group is illustrated (voxel-level $p < .05$ FWE small volume corrected and contrasted with the LC-mask based on Keren et al., 2009, yellow). The bar graph in the right upper corner depicts the parameter estimates from the LC for both Stroop task conditions as well as for patients and controls. In the right lower corner, the scatterplot illustrates the correlation between parameter estimates as extracted from the LC cluster (averaged over significant voxels) in the interference Stroop task condition and Stroop interference time (in ms) in patients and healthy controls. LC = locus coeruleus; CONGR = congruent Stroop task condition; INCON = incongruent condition; SZ = patients with schizophrenia; HC = healthy controls

We especially focused on the incongruent condition, because we expected to find the largest changes in neural activation due to decreasing demand in cognitive control over the course of the experiment. However, for the sake of completeness, results regarding the congruent condition are also reported in Table S3, Supporting Information.

Furthermore, a significant group difference was detected in practice-related signal changes over conditions (HC IC & CC vs. SZ IC & CC) at the whole-brain level with healthy controls showing a stronger BOLD activation decline in the occipital cortex compared to patients (Figure 4, Table 2). However, no significant group differences in the activation decline or increase in the LC and in the VTA/SN were observed.

4 | DISCUSSION

In accordance with our first hypothesis, a reduced activation pattern was found in the VTA in patients with schizophrenia during the

Stroop task, which negatively correlated with the degree of negative symptoms in schizophrenia. A comparable LC activation was observed in patients and controls and did not imply an abnormal LC functioning in patients. However, the finding of the lack of a significant association between the Stroop interference time and LC activation in patients might indicate an abnormally working LC-noradrenergic (NA) system.

4.1 | Dopaminergic VTA

The finding of reduced VTA activation in patients with schizophrenia lends further support to the dopamine hypothesis of schizophrenia (Howes et al., 2009). Despite the relevance of the dopaminergic system in schizophrenia, only few neuroimaging studies investigated the midbrain dopaminergic nuclei in schizophrenia. In two fMRI studies applying tasks designed to tap into executive functions, a hyperactive substantia nigra was detected during a working-memory task in medicated patients (Yoon et al., 2013) and, during CPT, in antipsychotic-naïve (Yoon et al., 2014) patients with schizophrenia going along with

TABLE 1 Univariate functional whole-brain data analysis: Main effect of GROUP (HC > SZ)

Region of activation	Right/left	Brodmann's area	Cluster size	MNI coordinate			T value
				x	y	z	
Medial frontal gyrus	R	9	1,631	2	44	22	5.42
Anterior cingulate gyrus	L	32		-2	18	36	5.38
Supplementary motor area	R	6		4	16	50	4.71
Middle frontal gyrus	R	10	379	32	56	4	5.30
Superior frontal gyrus	R	10		24	58	14	3.73
Middle frontal gyrus	R	6/8	1,212	38	4	58	5.24
Precentral gyrus	R	6		50	0	50	5.12
Inferior frontal gyrus	L	47	170	-40	24	-10	4.70
Cuneus	R	18	198	18	-78	16	4.52
Occipital cortex	R	18		32	-92	12	4.19
Cerebellum	L		25,205	-2	-80	-20	7.00
Caudate nucleus	R			22	-12	30	6.68
Nucleus Accumbens	L/R			6	10	-2	5.91
Supramarginal gyrus	L	40		-34	-38	30	6.59
Transverse temporal gyrus	L	42	220	-58	-12	10	6.22
Postcentral gyrus	L	43		-48	-14	16	4.15

Maxima of regions showing significant BOLD activation differences when comparing healthy controls vs. patients with schizophrenia at the whole-brain level (voxel-level $p < .001$ uncorr., cluster-level, $p < .05$, FDR corr.).

prefrontal and striatal hypoactivation. In both studies, patients were slower and less accurate compared to controls. The discrepancy in the midbrain activation between these two studies and our study could be due to several factors including the symptoms heterogeneity, antipsychotic treatment, and methodological differences. In accordance with the present findings, Cuervo-Lombard et al. (2012) demonstrated decreased fMRI activation in the VTA as well as in the fronto-cingulate network in patients with schizophrenia during an autobiographical memory retrieval task. Similarly, Rausch et al. (2014) detected reduced BOLD signal in the ventral striatum and VTA in medicated patients during probabilistic decision-making.

Furthermore, in our previous study we observed, in accordance with present results, decreased neural activation in the cortico-cerebellar-thalamic-cortical circuitry (CCTCC) in patients during execution of the same Stroop paradigm, while patients were significantly slower and less accurate than healthy controls (Wagner et al., 2015). Thus, similar performance accuracy between patients and controls in the current study makes an association with the reduced activation pattern in the CCTCC rather unlikely. Interestingly, studies investigating cognitive control processes in subjects with abnormal DA transmission due to cocaine or methamphetamine abuse also reported reduced regional cerebral blood flow (rCBF) or reduced BOLD activation in the fronto-cingulate network during the modified Stroop task (Bolla et al., 2004; Salo et al., 2009). Drug abusers did not show an impaired performance either. One supposed function of dopamine, for example, in the ACC or PFC, is modulation of high-frequency neural synchronization optimizing information processing during cognitive tasks (Furth et al., 2004). We assume that observed marked aberrant activation in the cortical networks modulated by the VTA-DA system and involved in specific executive processes, might be explained by a lack of coordinated activation within task-specific neural networks as a consequence of a disruption in

synchronized activity in schizophrenia (Uhlhaas & Singer, 2010). This might lead to prolonged response times on the behavioral level, as observed in the present investigation, but not necessarily to incorrect responses.

4.1.1 | Correlation between VTA and negative symptoms

A significant negative correlation was found between the VTA BOLD signal and the degree of negative symptoms in patients. Whereas positive symptoms of schizophrenia, that is, hallucinations and delusions, are thought to result from disturbances along the nigrostriatal pathway resulting in a hyperdopaminergic state (Howes et al., 2009), the negative symptoms of schizophrenia, that is, cognitive deficits, anhedonia, amotivation, and blunted affect, might be related to abnormal dopaminergic neurotransmission along the mesolimbic and mesocortical pathways (Toda & Abi-Dargham, 2007).

The VTA and NAc dopamine neurons are most commonly associated with reward anticipation and detection (Ikemoto, 2007). For example, reduced ventral striatal activation to reward-indicating cues was inversely correlated with the severity of negative symptoms in patients with schizophrenia (Juckel et al., 2006). VTA projection to the medial prefrontal cortex and amygdala/hippocampus are also supposed to be involved in reward-guided behavior and motivation (Haber & Knutson, 2010). Thus, even if we did not apply a classical reward task, the observed significant correlation points toward an association between VTA activation and abnormal goal-directed motivational processes in schizophrenia.

Another important question in the present study is whether the observed decreased BOLD signal in the VTA is an indicator of an abnormal dopaminergic transmission in SZ.

There is some evidence to support this notion. In a combined fMRI-PET study, Schott et al. (2008) demonstrated that the VTA BOLD responses to reward-predicting stimuli were positively

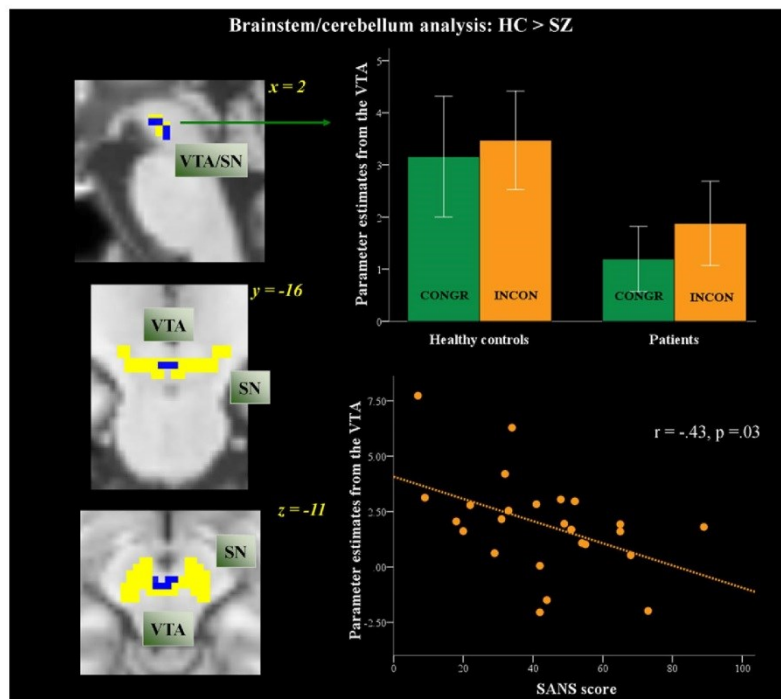


FIGURE 3 Brainstem/cerebellum fMRI analysis: On the left side of the figure, the difference in the BOLD activation between healthy controls vs. patients with schizophrenia is depicted (voxel-level $p < .05$ FWE small volume corrected and contrasted with the combined VTA/SN mask image [yellow]). The bar graph in the right top corner depicts parameter estimates from the VTA cluster (averaged over significant voxels) for both Stroop task condition and for patients and controls. In the right bottom corner, the scatterplot illustrates the significant negative correlation between parameter estimates from the VTA cluster in the incongruent versus congruent Stroop task condition and the SANS score in patients with schizophrenia. VTA = ventral tegmental area; SN = substantia nigra pars compacta; CONGR = congruent Stroop task condition; INCON = incongruent condition; SZ = patients with schizophrenia; HC = healthy controls

correlated with reward-related dopamine release in the nucleus accumbens (NAc), measured with [^{11}C]raclopride PET. Knutson and Gibbs (2007) provided evidence for the association between dopamine release in the NAc and increased local BOLD signal via agonism of postsynaptic D1 receptors.

Otherwise, activity of dopaminergic neurons in the VTA is also regulated by local glutamate-releasing and GABA-releasing neurons (Morales & Margolis, 2017). These VTA-GABA and glutamate neurons send long-range projections to cortical/subcortical regions innervated by VTA dopamine neurons (Morales & Margolis, 2017). Lavin et al. (2005) showed that the mesocortical system produced a fast postsynaptic response in the PFC via corelease of glutamate, which might be associated with signals about reward or salience. Furthermore, glutamate is considered to be centrally involved in cerebral blood flow and BOLD signal changes by putatively interacting with glutamate receptors on astrocytes and neurons (Lauritzen, 2005). Hence, present result of decreased activation in the VTA might be indicative of a dopaminergic disturbance, but might also support the hypothesis of abnormal glutamatergic neurotransmission. However, some caution is required since all patients received antipsychotic

medication influencing dopaminergic neurotransmission in addition to disease-specific alterations.

4.2 | Locus coeruleus

The noradrenergic LC is considered to modulate behavioral states such as arousal, mood and attention (Sara & Bouret, 2012). It is also thought to selectively optimize task-relevant behavioral responses (Coull et al., 1999). Prefrontal and anterior cingulate inputs were assumed to enable the transition between different activity levels of LC (Corbetta et al., 2008). Recently, we demonstrated increased LC activation in the Stroop interference condition in healthy subjects and detected stronger functional connectivity of the LC with the dorsal fronto-cingulo-parietal network (Köhler, Bär, & Wagner, 2016).

In the present study, a comparable LC activation magnitude was observed between patients and controls in both task conditions. However, the positive correlation between the LC BOLD signal and the Stroop interference time found in healthy controls but not in patients might indicate altered LC functioning during conflict resolution in schizophrenia. An abnormally working LC-NA system was supposed in schizophrenia (Friedman et al., 1999), which was related to the

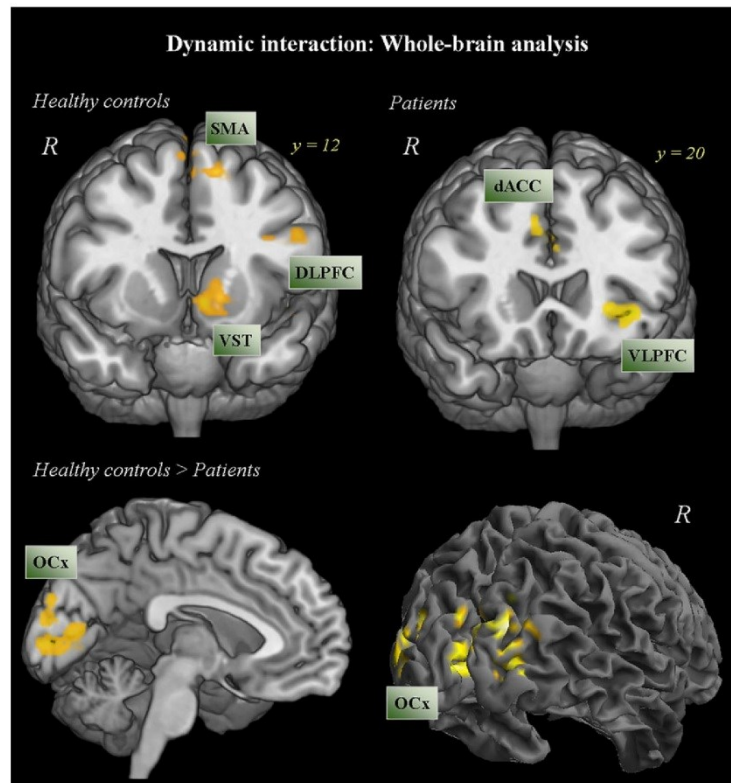


FIGURE 4 Whole-brain fMRI analysis: In the top corner on the left side of the figure the practice-related decline in fMRI activation in the incongruent condition is illustrated in healthy controls; in the top corner on the right side of the figure, the practice-related decline in fMRI activation in the incongruent condition is depicted in patients with schizophrenia; in the bottom half of the figure the practice-related decline in fMRI activation in healthy controls versus patients with schizophrenia is shown (voxel-level $p < .001$ uncorr., cluster-level, $p < .05$, FDR corr.). DLPFC = dorsolateral prefrontal cortex; VLPFC = ventrolateral prefrontal cortex; dACC = dorsal anterior cingulate cortex; SMA = supplementary motor area; VST = ventral striatum; OCx = occipital cortex

manifestation of cognitive deficits (Fields et al., 1988; van Kammen et al., 1989). However, only sparse empirical evidence exists to support this hypothesis (Lohr & Jeste, 1988; Shibata et al., 2008) and, thus, needs further investigations.

Finally, when analyzing the dynamics of the whole-brain activation patterns between groups, we found a significant linear BOLD signal decline in the occipital cortex in healthy controls but not in patients. This finding points toward a decreasing occipital cortex involvement over the course of the experiment.

One explanation might be related to the assumed role of the occipital cortex in tasks tapping the ability to use complex resolution strategies (Li et al., 2014; Pierce & McDowell, 2017). Thus, it is conceivable that healthy controls generate a strategy to visually resolve the Stroop conflict in a more efficient way than patients across the experiment. Visual processing deficits are considered to be important pathophysiological features of schizophrenia (Coleman et al., 2009; Kantrowitz et al., 2009).

4.3 | Limitations

Some limitations should be noted. Although, we did not detect a significant association between VTA as well as LC activation and the dose of antipsychotics, the impact of medication on brain activation cannot be ruled out. Moreover, in a typical fMRI experiment, we always investigate the statistical significance of BOLD signal changes during a specific task condition relative to an investigator-defined control condition, which is a fixation baseline here. Thus, we cannot definitely state whether the detected lower task-related cortical/subcortical activation in schizophrenia patients is due to a higher “baseline” activation or a lower task-related activation or both. To resolve this problem, PET studies are required to determine the activity level of the baseline condition in schizophrenia patients. In our present study, we found an activation cluster which we assumed to be the LC, because the voxels of this cluster were lying within the anatomical LC mask image provided by Keren et al. (2009). However, in the unmasked contrast we noticed that there are some voxels within the

TABLE 2 Univariate functional whole-brain data analysis: Practice-related signal changes in neuronal activation

Region of activation	Right/left	Brodmann's area	Cluster size	MNI coordinate			T value
				x	y	z	
Healthy controls							
Inferior frontal gyrus	L	47	179	-44	20	-8	5.17
Supplementary motor area	L/R	6	351	-6	20	58	5.04
Occipital cortex	L	18/19	541	-6	-76	2	4.75
Middle frontal gyrus	L	46	219	-50	24	26	4.64
Inferior frontal gyrus	L	9		-54	12	26	4.10
Cerebellum	R		322	18	-78	-24	4.63
Nucleus Accumbens	L		356	-8	14	-4	4.59
Caudate nucleus	L			-14	4	10	4.35
Putamen	L			-22	8	-4	4.28
Occipital cortex	L	18/19	324	-40	-84	0	4.57
Occipital cortex	R	18/19	916	28	-94	8	4.51
Medial frontal gyrus	L/R	6	127	6	-20	66	4.10
Patients							
Supplementary motor area	L/R	6	282	6	6	52	5.23
Inferior frontal gyrus	L	47	168	-38	24	-4	4.82
Insula	L	13		-28	22	-4	4.57
Brainstem	L		134	-2	-40	-42	4.68
Medial frontal gyrus	L/R	9	225	8	36	28	4.38
Anterior cingulate gyrus	L	32		-4	24	26	4.10
Healthy controls > patients							
Occipital cortex	L	17/18	864	-10	-84	2	4.73
Occipital cortex	R	17/18	169	30	-90	2	4.64

Maxima of regions showing significant practice-related BOLD signal decreases in the incongruent Stroop task condition in healthy controls and patients with schizophrenia as well as in the main effect of task, that is, healthy controls versus patients at the whole-brain (voxel-level $p < .001$ uncorr., cluster-level $p < .05$, FDR corr.).

significant cluster, which were lying outside of the LC mask image. Therefore, it is conceivable that further brainstem nuclei in close proximity to LC are activated during the Stroop interference contrast. Furthermore, nuclei within the brainstem/midbrain are small compared to cortical regions. Therefore, a certain degree of uncertainty remains when assigning an activation cluster to a specific nucleus. Although anatomically defined a priori ROIs of the VTA/SN and the LC were used, future studies might use high-resolution fMRI and apply structural neuromelanin-sensitive MRI scans to improve detection of dopaminergic and noradrenergic brainstem/midbrain nuclei. Moreover, to account for potential movement related confounds in the schizophrenia group, we tested for significant between-group differences in the motion parameters. No significant differences could be found in these parameters. However, even if this comparison was nonsignificant, we cannot fully exclude an effect of stronger movement in patients with schizophrenia on the fMRI signal. It is also important to note, that abnormal VTA/SN activation patterns cannot be solely related to a specific deficit in cognitive control functions. Since a significant activation difference was observed in both, the congruent and incongruent Stroop task conditions and given the numerous dopaminergic projections to cortical/subcortical regions, present finding can be also interpreted as a neurofunctional correlate of a global cognitive deficit in schizophrenia. The improved normalization of the brainstem/cerebellum using SUI toolbox was originally validated for the cerebellum (Diedrichsen, 2006), but not for the brainstem. However, by creating a

high-resolution atlas template of both, cerebellum and brainstem, Diedrichsen (2006) also intended to improve the normalization of brainstem structures as well.

ORCID

Karl-Jürgen Bär  <http://orcid.org/0000-0003-3861-5679>

REFERENCES

- Andreasen, N. C. (1999). A unitary model of schizophrenia: Bleuler's "fragmented phre" as schizencephaly. *Archives of General Psychiatry*, *56*(9), 781–787.
- Andreasen, N. C., Pressler, M., Nopoulos, P., Miller, D., & Ho, B. C. (2010). Antipsychotic dose equivalents and dose-years: A standardized method for comparing exposure to different drugs. *Biological Psychiatry*, *67*(3), 255–262. <https://doi.org/10.1016/j.biopsych.2009.08.040>
- Arnsten, A. F., & Rubia, K. (2012). Neurobiological circuits regulating attention, cognitive control, motivation, and emotion: Disruptions in neurodevelopmental psychiatric disorders. *Journal of the American Academy of Child and Adolescent Psychiatry*, *51*(4), 356–367. <https://doi.org/10.1016/j.jaac.2012.01.008>
- Artiges, E., Leroy, C., Dubol, M., Prat, M., Pepin, A., Mabondo, A., ... Trichard, C. (2017). Striatal and Extrastriatal dopamine transporter availability in schizophrenia and its clinical correlates: A voxel-based and high-resolution PET study. *Schizophrenia Bulletin*, *43*(5), 1134–1142. <https://doi.org/10.1093/schbul/sbw192>
- Aston-Jones, G., & Cohen, J. D. (2005). An integrative theory of locus coeruleus-norepinephrine function: Adaptive gain and optimal performance. *Annual Review of Neuroscience*, *28*, 403–450. <https://doi.org/10.1146/annurev.neuro.28.061604.135709>

- Aston-Jones, G., & Waterhouse, B. (2016). Locus coeruleus: From global projection system to adaptive regulation of behavior. *Brain Research*, 1645, 75–78. <https://doi.org/10.1016/j.brainres.2016.03.001>
- Bär, K. J., de la Cruz, F., Schumann, A., Köhler, S., Sauer, H., Critchley, H., & Wagner, G. (2016). Functional connectivity and network analysis of midbrain and brainstem nuclei. *NeuroImage*, 134, 53–63. <https://doi.org/10.1016/j.neuroimage.2016.03.071>
- Barch, D. M., & Sheffield, J. M. (2014). Cognitive impairments in psychotic disorders: Common mechanisms and measurement. *World Psychiatry*, 13(3), 224–232. <https://doi.org/10.1002/wps.20145>
- Bolla, K., Ernst, M., Kiehl, K., Mouratidis, M., Eldreth, D., Contoreggi, C., ... London, E. (2004). Prefrontal cortical dysfunction in abstinent cocaine abusers. *The Journal of Neuropsychiatry and Clinical Neurosciences*, 16(4), 456–464. <https://doi.org/10.1176/jnp.16.4.456>
- Briggs, G. G., & Nebes, R. D. (1975). Patterns of hand preference in a student population. *Cortex*, 11(3), 230–238.
- Callicott, J. H., Bertolino, A., Mattay, V. S., Langheim, F. J., Duyn, J., Coppola, R., ... Weinberger, D. R. (2000). Physiological dysfunction of the dorsolateral prefrontal cortex in schizophrenia revisited. *Cerebral Cortex*, 10(11), 1078–1092.
- Coleman, M. J., Cestnick, L., Krastoshevsky, O., Krause, V., Huang, Z., Mendell, N. R., & Levy, D. L. (2009). Schizophrenia patients show deficits in shifts of attention to different levels of global-local stimuli: Evidence for magnocellular dysfunction. *Schizophrenia Bulletin*, 35(6), 1108–1116. <https://doi.org/10.1093/schbul/sbp090>
- Corbetta, M., Patel, G., & Shulman, G. L. (2008). The reorienting system of the human brain: From environment to theory of mind. *Neuron*, 58(3), 306–324. <https://doi.org/10.1016/j.neuron.2008.04.017>
- Coull, J. T., Buchel, C., Friston, K. J., & Frith, C. D. (1999). Noradrenergically mediated plasticity in a human attentional neuronal network. *NeuroImage*, 10(6), 705–715. <https://doi.org/10.1006/nimg.1999.0513>
- Cuervo-Lombard, C., Lemogne, C., Gierski, F., Bera-Potelle, C., Tran, E., Portefaix, C., ... Limosin, F. (2012). Neural basis of autobiographical memory retrieval in schizophrenia. *The British Journal of Psychiatry*, 201(6), 473–480. <https://doi.org/10.1192/bjp.bp.111.099820>
- Diedrichsen, J. (2006). A spatially unbiased atlas template of the human cerebellum. *NeuroImage*, 33(1), 127–138. <https://doi.org/10.1016/j.neuroimage.2006.05.056>
- Eklund, A., Nichols, T. E., & Knutsson, H. (2016). Cluster failure: Why fMRI inferences for spatial extent have inflated false-positive rates. *Proceedings of the National Academy of Sciences of the United States of America*, 113(28), 7900–7905. <https://doi.org/10.1073/pnas.1602413113>
- Fields, R. B., Van Kammen, D. P., Peters, J. L., Rosen, J., Van Kammen, W. B., Nugent, A., ... Linnoila, M. (1988). Clonidine improves memory function in schizophrenia independently from change in psychosis. Preliminary findings. *Schizophrenia Research*, 1(6), 417–423.
- Fitzgerald, P. J. (2014). Is elevated norepinephrine an etiological factor in some cases of schizophrenia? *Psychiatry Research*, 215(3), 497–504. <https://doi.org/10.1016/j.psychres.2014.01.011>
- Friedman, J. I., Adler, D. N., & Davis, K. L. (1999). The role of norepinephrine in the pathophysiology of cognitive disorders: Potential applications to the treatment of cognitive dysfunction in schizophrenia and Alzheimer's disease. *Biological Psychiatry*, 46(9), 1243–1252.
- Furth, K. E., Mastwal, S., Wang, K. H., Buonanno, A., & Vullhorst, D. (2013). Dopamine, cognitive function, and gamma oscillations: Role of D4 receptors. *Frontiers in Cellular Neuroscience*, 7, 102. <https://doi.org/10.3389/fncel.2013.00102>
- Goghari, V. M., Sponheim, S. R., & MacDonald, A. W., 3rd. (2010). The functional neuroanatomy of symptom dimensions in schizophrenia: A qualitative and quantitative review of a persistent question. *Neuroscience and Biobehavioral Reviews*, 34(3), 468–486. <https://doi.org/10.1016/j.neubiorev.2009.09.004>
- Haber, S. N., & Knutson, B. (2010). The reward circuit: Linking primate anatomy and human imaging. *Neuropsychopharmacology*, 35(1), 4–26. <https://doi.org/10.1038/npp.2009.129>
- Howes, O. D., Egerton, A., Allan, V., McGuire, P., Stokes, P., & Kapur, S. (2009). Mechanisms underlying psychosis and antipsychotic treatment response in schizophrenia: Insights from PET and SPECT imaging. *Current Pharmaceutical Design*, 15(22), 2550–2559.
- Howes, O. D., & Kapur, S. (2009). The dopamine hypothesis of schizophrenia: Version III—the final common pathway. *Schizophrenia Bulletin*, 35(3), 549–562. <https://doi.org/10.1093/schbul/sbp006>
- Ikemoto, S. (2007). Dopamine reward circuitry: Two projection systems from the ventral midbrain to the nucleus accumbens-olfactory tubercle complex. *Brain Research Reviews*, 56(1), 27–78. doi:10.1016/j.brainresrev.2007.05.004
- Juckel, G., Schlagenhauf, F., Koslowski, M., Filonov, D., Wustenberg, T., Villringer, A., ... Heinz, A. (2006). Dysfunction of ventral striatal reward prediction in schizophrenic patients treated with typical, not atypical, neuroleptics. *Psychopharmacology*, 187(2), 222–228. <https://doi.org/10.1007/s00213-006-0405-4>
- Kantrowitz, J. T., Butler, P. D., Schecter, I., Silipo, G., & Javitt, D. C. (2009). Seeing the world dimly: The impact of early visual deficits on visual experience in schizophrenia. *Schizophrenia Bulletin*, 35(6), 1085–1094. <https://doi.org/10.1093/schbul/sbp100>
- Keren, N. I., Lozar, C. T., Harris, K. C., Morgan, P. S., & Eckert, M. A. (2009). In vivo mapping of the human locus coeruleus. *NeuroImage*, 47(4), 1261–1267. <https://doi.org/10.1016/j.neuroimage.2009.06.012>
- Knutson, B., & Gibbs, S. E. (2007). Linking nucleus accumbens dopamine and blood oxygenation. *Psychopharmacology*, 191(3), 813–822. <https://doi.org/10.1007/s00213-006-0686-7>
- Koch, K., Wagner, G., Nenadic, I., Schachtzabel, C., Roebel, M., Schultz, C., Axer, M., ... Schlosser, R. G. (2006). Temporal modeling demonstrates preserved overlearning processes in schizophrenia: an fMRI study. *Neuroscience*, 146, 1474–1483.
- Koch, K., Schachtzabel, C., Wagner, G., Schikora, J., Schultz, C., Reichenbach, J. R., ... Schlosser, R. G. (2010). Altered activation in association with reward-related trial-and-error learning in patients with schizophrenia. *NeuroImage*, 50(1), 223–232. <https://doi.org/10.1016/j.neuroimage.2009.12.031>
- Köhler, S., Bär, K. J., & Wagner, G. (2016). Differential involvement of brainstem noradrenergic and midbrain dopaminergic nuclei in cognitive control. *Human Brain Mapping*, 37(6), 2305–2318. <https://doi.org/10.1002/hbm.23173>
- Lauritzen, M. (2005). Reading vascular changes in brain imaging: Is dendritic calcium the key? *Nature Reviews Neuroscience*, 6(1), 77–85. <https://doi.org/10.1038/nrn1589>
- Lavin, A., Nogueira, L., Lapiush, C. C., Wightman, R. M., Phillips, P. E. M., & Seamans, J. K. (2005). Mesocortical dopamine neurons operate in distinct temporal domains using multimodal signaling. *Journal of Neuroscience*, 25(20), 5013–5023. <https://doi.org/10.1523/Jneurosci.0557-05.2005>
- Li, L., Men, W. W., Chang, Y. K., Fan, M. X., Ji, L., & Wei, G. X. (2014). Acute aerobic exercise increases cortical activity during working memory: A functional MRI study in female college students. *PLoS One*, 9(6), e99222. <https://doi.org/10.1371/journal.pone.0099222>
- Lohr, J. B., & Jeste, D. V. (1988). Locus ceruleus morphometry in aging and schizophrenia. *Acta Psychiatrica Scandinavica*, 77(6), 689–697.
- Milham, M. P., Banich, M. T., Claus, E. D., & Cohen, N. J. (2003). Practice-related effects demonstrate complementary roles of anterior cingulate and prefrontal cortices in attentional control. *NeuroImage*, 18, 483–493.
- Morales, M., & Margolis, E. B. (2017). Ventral tegmental area: Cellular heterogeneity, connectivity and behaviour. *Nature Reviews Neuroscience*, 18(2), 73–85. <https://doi.org/10.1038/nrn.2016.165>
- Naidich, T. P., Duvernoy, H. M., Delman, B. N., Sorensen, A. G., Kollias, S. S., & Haacke, E. M. (2009). *Duvernoy's atlas of the human brain stem and cerebellum*. Wien: Springer.
- Pierce, J. E., & McDowell, J. E. (2017). Contextual effects on cognitive control and BOLD activation in single versus mixed saccade tasks. *Brain and Cognition*, 115, 12–20. <https://doi.org/10.1016/j.bandc.2017.03.003>
- Rausch, F., Mier, D., Eifler, S., Esslinger, C., Schilling, C., Schirmbeck, F., ... Zink, M. (2014). Reduced activation in ventral striatum and ventral tegmental area during probabilistic decision-making in schizophrenia. *Schizophrenia Research*, 156(2–3), 143–149. <https://doi.org/10.1016/j.schres.2014.04.020>
- Repovs, G., Csernansky, J. G., & Barch, D. M. (2011). Brain network connectivity in individuals with schizophrenia and their siblings. *Biological*

- Psychiatry*, 69(10), 967–973. <https://doi.org/10.1016/j.biopsych.2010.11.009>
- Salo, R., Ursu, S., Buonocore, M. H., Leamon, M. H., & Carter, C. (2009). Impaired prefrontal cortical function and disrupted adaptive cognitive control in methamphetamine abusers: A functional magnetic resonance imaging study. *Biological Psychiatry*, 65(8), 706–709. <https://doi.org/10.1016/j.biopsych.2008.11.026>
- Sara, S. J., & Bouret, S. (2012). Orienting and reorienting: The locus coeruleus mediates cognition through arousal. *Neuron*, 76(1), 130–141. <https://doi.org/10.1016/j.neuron.2012.09.011>
- Schlösser, R. G., Koch, K., Wagner, G., Nenadic, I., Roebel, M., Schachtzabel, C., ... Sauer, H. (2008). Inefficient executive cognitive control in schizophrenia is preceded by altered functional activation during information encoding: An fMRI study. *Neuropsychologia*, 46(1), 336–347. <https://doi.org/10.1016/j.neuropsychologia.2007.07.006>
- Schott, B. H., Minuzzi, L., Krebs, R. M., Elmenhorst, D., Lang, M., Winz, O. H., ... Bauer, A. (2008). Mesolimbic functional magnetic resonance imaging activations during reward anticipation correlate with reward-related ventral striatal dopamine release. *Journal of Neuroscience*, 28(52), 14311–14319. <https://doi.org/10.1523/Jneurosci.2058-08.2008>
- Sheehan, D. V., Lecrubier, Y., Sheehan, K. H., Amorim, P., Janavs, J., Weiller, E., ... Dunbar, G. C. (1998). The mini-international neuropsychiatric interview (M.I.N.I.): The development and validation of a structured diagnostic psychiatric interview for DSM-IV and ICD-10. *The Journal of Clinical Psychiatry*, 59 Suppl 20, 22–33;quiz 34–57.
- Sheffield, J. M., & Barch, D. M. (2016). Cognition and resting-state functional connectivity in schizophrenia. *Neuroscience and Biobehavioral Reviews*, 61, 108–120. <https://doi.org/10.1016/j.neubiorev.2015.12.007>
- Shibata, E., Sasaki, M., Tohyama, K., Otsuka, K., Endoh, J., Terayama, Y., & Sakai, A. (2008). Use of neuromelanin-sensitive MRI to distinguish schizophrenic and depressive patients and healthy individuals based on signal alterations in the substantia nigra and locus coeruleus. *Biological Psychiatry*, 64(5), 401–406. <https://doi.org/10.1016/j.biopsych.2008.03.021>
- Silfstein, M., van de Giessen, E., Van Snellenberg, J., Thompson, J. L., Narendran, R., Gil, R., ... Abi-Dargham, A. (2015). Deficits in prefrontal cortical and extrastriatal dopamine release in schizophrenia: A positron emission tomographic functional magnetic resonance imaging study. *JAMA Psychiatry*, 72(4), 316–324. <https://doi.org/10.1001/jamapsychiatry.2014.2414>
- Su, T. W., Lan, T. H., Hsu, T. W., Biswal, B. B., Tsai, P. J., Lin, W. C., & Lin, C. P. (2013). Reduced neuro-integration from the dorsolateral prefrontal cortex to the whole brain and executive dysfunction in schizophrenia patients and their relatives. *Schizophrenia Research*, 148(1–3), 50–58. <https://doi.org/10.1016/j.schres.2013.05.005>
- Tanaka, S. (2006). Dopaminergic control of working memory and its relevance to schizophrenia: A circuit dynamics perspective. *Neuroscience*, 139(1), 153–171. <https://doi.org/10.1016/j.neuroscience.2005.08.070>
- Toda, M., & Abi-Dargham, A. (2007). Dopamine hypothesis of schizophrenia: Making sense of it all. *Current Psychiatry Reports*, 9(4), 329–336.
- Uhlhaas, P. J., & Singer, W. (2010). Abnormal neural oscillations and synchrony in schizophrenia. *Nature Reviews Neuroscience*, 11(2), 100–113. doi:nm2774 [pii] 10.1038/nm2774
- van Dijk, K. R., Sabuncu, M. R., & Buckner, R. L. (2012). The influence of head motion on intrinsic functional connectivity MRI. *NeuroImage*, 59, 431–438.
- van Kammen, D. P., Peters, J. L., van Kammen, W. B., Rosen, J., Yao, J. K., McAdam, D., & Linnola, M. (1989). Clonidine treatment of schizophrenia: Can we predict treatment response? *Psychiatry Research*, 27(3), 297–311.
- Wagner, G., De la Cruz, F., Schachtzabel, C., Gullmar, D., Schultz, C. C., Schlösser, R. G., ... Koch, K. (2015). Structural and functional dysconnectivity of the fronto-thalamic system in schizophrenia: A DCM-DTI study. *Cortex*, 66, 35–45. <https://doi.org/10.1016/j.cortex.2015.02.004>
- Wagner, G., Koch, K., Schachtzabel, C., Schultz, C. C., Gaser, C., Reichenbach, J. R., ... Schlösser, R. G. (2013). Structural basis of the fronto-thalamic dysconnectivity in schizophrenia: A combined DCM-VBM study. *NeuroImage Clinical*, 3, 95–105. <https://doi.org/10.1016/j.nicl.2013.07.010>
- Wagner, G., Sinsel, E., Sobanski, T., Köhler, S., Marinou, V., Mentzel, H. J., ... Schlösser, R. G. (2006). Cortical inefficiency in patients with unipolar depression: An event-related fMRI study with the Stroop task. *Biological Psychiatry*, 59(10), 958–965. <https://doi.org/10.1016/j.biopsych.2005.10.025>
- Wang, L., Zou, F., Shao, Y., Ye, E., Jin, X., Tan, S., ... Yang, Z. (2014). Disruptive changes of cerebellar functional connectivity with the default mode network in schizophrenia. *Schizophrenia Research*, 160(1–3), 67–72. <https://doi.org/10.1016/j.schres.2014.09.034>
- Watanabe, Y., Tanaka, H., Tsukabe, A., Kunitomi, Y., Nishizawa, M., Hashimoto, R., ... Tomiyama, N. (2014). Neuromelanin magnetic resonance imaging reveals increased dopaminergic neuron activity in the substantia nigra of patients with schizophrenia. *PLoS One*, 9(8), e104619. <https://doi.org/10.1371/journal.pone.0104619>
- Winterer, G., & Weinberger, D. R. (2004). Genes, dopamine and cortical signal-to-noise ratio in schizophrenia. *Trends in Neurosciences*, 27(11), 683–690. <https://doi.org/10.1016/j.tins.2004.08.002>
- Yamamoto, K., & Hornykiewicz, O. (2004). Proposal for a noradrenergic hypothesis of schizophrenia. *Progress in Neuro-Psychopharmacology & Biological Psychiatry*, 28(5), 913–922. <https://doi.org/10.1016/j.pnpb.2004.05.033>
- Yamashita, F., Sasaki, M., Fukumoto, K., Otsuka, K., Uwano, I., Kameda, H., ... Sakai, A. (2016). Detection of changes in the ventral tegmental area of patients with schizophrenia using neuromelanin-sensitive MRI. *NeuroReport*, 27(5), 289–294. <https://doi.org/10.1097/wnr.0000000000000530>
- Yoon, J. H., Minzenberg, M. J., Raouf, S., D'Esposito, M., & Carter, C. S. (2013). Impaired prefrontal-basal ganglia functional connectivity and substantia nigra hyperactivity in schizophrenia. *Biological Psychiatry*, 74(2), 122–129. <https://doi.org/10.1016/j.biopsych.2012.11.018>
- Yoon, J. H., Westphal, A. J., Minzenberg, M. J., Niendam, T., Ragland, J. D., Lesh, T., ... Carter, C. S. (2014). Task-evoked substantia nigra hyperactivity associated with prefrontal hypofunction, prefrontonigral disconnection and nigrostriatal connectivity predicting psychosis severity in medication naive first episode schizophrenia. *Schizophrenia Research*, 159(2–3), 521–526. <https://doi.org/10.1016/j.schres.2014.09.022>
- Zysset, S., Müller, K., Lohmann, G., & von Cramon, D. Y. (2001). Color-word matching stroop task: Separating interference and response conflict. *NeuroImage*, 13(1), 29–36. <https://doi.org/10.1006/nimg.2000.0665>

SUPPORTING INFORMATION

Additional supporting information may be found online in the Supporting Information section at the end of the article.

How to cite this article: Köhler S, Wagner G, Bär K-J. Activation of brainstem and midbrain nuclei during cognitive control in medicated patients with schizophrenia. *Hum Brain Mapp*. 2018;1–12. <https://doi.org/10.1002/hbm.24365>



The Use of Physiological Signals in Brainstem/Midbrain fMRI

Andy Schumann¹, Stefanie Köhler¹, Feliberto de la Cruz¹, Daniel Güllmar², Jürgen R. Reichenbach^{2,3}, Gerd Wagner¹ and Karl-Jürgen Bär^{1*}

¹ Psychiatric Brain and Body Research Group Jena, Department of Psychiatry and Psychotherapy, Jena University Hospital, Jena, Germany, ² Medical Physics Group, Institute of Diagnostic and Interventional Radiology, Jena University Hospital, Jena, Germany, ³ Michael Stifel Center for Data-driven and Simulation Science Jena, Friedrich Schiller University Jena, Jena, Germany

OPEN ACCESS

Edited by:

Erwin Lemche,
King's College London,
United Kingdom

Reviewed by:

Anthony E. Pickering,
University of Bristol, United Kingdom
Hoon-Ki Min,
Mayo Clinic, United States
Todd S. Braver,
Washington University in St. Louis,
United States

*Correspondence:

Karl-Jürgen Bär
Karl-Juergen.Baer@med.uni-jena.de

Specialty section:

This article was submitted to
Autonomic Neuroscience,
a section of the journal
Frontiers in Neuroscience

Received: 02 April 2018

Accepted: 19 September 2018

Published: xx September 2018

Citation:

Schumann A, Köhler S,
de la Cruz F, Güllmar D,
Reichenbach JR, Wagner G and
Bär K-J (2018) The Use
of Physiological Signals
in Brainstem/Midbrain fMRI.
Front. Neurosci. 12:718.
doi: 10.3389/fnins.2018.00718

Brainstem and midbrain nuclei are closely linked to cognitive performance and autonomic function. To advance the localization in this area, precise functional imaging is fundamental. In this study, we used a sophisticated fMRI technique as well as physiological recordings to investigate the involvement of brainstem/midbrain nuclei in cognitive control during a Stroop task. The temporal signal-to-noise ratio (tSNR) increased due to physiological noise correction (PNC) especially in regions adjacent to arteries and cerebrospinal fluid. Within the brainstem/cerebellum template an average tSNR of 68 ± 16 was achieved after the simultaneous application of a high-resolution fMRI, specialized co-registration, and PNC. The analysis of PNC data revealed an activation of the substantia nigra in the Stroop interference contrast whereas no significant results were obtained in the midbrain or brainstem when analyzing uncorrected data. Additionally, we found that pupil size indicated the level of cognitive effort. The Stroop interference effect on pupillary responses was correlated to the effect on reaction times ($R^2 = 0.464$, $p < 0.05$). When Stroop stimuli were modulated by pupillary responses, we observed a significant activation of the LC in the Stroop interference contrast. Thus, we demonstrated the beneficial effect of PNC on data quality and statistical results when analyzing neuronal responses to a cognitive task. Parametric modulation of task events with pupillary responses improved the model of LC BOLD activations in the Stroop interference contrast.

Keywords: locus coeruleus, Stroop task, substantia nigra, pupil diameter, skin conductance

INTRODUCTION

Accumulating research has revealed the close interrelationship between the autonomic state and motivation, attention, mood, and cognition. For instance, in addition to the strong influence of cognitive strains on autonomic function, feelings in the body that are associated with emotions (somatic markers) profoundly influence our decisions (Damasio et al., 1991; Bechara and Damasio, 2005). Thus, the internal state determines the way we react to the environment (Critchley, 2009). It has been assumed that behavioral states might be related closely to neuromodulatory brainstem systems. Thus, assessing the activity of the autonomic nervous system is indicative of the functional state (Samuels and Szabadi, 2008b; Urai et al., 2017). Therefore, inclusion of peripheral indicators of autonomic function is an important addendum to research in neurosciences.

MATERIALS AND METHODS

Subjects

Fourteen healthy subjects (nine females, five males, age: 27 ± 7 years) participated in this study. The following exclusion criteria were applied: any disease or impairment of the circulatory system, the peripheral nervous system or the endocrine system, alcohol- or drug abuse. Subjects with past or current neurological or psychiatric diseases according to M.I.N.I (Sheehan et al., 1998) and/or first-degree relatives with Axis I psychiatric disorders were excluded from the study. None of the study participants was taking any psychopharmacological medication.

Three subjects were excluded due to inadequate quality of the eye tracker signal (see below). Thus, eleven subjects were analyzed (seven males, four females, age: 28 ± 7 years). All participants were German native speakers, right-handed according to the modified version of Annett's Handedness Inventory (Briggs and Nebes, 1975). All participants gave written consent to a protocol approved by the Ethics Committee of the University Hospital Jena in accordance with the Declaration of Helsinki.

Experimental Paradigm

Participants conducted the manual version of the Stroop color word task (Stroop, 1935; Wagner et al., 2015). In brief, participants had to choose the color of the word written in the center of the projected screen. In the congruent condition, the color of the word matches its meaning. In the IC, the color word is displayed in a color, which is not denoted by the word. Subjects were instructed to indicate one of two possible answers presented at the bottom of the screen by pressing a button of the pad with the right index or middle finger. Correct answers were counterbalanced on the right and left sides of the display. In a pseudorandomized order, 18 congruent and 18 incongruent stimuli were presented for 1500 ms each, with an inter-stimulus interval of 10.5 s. Additionally, a temporal jitter was introduced to enhance the temporal resolution.

MRI Parameters

Functional data was collected on a 3 T Magnetom PRISMA fit whole-body system (Siemens Healthineers, Erlangen, Germany) equipped with a 64-element receive-only head matrix coil. Head immobilization was achieved using head pads within the coil. T2*-weighted images were obtained using a gradient-echo EPI sequence (TR = 2040 ms, TE = 33 ms, flip angle = 75°) with 100 contiguous transverse slices of 1.4 mm thickness and a multi-band acceleration factor of four covering the entire brain and including the lower brainstem. Matrix size was 138×138 pixels with in-plane resolution of (1.4×1.4) mm². A series of 220 whole-brain volume sets were acquired in one session. High-resolution anatomical T1-weighted volume scans (MP-RAGE) were obtained in sagittal orientation (TR = 2300 ms, TE = 2.07 ms, TI = 900 ms, flip angle = 9°, FOV = 256 mm, matrix = (256×256) mm², number of sagittal slices = 192, with an isotropic resolution of $(1 \times 1 \times 1)$ mm³.

Physiological Recordings

Photoplethysmogram (PPG), respiration and skin conductance were recorded throughout MR image acquisition at 500 Hz using an MR-compatible polygraph MP150 (BIOPAC Systems Inc., Goleta, CA, United States). Respiratory activity was assessed by a strain gage transducer incorporated in a belt that was tied around the chest, approximately at the level of the processus xiphoideus. The respiratory signal was amplified between 0.05 and 10 Hz and temporally smoothed (250 samples). The PPG sensor was attached to the proximal phalanx of the left index finger. The finger pulse signal was recorded in a frequency range of 0.05–3 Hz and smoothed over 50 samples. Skin conductance was measured continuously (constant voltage 1 technique) at the left hand's palm with Ag/AgCl electrodes placed at the thenar and hypothenar eminence. The signal was amplified below 10 Hz, median filtered (150 samples) and smoothed (250 samples).

Pupillometric recordings were conducted using a MR-compatible ASL Long Range Optic Eye Tracker (Applied Science Laboratories, Bedford, MA, United States). Pupil diameter (PD) and gaze position were extracted from the video stream and sampled at 120 Hz. Artifacts and closed eyes were automatically detected by the software and replaced offline by linear interpolation of adjacent values. PD was smoothed over 100 samples. Only recordings with artificial samples less than 10% of all acquired data during the recording were analyzed (mean artifact rate of the final sample was 3.3%). Trigger output of the MR scanner was logged by the presentation software and recorded by the polygraph and the eye tracker to synchronize all the acquired data with the task paradigm.

Physiological Noise Correction

Prior to preprocessing, physiological fluctuations synchronized with cardiac and respiratory cycles were removed using the RETROICOR approach (Glover et al., 2000). To account for low frequency variations in the BOLD signal through slow blood oxygenation level fluctuations, five respiration volumes per time (RVT) regressors were additionally removed (Birn et al., 2006). The RVT regressors consisted of the RVT function and four delayed terms at 5, 10, 15, and 20 s (Birn et al., 2008; Jo et al., 2010), while eight low-order Fourier time series (four based on the cardiac phase and four on the respiratory phase) were created using the RETROICOR algorithm. All regressors were generated on a slice-wise basis by AFNI's RetroTS.m script implemented in MATLAB 2016b, which takes the cardiac and respiratory time series synchronized with the fMRI acquisition as input.

Image Data Preprocessing

For image processing and statistical analyses, we used SPM12¹. The first four images were discarded to avoid contributions from non-steady-state tissue magnetization. The remaining 216 images were corrected for differences in time acquisition by sinc-interpolation and realigned to the first image. The co-registered anatomical images were segmented using the tissue probability maps. Functional images were then spatially normalized to the

¹<http://www.fil.ion.ucl.ac.uk/spm>

115 One excellent example of such a close interaction is the
 116 human pupil reflecting both the autonomic state as well as
 117 cognitive demand (Granholm and Steinhauer, 2009; Laeng
 118 et al., 2012). Thus, pupillometry has become a powerful tool
 119 in psychophysiology (e.g., see review by Sirois and Brisson,
 120 2014). Pupils have been shown to react to various types of
 121 cognitive demand, such as memory load (Attar et al., 2013),
 122 arithmetic tests (Vö et al., 2008), or speech processing (Zekveld
 123 et al., 2010). A higher level of cognitive effort leads to a
 124 greater magnitude of pupillary reaction (Laeng et al., 2012;
 125 Querino et al., 2015). The size of the pupil is determined by
 126 the sympathetic and parasympathetic outflow to the muscles
 127 of the iris (Steinhauer et al., 2004). Parasympathetic activation
 128 leads to constriction, whereas sympathetic activation results in
 129 dilation of the pupil. Preganglionic sympathetic neurons receive
 130 input from the posterior nuclei of the hypothalamus and project
 131 from the intermediolateral nucleus in the spinal cord through
 132 the sympathetic trunk to the iris. The Edinger-Westphal nucleus
 133 (EWN) is considered to be the primary origin of parasympathetic
 134 influence on the pupils. In addition, the locus coeruleus (LC), the
 135 main source of noradrenaline in the brain, exhibits inhibitory
 136 influences on the EWN (Samuels and Szabadi, 2008a; Murphy
 137 et al., 2014; Joshi et al., 2016). Given the reported co-variation of
 138 LC firing rate and pupillary responses (Aston-Jones and Cohen,
 139 2005; Costa and Rudebeck, 2016), the dilation of the pupil has
 140 been considered as a proxy of noradrenergic activity in humans
 141 (Sirois and Brisson, 2014; Eckstein et al., 2017).

142 The LC has been proposed to facilitate the dynamic
 143 reorganization of neural networks in response to external stimuli
 144 (Bouret and Sara, 2005). Corbetta et al. (2008) highlighted
 145 its role in attention shifting and cognitive flexibility. They
 146 postulated that the LC is significantly involved in the dynamic
 147 switch between functional networks. The dorsal fronto-parietal
 148 network including the dorsolateral prefrontal cortex and the
 149 dorsal parietal cortex is important for the selection of stimuli and
 150 generation of responses. The ventral fronto-parietal network with
 151 the temporo-parietal junction, ventrolateral prefrontal cortex and
 152 anterior insula as core regions, detects salient stimuli, interrupts
 153 and redirects attention (Corbetta et al., 2008).

154 Another physiological marker that has been proposed to
 155 indicate mental effort is the level of skin conductance (Jacobs
 156 et al., 1994; Kohlisch and Schaefer, 1996; Mehler et al., 2009;
 157 Reimer and Mehler, 2011). The secretion of sweat changes the
 158 electrical properties of the skin that can be recorded superficially
 159 (Edelberg, 1993). In competitive analyses, Kahneman et al.
 160 (1969) and Fritz et al. (2014) demonstrated measures of skin
 161 conductance and pupil size to be similarly suitable for indicating
 162 mental workload. Hogervorst et al. (2014) reported that pupil size
 163 was the index far more applicable.

164 The differential involvement of neurotransmitter systems
 165 in the generation of skin conductance responses (SCR) is
 166 still unclear. Yamamoto et al. (1990) showed that lesions to
 167 noradrenergic fiber bundles in cats abolish SCR and spontaneous
 168 fluctuation of skin conductance. In contrast, microinjections into
 169 the ventral tegmental area (VTA), the midbrain's dopaminergic
 170 center, had no effect on skin conductance. Neuroimaging
 171 studies reported that BOLD changes and metabolism in regions

congruent to LC and VTA are related to spontaneous skin
 conductance fluctuations at rest (Patterson, 2002), and responses
 to fear (Linnman et al., 2013). Sequeira and Roy (1993) proposed
 a crucial influence of the reticular formation, a brainstem
 network including the LC, on skin conductance. Thus, the
 noradrenergic system might have a decisive role in generating
 SCR.

172 Recently, we reported that the LC and VTA/Substantia
 173 nigra (SN) are significantly involved in cognitive and especially
 174 inhibitory control (Köhler et al., 2016, 2018b). We used the well-
 175 established *Stroop Color-Word Test* [SCWT, (Stroop, 1935)] to
 176 investigate the neural correlates of cognitive control processes in
 177 the brainstem/midbrain. In the SCWT, participants shall name
 178 the color in which a word is presented ignoring the word itself.
 179 The color either matches the meaning of the word (congruent
 180 condition) or not [incongruent condition (IC)]. Incongruent
 181 trials require an inhibition of an overlearned, pre-potent response
 182 tendency (reading the word) in favor of an unusual, less pre-
 183 potent action (naming the color of the ink). We observed that
 184 BOLD activation of the LC and VTA/SN was higher in
 185 incongruent than in congruent trials. Compared to the VTA/SN,
 186 the LC was functionally connected to the dorsal fronto-parietal
 187 network. We additionally demonstrated differential activation of
 188 VTA/SN and LC modulated by demands of cognitive control.
 189 Our data gave additional evidence that phasic activation of LC
 190 facilitates cognitive conflict resolution and optimizes behavioral
 191 responses by activating specific task-related brain networks.

192 However, brainstem and midbrain nuclei are small compared
 193 with the cortical regions involved in cognitive control, and are
 194 more susceptible to signal distortion and artifacts arising from
 195 local tissue interfaces and physiological noise (Köhler et al., 2016).
 196 Especially the position of the LC at the posterior border of
 197 the brainstem impedes its functional imaging. Neuromelanin-
 198 sensitive scans have added significant information on the
 199 anatomical location of the LC (Keren et al., 2009, 2015;
 200 Hämmerer et al., 2017) that can be used to validate the
 201 identification of LC (Astafiev et al., 2010; Murphy et al., 2014;
 202 Clewett et al., 2018). Standard anatomical scans can also be used
 203 to detect activation of the LC (Brooks et al., 2017; de Gee et al.,
 204 2017). To link structures such as the LC with specific functions
 205 using fMRI, a precise match of anatomical and functional
 206 information is essential. To really advance our understanding in
 207 this field, improvement of functional data analysis is needed.

208 In our present study, we used the SCWT to corroborate
 209 the involvement of LC and VTA/SN in cognitive control.
 210 To further enhance image quality, we prepared our data by
 211 applying physiological noise correction (PNC) and a specialized
 212 brainstem/cerebellum normalization technique. To improve
 213 anatomical and functional distinction between brainstem and
 214 midbrain nuclei, we applied functional scans with a high spatial
 215 resolution of 1.4 mm³ and assessed simultaneously physiological
 216 responses of pupils and skin conductance to indicate cognitive
 217 efforts. We assumed a close association of LC activation
 218 and pupillary dilation in the Stroop interference contrast.
 219 Therefore, we hypothesize that including pupillary responses
 220 to model BOLD activation within the LC might enhance its
 221 identification.
 222
 223
 224
 225
 226
 227
 228

MNI space using parameters estimated during the segmentation process.

Specialized Brainstem/Midbrain

Co-registration

To improve the image normalization at the brainstem level, data was normalized to the spatially unbiased infra-tentorial template [SUIT; version 3.1, (Diedrichsen, 2006)]. Using the SUIT toolbox, we applied the following preprocessing steps: (i) segmentation of the whole-brain image; (ii) cropping of the image, retaining only the cerebellum and brainstem; (iii) normalization using the DARTEL engine (Ashburner, 2007) that uses gray and white matter segmentation maps produced during cerebellar isolation to generate a flow field using Large Deformation Diffeomorphic Metric Mapping (Beg et al., 2005), and (iv) re-slicing to a voxel size of $(1.5 \times 1.5 \times 1.5) \text{ mm}^3$.

Whole brain and cropped data were smoothed with a Gaussian filter of 4 mm FWHM and high-pass filtered with a cutoff period of 128 s and corrected for serial correlations choosing AR (1).

Temporal Signal-to-Noise Ratio (tSNR)

The quality of the data was quantified in terms of the temporal signal-to-noise ratio (tSNR). It was calculated voxel-wise as the BOLD signals temporal mean divided by its standard deviation (Brooks et al., 2013). To compare the change of quality due to PNC at the brainstem level, we calculated mean tSNR maps after standard preprocessing of corrected and uncorrected data (standard co-registration, unsmoothed). Additionally, we estimated a mean tSNR map of the data used for our analyses (with specialized co-registration, PNC and smoothing).

Physiological Recordings: Event-Related SCR and PDR

Physiological responses were extracted at the onset of stimulus presentation (reference time $t = 0$) with a duration of 10 s and referenced to baseline (mean value within 1 s before stimulus onset). We averaged reactions in congruent and incongruent Stroop trials. The area under the curve (AUC) and maximum of each PD and SC reaction was estimated and compared in terms of a paired t -test between conditions. The AUC per subject was used as measure of the strength of PD and SCR in all further analyses. The pupillary Stroop effect was defined as percentage increases of PDR in IC compared to CC (Rondeel et al., 2015). Stroop interference effect, i.e., the percentage increase of reaction times from CC to IC was correlated to the pupillary Stroop effect.

fMRI Statistical Data Analysis

Reaction times and characteristics of physiological responses to congruent and incongruent Stroop stimuli were compared by a paired t -test. To assess a possible decline of physiological reactions over trials, we standardized all reactions (AUC) to the first trial and correlated these ratios to the trial number.

In *model 1*, neural responses to incongruent (IC) and congruent Stroop stimuli (CC) were modeled by convolving a series of impulses at stimulus onset times by the hemodynamic response function. The single-subject general linear model

(GLM) included the regressors of CC and IC, as well as six head motion parameters estimated during image realignment.

In *model 2*, each Stroop stimulus was weighted by the evoked SCR. Therefore, SCR was added as a parametric modulator to *model 1*. Single subjects GLMs included modulated task regressors (CC and IC) and six head motion parameters as covariates.

In *model 3*, pupillary responses were used for parametric modulation of Stroop stimuli in the same manner as in *model 2*.

Subject-specific parameter estimates were then entered into a second-level RFX analysis. We set up an ANOVA design with the within-subject factor TASK (CC and IC) and tested for the interference contrast IC vs. CC. All statistical maps were thresholded at the voxel-level with $p < 0.005$ (uncorrected) and cluster-level corrected with the number of expected voxels per cluster (Köhler et al., 2016). To investigate the influence of PNC, *model 1* was estimated on data corrected for physiological noise as well as uncorrected data. *Model 2* and *model 3* were estimated on PNC data. To assess an overlap between activated brainstem clusters and LC location, we used the anatomical mask image in the MNI coordinate space based on Keren et al. (2009). This mask represents the extent of peak LC signal distribution, obtained from a sample of 44 healthy adults using high-resolution T1-weighted Turbo Spin Echo MRI.

We investigated the changes of luminance due to the presentation of color words of different length and ink color. In our lab outside the scanner, we used the toolbox *phyphox*² (RWTH Aachen University, Aachen, Germany) running on a Samsung Galaxy tablet to record luminance during the Stroop task. Mean luminance changes during stimulus presentation were calculated to check for a difference of luminance between task conditions.

RESULTS

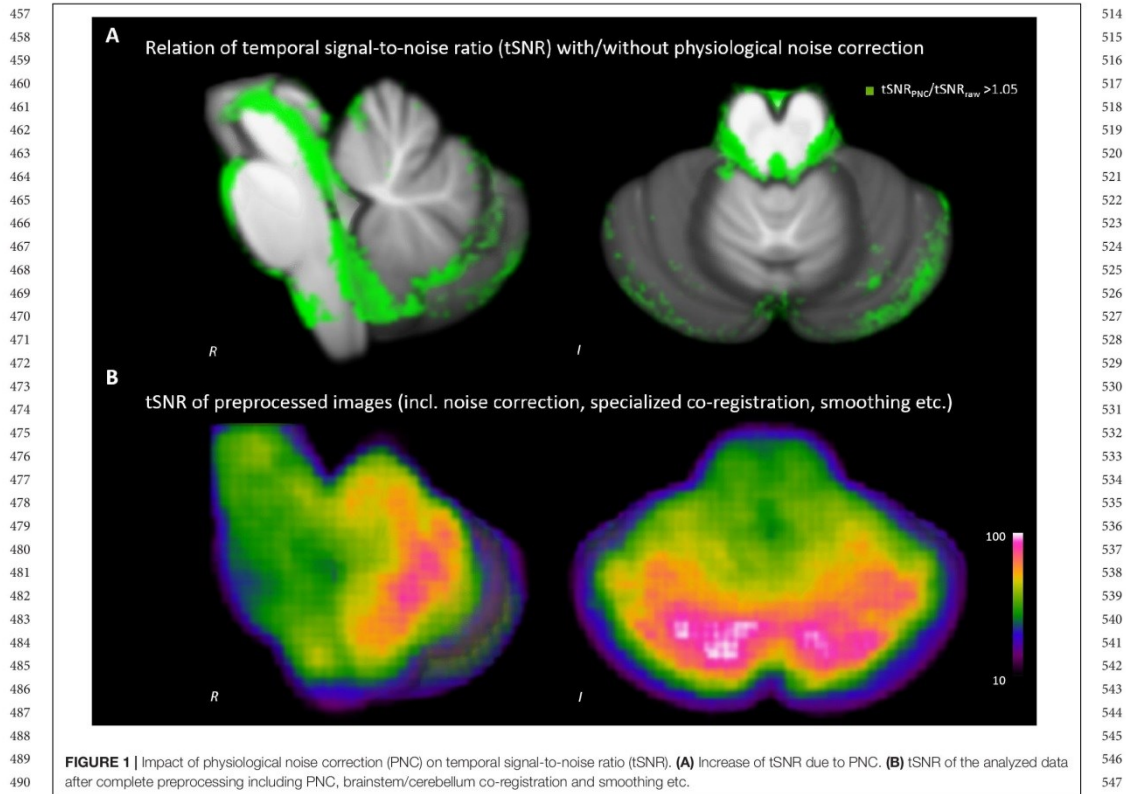
Effect of Physiological Noise Correction on tSNR

We detected increases of the tSNR throughout the brainstem (see **Figure 1A**). The improvement was most pronounced around tissue borders to cerebral spinal fluid, but also within the midbrain, brainstem and cerebellum. The tSNR of our data used for analyses was 67.8 ± 15.9 on average within the SUIT template (**Figure 1B**).

Effect of Physiological Noise Correction on Statistical Results (Stroop Interference Contrast)

Without PNC, a cluster in the upper anterior pons showed increased activations in the incongruent compared to the congruent condition ($x = 0, y = -24, z = -21, t = 3.69, p < 0.005, k = 12$). Three clusters in the cerebellum also showed significant activation in the Stroop interference contrast (see **Figure 2A** and **Table 1**).

²www.phyphox.org



After PNC, we found that three clusters in the midbrain were more activated in the incongruent than in the congruent condition (**Figure 2B**). One cluster most probably overlapped with the substantia nigra (SN, $x = -6$, $y = -19$, $z = -16$, $t = 4.29$, $p < 0.005$, $k = 28$) and one was situated adjacent to the aqueduct (periaqueductal gray, PAG, $x = -7$, $y = -30$, $z = -4$, $t = 3.89$, $p < 0.005$, $k = 56$). Additional activations were found in the cerebellum (see **Table 1**). There was no overlap of significant clusters of uncorrected and PNC data in the Stroop interference contrast.

Behavioral and Physiological Reactions to the Stroop Task

Subjects responded significantly slower in incongruent (1223 ± 328 ms) than in congruent trials (1036 ± 216 ms, $t = -4.16$, $p < 0.01$), indicating a reliable induction of the Stroop effect. Errors and missing responses ($n = 11$) occurred in the IC only. Reaction times decreased with increasing trial number of the IC ($R^2 = 0.333$, $p < 0.05$) and

the CC ($R^2 = 0.349$, $p < 0.01$) revealing a general learning effect.

As shown in **Figures 3A–C**, pupil diameter responses (PDR) were higher in incongruent (IC, green) than in congruent trials (CC, blue). The area under PDR was lower in the CC (1241 ± 1043 n.u.) compared to the IC (2155 ± 1110 n.u., $t = -2.24$, $p < 0.05$; **Figure 3B**). The maximum pupil size was 1.135 ± 0.038 n.u. in CC trials and 1.159 ± 0.041 n.u. in IC trials ($t = -2.45$, $p < 0.05$; **Figure 3C**). There was a significant habituation of pupillary responses during CC ($R^2 = 0.459$, $p < 0.01$) and IC ($R^2 = 0.223$, $p < 0.05$). The pupillary Stroop effect correlated to the Stroop interference effect ($R^2 = 0.464$, $p < 0.05$).

There was no significant difference between SCR during the incongruent and congruent condition (**Figure 3D**). Similarly, the maximum, the area under SCR and the latency of SCR were not different (**Figures 3E,F**). We found no linear decrease of SCR indices over trials and no correlation to reaction times.

During the task, luminance decreased by $2.15 \pm 1.45\%$ in CC and $2.11 \pm 1.44\%$ in IC trials. There was no significant difference of luminance between the two conditions.

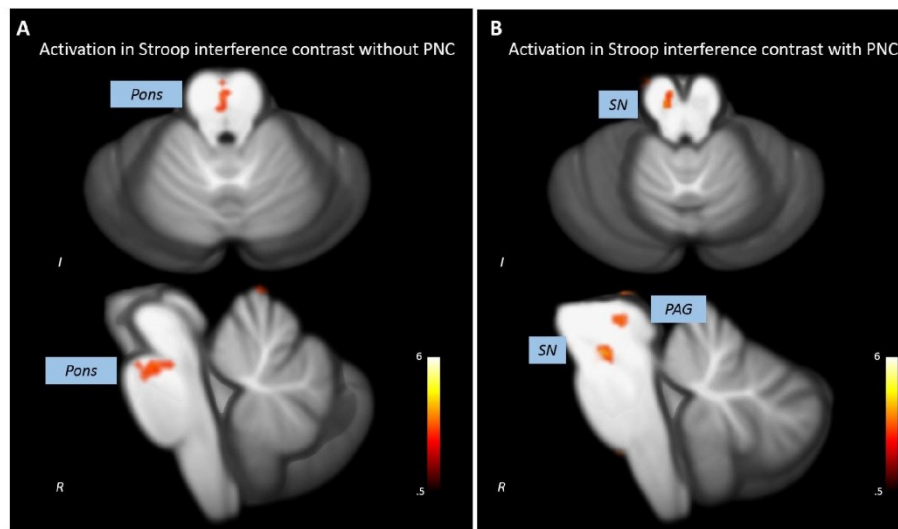
571
572
573
574
575
576
577
578
579
580
581
582
583
584
585
586
587
588
589
590
591
592
593
594

FIGURE 2 | Impact of PNC on the statistical results revealed by the analysis of the Stroop interference contrast. **(A)** The analysis of uncorrected data leads to a statistical significant activation cluster in the upper pons and no midbrain/brainstem activations. **(B)** A significant activation in the substantia nigra (SN) and the periaqueductal gray (PAG) was detected when analyzing PNC data.

595
596
597
598
599
600
601
602
603
604
605
606
607
608
609

SCR Parametric Modulation of Stroop Stimuli

Modulating Stroop stimuli using SCR, a significant activation of the SN in the Stroop interference contrast was replicated ($x = -6$, $y = -24$, $z = -15$, $t = 3.91$, $p < 0.005$, $k = 39$) together with most cerebellar clusters (see Table 2). In contrast, no activation of the periaqueductal gray was detected.

PDR Parametric Modulation of Stroop Stimuli

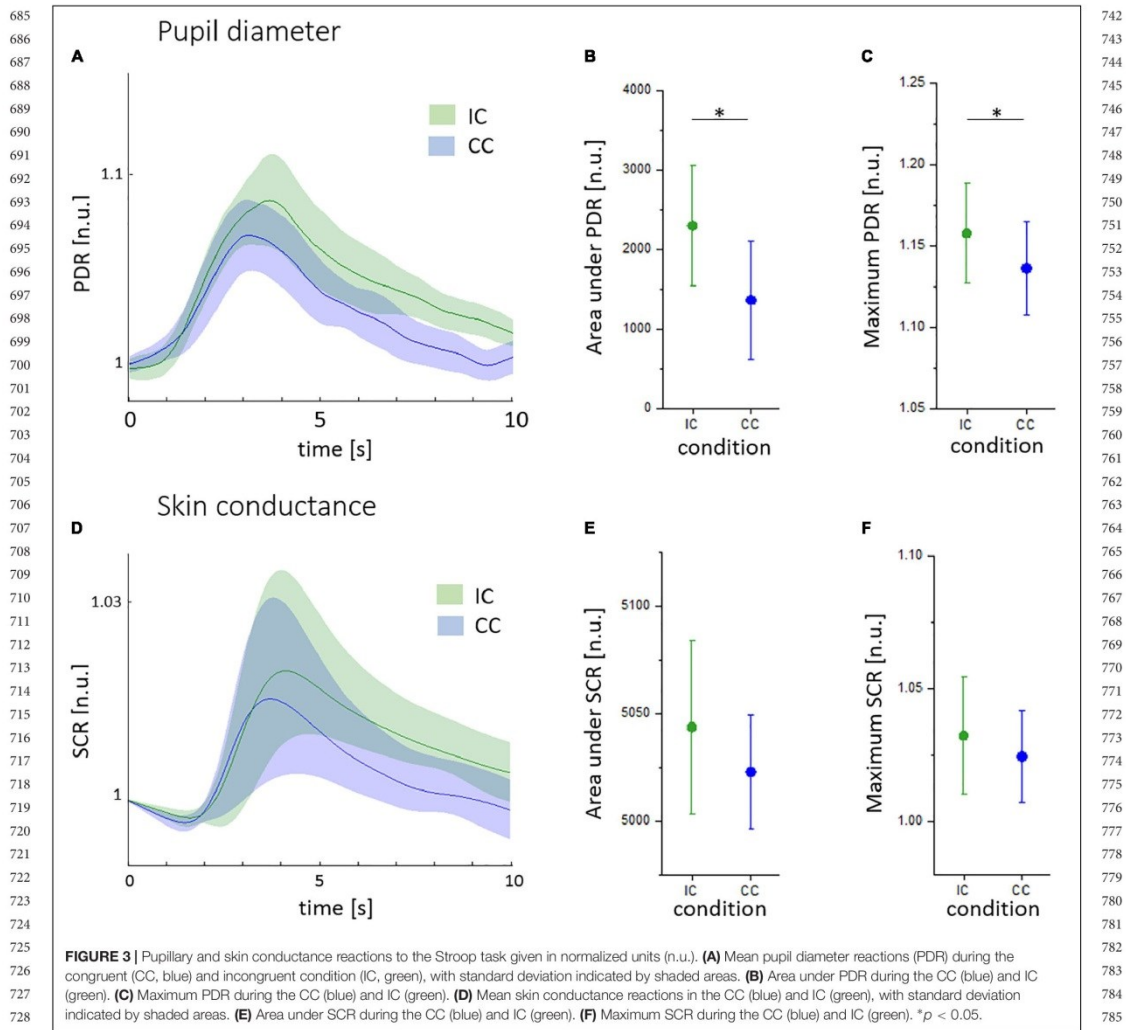
When Stroop stimuli were weighted by PDR, the Stroop interference contrast revealed a significant activation of a tube-like cluster at the posterior brainstem (Figure 4A and Table 2). The overlap with the anatomical mask of the LC suggested that the activated cluster overlaps with both lateral branches of the upper LC (Figure 4B).

610

TABLE 1 | Clusters with significant BOLD activations in the Stroop interference contrast with and without physiological noise correction of underlying data.

611
612
613
614
615
616
617
618
619
620
621
622
623
624
625
626
627

Region	Side	Cluster size	MNI coordinates			t
			X	Y	Z	
Without physiological noise correction						
Thalamus	R	17	18	-32	-1	3.8
Pons	R	16	0	-24	-21	3.69
Culmen	L	13	-2	-58	3	3.96
Dentate	L	20	-10	-48	-31	4.04
Anterior cerebellar lobe	R	12	14	-66	-33	4.55
With physiological noise correction						
Thalamus	R	69	11	-26	6	5.02
PAG	L	56	-7	-30	-4	3.89
SN	L	28	-6	-19	-16	4.29
Culmen	R	10	17	-48	-9	3.34
Nodule	L	16	-8	-49	-30	3.79
Cerebellar Tonsil	L	10	-25	-46	-44	3.41



DISCUSSION

In this study, we combined high-resolution fMRI, advanced brainstem co-registration, PNC and physiological recordings in order to precisely identify brainstem and midbrain regions involved in cognitive control. We demonstrate the enhancement of signal quality due to PNC as well as its beneficial effect on the statistical results. The signal to noise ratio was increased especially in tissue adjacent to arteries and spaces filled with cerebrospinal fluid. The analysis of PNC data replicated the involvement of the nigro-striatal dopaminergic system

in cognitive control whereas uncorrected data revealed no brainstem/midbrain activations. We found that pupil size was a sensitive indicator of the level of cognitive demand. When Stroop stimuli were modulated by pupillary responses, we observed a significant activation of the LC.

About 20,000–50,000 neurons build the LC as a symmetric structure at the dorsal brainstem with a rostrocaudal extent of 12–17 mm and a diameter of about 2.5 mm (German et al., 1988; Fernandes et al., 2012). It begins rostrally in the caudolateral part of the mesencephalic central gray, at the level of the inferior colliculus, and extends caudally to a position in the lateral wall

799 of the fourth ventricle (German et al., 1988; Köhler et al., 2016).
800 Neurons of the LC project to various regions throughout the
801 cerebral cortex, thalamus, hippocampus, brainstem, midbrain,
802 cerebellum, and the spinal cord (Aston-Jones et al., 1999;
803 Berridge and Waterhouse, 2003; Samuels and Szabadi, 2008a).

856 Electrophysiological studies have shown that the LC selectively
857 responds to salient stimuli that entail attention disruption and
858 reorientation (Grant et al., 1988; Aston-Jones et al., 1999). The
859 recorded LC activity was previously decomposed into a tonic
860 and phasic component (Aston-Jones and Cohen, 2005). Tonic
861

806 **TABLE 2 |** Clusters with significant BOLD activations in the Stroop interference contrast after modulating task events by skin conductance responses (SCR) and pupil
807 diameter responses (PDR) (with complete preprocessing).
808

809 Region	810 Side	811 Cluster size	812 MNI coordinates			813 t
			814 X	815 Y	816 Z	
817 Parametric modulation with SCR						
818 Thalamus	R	56	6	-24	8	4.7
819 Substantia nigra	L	39	-13	-13	-12	3.91
820 Dentate	L	33	-16	-54	-28	4.5
821 Fastigium	L	23	-7	-49	-30	3.89
822 Anterior cerebellar lobe	R	42	5	-48	-33	5.94
823 Parametric modulation with PDR						
824 Thalamus	R	33	4	-18	8	3.17
825 Inferior colliculus	R	25	8	-38	-12	4.25
826 LC	L	39	-2	-36	-18	3.76
827 Medulla	L	23	-4	-37	-44	3.88
828 Culmen	L	10	-10	-62	-9	4.68
829 Culmen	R	13	6	-49	-10	3.27
830 Culmen	L	20	-19	-40	-18	4.38
831 Declive	R	19	29	-70	-20	4.83
832 Culmen	R	14	32	-54	-21	3.86
833 Cerebellar Lingual	R	13	8	-48	-24	3.38
834 Culmen	R	30	28	-40	-26	3.83
835 Culmen	R	15	11	-55	-27	4.22
836 Culmen	R	10	17	-42	-27	3.73
837 Declive of Vermis	R	22	0	-76	-27	3.47
838 Culmen	L	41	-12	-48	-28	4.57
839 Declive	L	10	-43	-68	-28	3.75
840 Declive	R	17	46	-54	-28	3.62
841 Declive	L	26	-30	-74	-28	3.56
842 Culmen	L	13	-40	-52	-30	4
843 Declive	R	45	42	-66	-30	3.83
844 Declive	R	10	11	-73	-30	3.72
845 Nodule	R	59	4	-56	-32	4.14
846 Uvula	R	13	8	-66	-36	3.49
847 Culmen	L	23	-42	-44	-38	4.48
848 Culmen	L	11	-28	-37	-38	3.86
849 Tuber	R	18	48	-60	-38	3.52
850 Pyramis	L	11	-12	-68	-38	3.39
851 Tuber	R	55	34	-74	-39	4.35
852 Tuber	L	13	-22	-85	-39	3.15
853 Pyramis	R	14	44	-70	-42	4.78
854 Uvula	L	26	-7	-66	-44	3.76
855 Cerebellar Tonsil	R	14	29	-62	-48	3.75
856 Cerebellar Tonsil	L	40	-32	-54	-50	6.08
857 Cerebellar Tonsil	R	12	12	-42	-50	3.41
858 Inferior Semi-Lunar Lobule	L	28	-30	-62	-52	3.47
859 Cerebellar Tonsil	R	44	5	-44	-54	3.91

860 LC, locus coeruleus.

913
914
915
916
917
918
919
920
921
922
923
924
925
926
927
928
929
930
931
932
933
934
935
936
937
938
939
940
941
942
943
944
945
946
947
948
949
950
951
952
953
954
955
956
957
958
959
960
961
962
963
964
965
966
967
968
969

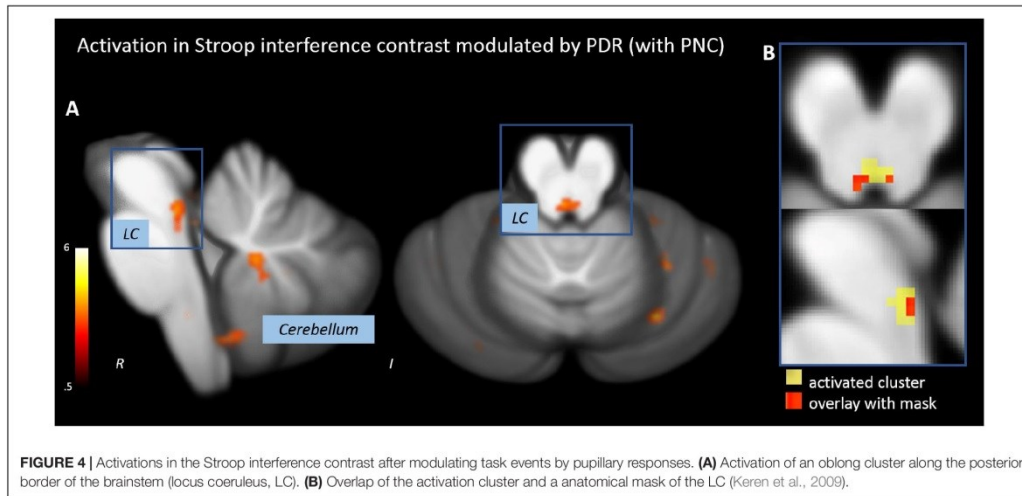


FIGURE 4 | Activations in the Stroop interference contrast after modulating task events by pupillary responses. **(A)** Activation of an oblong cluster along the posterior border of the brainstem (locus coeruleus, LC). **(B)** Overlap of the activation cluster and an anatomical mask of the LC (Keren et al., 2009).

activity represents a kind of baseline arousal and is low during certain automatic behavior and drowsiness. LC neurons become phasically activated by salient stimuli (Rajkowski et al., 1994; Aston-Jones et al., 1999).

The LC is an important relay of the noradrenergic and dopaminergic circuitry of the brainstem (Fernandes et al., 2012). The LC-noradrenergic system regulates the balance between selective and flexible attention. At rest, we have recently shown that the LC is functionally integrated into the executive-control network (Bär et al., 2016). Under external stimulation, the LC seems to dynamically moderate the switch between distinct functional networks depending on the salience of incoming stimuli (Bouret and Sara, 2005; Corbetta et al., 2008). It has been demonstrated previously that the incongruent Stroop task condition, requiring inhibitory control, activates the neural cognitive control network consisting of the prefrontal cortex, the anterior cingulate cortex, the posterior parietal cortex and subcortical structures (Miller and Cohen, 2001; Critchley et al., 2005; Wagner et al., 2006). In our recent study, we additionally found that incongruent Stroop stimuli trigger the activation of the LC (Köhler et al., 2016). In the current study, we wanted to investigate the influence of enhanced preprocessing techniques on BOLD activations during the Stroop task.

Considering the spatial extent of brainstem nuclei, functional MR imaging requires highly precise approaches (Beissner et al., 2014). In our current analysis, the spatial resolution is far more sensitive compared to previous investigations (Murphy et al., 2014; Köhler et al., 2016). Additionally, we prepared the acquired functional data by PNC involving cardiac and respiratory signals. We demonstrated that the signal-to-noise ratio (SNR) of brainstem images benefits from PNC due to the presence of nearby major arteries and cerebrospinal fluid filled spaces (Brooks et al., 2013). Especially along the posterior border of the brainstem, an increase of temporal SNR was

detected. In this region important nuclei of the ascending reticular system, the serotonergic system, the noradrenergic system etc. are located. After PNC and brainstem/cerebellum specialized co-registration an average temporal SNR of 67.8 was achieved. The SNR map resamples the results reported by Brooks et al. (2013). He highlighted the effect of noise from non-neural sources and reviewed different correction approaches (e.g., RETROICOR). In brainstem fMRI, the increase of signal quality by using RETROICOR was documented previously (see Harvey et al., 2008; Brooks et al., 2013). In our approach here, we use five respiration volume per time regressors additionally to the RETROICOR cardiac and respiratory phase regressors (Birn et al., 2008).

In this study, we show that PNC has a crucial impact on the results that revealed the analysis of BOLD activations during the Stroop task. Without PNC, the only activated cluster outside the cerebellum was located along the midline of the upper anterior pons. When analyzing PNC data, significant activations within the SN and a region adjacent to the aqueduct, presumably in the periaqueductal gray, were detected. The activation of the dopaminergic VTA and SN in the Stroop interference contrast was demonstrated previously (Köhler et al., 2016). The periaqueductal gray is an important interface of the midbrain/brainstem to cortical area with connections to areas involved in cognitive control such as the prefrontal and cingulate cortex as well as the ventral striatum (Wager et al., 2004; Faull and Pattinson, 2017). Via nigrostriatal and mesolimbic pathways, BOLD activations of the VTA/SN are associated with goal-directed motivational behavior (Amalric and Koob, 1993; Mannella et al., 2013). Therefore, the detected activations appear far more plausible when underlying data was corrected for the influence of physiological noise. As significant clusters in the Stroop interference contrast of corrected and uncorrected data did not overlap, PNC has fundamental influence on the results of

970
971
972
973
974
975
976
977
978
979
980
981
982
983
984
985
986
987
988
989
990
991
992
993
994
995
996
997
998
999
1000
1001
1002
1003
1004
1005
1006
1007
1008
1009
1010
1011
1012
1013
1014
1015
1016
1017
1018
1019
1020
1021
1022
1023
1024
1025
1026

our study. The analysis of uncorrected data revealed an activation running along the midline of the upper pons – an area susceptible to physiological noise. As our sample is rather small, statistical analyses are particularly vulnerable to spurious results due to artifacts and inaccurate co-registration. Thus, the correction for physiological noise seem essential to reveal adequate results.

In agreement with previous reports, the pupillary response (PDR) was sensitive to different demands of cognitive control in the Stroop task (Siegle et al., 2004; Laeng et al., 2011; Rondeel et al., 2015). Similar to reaction times, PDR decreased over the course of the experiment with a more pronounced decline in the congruent than in the IC. Thus, the learning effect during the task seems to be reflected in pupillary reactions.

Skin conductance responses were not different between both task conditions and were neither related to reaction times nor trial number. However, we observed a marked increase of SCR in the incongruent compared to the congruent condition, which might be statistically detectable in a bigger sample. The time course of skin conductance is determined by a tonic and a phasic component. Stimuli might elicit multiple overlapping SCR as well as an increase of the tonic level (Lim et al., 1997). Although the area under curve was demonstrated to capture SCR characteristics appropriately (Bach et al., 2010; Köhler et al., 2018a), the variance of SCR measures seems to be higher than pupillary indices.

The reactions of physiological signals were used to weight Stroop stimuli. Parametric modulation with SCR led to similar results as the analysis without modulation. In the brainstem/midbrain, the only activation was found in the SN. When events are combined with pupillary responses, a significant activation of a tube-like cluster at the posterior brainstem was found. The activated cluster overlapped with both lateral branches of the upper LC as indicated by the anatomical mask of the LC (Keren et al., 2009). Given the strong co-variation of LC activity during task performance and PD, we hypothesized that the pupillary signal might be useful to track LC activity (Rajkowski et al., 1994; Joshi et al., 2016; Eckstein et al., 2017). It seems that the modulation of Stroop events with physiological information was more accurately modeling the BOLD activation in the LC than the standard GLM.

However, the activated cluster is not completely matching the anatomical demarcation of the LC. The remaining activation between the two lateral branches of the LC might be due to a response of other nuclei located in this region, such as medial reticular nuclei or the dorsal raphe nucleus. Spatial smoothing might blur individual blobs of activation to a great cluster. However, smoothing improves the validity of statistical tests by normalizing the error distribution and compensating for small variations of individual brain anatomy.

Some limitations of our study have to be addressed. A drawback of our experimental design is the lack of luminance control as words presented on the screen vary in length and color. Because luminance was not different in both conditions, a systematic influence on our results seems unlikely. Furthermore,

the statistical power is limited with respect to sample size and number of Stroop stimuli. The parametric modulator had a strong impact on our results, which might be due to the restricted statistical power. However, our results indicate that the statistical analysis benefits from a precise modulation of BOLD activation using physiological markers.

CONCLUSION

In conclusion, we used a sophisticated fMRI technique and physiological recordings to investigate the involvement of brainstem/midbrain nuclei in cognitive control. We demonstrated a positive effect of PNC on data quality and statistical results. Finally, we corroborated previous findings that the dopaminergic SN and noradrenergic LC play a central role in cognitive control and demonstrated the reproducibility of this result on a small sample (Köhler et al., 2016). We investigated PD and skin conductance as autonomic markers of cognitive demand. By including the pupillary responses in our functional data analysis, we validated the location and functional role of the LC. We conclude that physiological signals are useful for modeling noise contaminating the BOLD signal but also BOLD signal changes of interest.

ETHICS STATEMENT

This study was carried out in accordance with the recommendations of the Ethics Committee of the University Hospital Jena. The protocol was approved by the Ethics Committee of the University Hospital Jena. All subjects gave written informed consent in accordance with the Declaration of Helsinki.

AUTHOR CONTRIBUTIONS

AS conceived and designed the study, analyzed and interpreted the data, and prepared the manuscript. SK acquired the data and prepared the manuscript. FC analyzed the data and prepared the manuscript. GW conceived and designed the study, prepared the manuscript, and critically revised the manuscript. DG and JR critically revised the manuscript. K-JB conceived the study, prepared the manuscript, and critically revised the manuscript.

FUNDING

The study was financed by internal funds only.

ACKNOWLEDGMENTS

We thank Dr. Jöran Lepsien and Lina Schaare (Max Planck Institute for Human Cognitive and Brain Sciences, Leipzig, Germany) for their expert technical assistance.

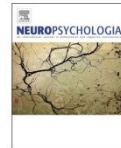
1141 REFERENCES

- 1142
1143 Amalric, M., and Koob, G. F. (1993). Functionally selective neurochemical afferents
1144 and efferents of the mesocorticolimbic and nigrostriatal dopamine system. *Prog.*
1145 *Brain Res.* 99, 209–226. doi: 10.1016/S0079-6123(08)61348-5
- 1146 Ashburner, J. (2007). A fast diffeomorphic image registration algorithm.
1147 *Neuroimage* 38, 95–113. doi: 10.1016/j.neuroimage.2007.07.007
- 1148 Astafiev, S. V., Snyder, A. Z., Shulman, G. L., and Corbetta, M. (2010). Comment
1149 on “Modafinil Shifts Human in the Suprachiasmatic Area”. *Science* 328:309.
1150 doi: 10.1126/science.1177200
- 1151 Aston-Jones, G., and Cohen, J. D. (2005). An integrative theory of locus coeruleus-
1152 norepinephrine function: adaptive gain and optimal performance. *Annu. Rev.*
1153 *Neurosci.* 28, 403–450. doi: 10.1146/annurev.neuro.28.061604.135709
- 1154 Aston-Jones, G., Rajkowski, J., and Cohen, J. (1999). Role of locus coeruleus in
1155 attention and behavioral flexibility. *Biol. Psychiatry* 46, 1309–1320. doi: 10.1016/
1156 S0006-3223(99)00140-7
- 1157 Attar, N., Schneps, M., and Pomplun, M. (2013). Pupil size as a measure of
1158 working memory load during a complex visual search task. *J. Vis.* 13, 160–160.
1159 doi: 10.1167/13.9.160
- 1160 Bach, D. R., Friston, K. J., and Dolan, R. J. (2010). Analytic measures for
1161 quantification of arousal from spontaneous skin conductance fluctuations. *Int.*
1162 *J. Psychophysiol.* 76, 52–55. doi: 10.1016/j.ijpsycho.2010.01.011
- 1163 Bär, K. J., De la Cruz, F., Schumann, A., Koehler, S., Sauer, H., Critchley, H.,
1164 et al. (2016). Functional connectivity and network analysis of midbrain and
1165 brainstem nuclei. *Neuroimage* 134, 53–63. doi: 10.1016/j.neuroimage.2016.
1166 03.071
- 1167 Bechara, A., and Damasio, A. R. (2005). The somatic marker hypothesis: a neural
1168 theory of economic decision Games. *Econ. Behav.* 52, 336–372. doi: 10.1016/j.
1169 geb.2004.06.010
- 1170 Beg, M. F., Miller, M. I., Trounev, A., and Younes, L. (2005). Computing large
1171 deformation metric mappings via geodesic flows of diffeomorphisms. *Int. J.*
1172 *Comput. Vis.* 61, 139–157. doi: 10.1016/j.neuroimage.2009.08.026
- 1173 Beissner, F., Schumann, A., Brunn, F., Eisenträger, D., and Bär, K.-J. (2014).
1174 Advances in functional magnetic resonance imaging of the human
1175 brainstem. *Neuroimage* 86, 91–98. doi: 10.1016/j.neuroimage.2013.
1176 07.081
- 1177 Berridge, C. W., and Waterhouse, B. D. (2003). The locus coeruleus-
1178 noradrenergic system: modulation of behavioral state and state-dependent
1179 cognitive processes. *Brain Res. Rev.* 42, 33–84. doi: 10.1016/S0165-0173(03)
1180 00143-7
- 1181 Birn, R. M., Diamond, J. B., Smith, M. A., and Bandettini, P. A. (2006).
1182 Separating respiratory-variation-related fluctuations from neuronal-activity-
1183 related fluctuations in fMRI. *Neuroimage* 31, 1536–1548. doi: 10.1016/j.
1184 neuroimage.2006.02.048
- 1185 Birn, R. M., Smith, M. A., Jones, T. B., and Bandettini, P. A. (2008). The respiration
1186 response function: the temporal dynamics of fMRI signal fluctuations related
1187 to changes in respiration. *Neuroimage* 40, 644–654. doi: 10.1016/j.neuroimage.
1188 2007.11.059
- 1189 Bouret, S., and Sara, S. J. (2005). Network reset: a simplified overarching theory
1190 of locus coeruleus noradrenergic function. *Trends Neurosci.* 28, 574–582.
1191 doi: 10.1016/j.tins.2005.09.002
- 1192 Briggs, G. G., and Nebes, R. D. (1975). Patterns of hand preference in a student
1193 population. *Cortex* 11, 230–238. doi: 10.1016/S0010-9452(75)80005-0
- 1194 Brooks, J. C. W., Davies, W., and Pickering, A. E. (2017). Resolving the brainstem
1195 contributions to attentional analgesia in man. *J. Neurosci.* 37, 2279–2291.
1196 doi: 10.1523/JNEUROSCI.2193-16.2016
- 1197 Brooks, J. C. W., Faull, O. K., Pattinson, K. T. S., and Jenkinson, M. (2013).
1198 Physiological noise in brainstem fMRI. *Front. Hum. Neurosci.* 7:623. doi: 10.
1199 3389/fnhum.2013.00623
- 1200 Clewett, D. V., Huang, R., Velasco, R., Lee, T.-H., and Mather, M. (2018). Locus
1201 coeruleus activity strengthens prioritized memories under arousal. *J. Neurosci.*
1202 38, 1558–1574. doi: 10.1523/JNEUROSCI.2097-17.2017
- 1203 Corbetta, M., Patel, G., and Shulman, G. L. (2008). The Reorienting system of
1204 the human brain: from environment to theory of mind. *Neuron* 58, 306–324.
1205 doi: 10.1016/j.neuron.2008.04.017
- 1206 Costa, V. D., and Rudebeck, P. H. (2016). More than meets the eye: the relationship
1207 between pupil size and locus coeruleus activity. *Neuron* 89, 8–10. doi: 10.1016/
1208 j.neuron.2015.12.031
- 1209 Critchley, H. D. (2009). Psychophysiology of neural, cognitive and affective
1210 integration: fMRI and autonomic indicators. *Int. J. Psychophysiol.* 73, 88–94.
1211 doi: 10.1016/j.ijpsycho.2009.01.012
- 1212 Critchley, H. D., Tang, J., Glaser, D., Butterworth, B., and Dolan, R. J. (2005).
1213 Anterior cingulate activity during error and autonomic response. *Neuroimage*
1214 27, 885–895. doi: 10.1016/j.neuroimage.2005.05.047
- 1215 Damasio, A. R., Tranel, D., and Damasio, H. C. (1991). “Somatic markers and the
1216 guidance of behavior: theory and preliminary testing,” in *Frontal Lobe Function*
1217 *and Dysfunction*, eds H. S. Levin, H. M. Eisenberg, and A. L. Benton (New York,
1218 NY: Oxford University Press), 217–229.
- 1219 de Gee, J. W., Colizoli, O., Kloosterman, N. A., Knapen, T., Nieuwenhuis, S., and
1220 Donner, T. H. (2017). Dynamic modulation of decision biases by brainstem
1221 arousal systems. *eLife* 6:23232. doi: 10.7554/eLife.23232
- 1222 Diedrichsen, J. (2006). A spatially unbiased atlas template of the human cerebellum.
1223 *Neuroimage* 33, 127–138. doi: 10.1016/j.neuroimage.2006.05.056
- 1224 Eckstein, M. K., Guerra-Carrillo, B., Miller Singley, A. T., and Bunge, S. A. (2017).
1225 Beyond eye gaze: what else can eyetracking reveal about cognition and cognitive
1226 development? *Dev. Cogn. Neurosci.* 25, 69–91. doi: 10.1016/j.dcn.2016.11.001
- 1227 Edelberg, R. (1993). “Electrodermal mechanisms: a critique of the two-effector
1228 hypothesis and a proposed replacement,” in *Progress Electrodermal Research*,
1229 eds J. Roy, W. Boucsein, D. C. Fowles, and J. H. G. Ruzelie (New York, NY:
1230 Plenum Press), 7–29.
- 1231 Faull, O. K., and Pattinson, K. T. S. (2017). The cortical connectivity of the
1232 periaqueductal gray and the conditioned response to the threat of
1233 breathlessness. *eLife* 6:21749. doi: 10.7554/eLife.21749
- 1234 Fernandes, P., Regala, J., Correia, F., and Gonçalves-Ferreira, A. J. (2012). The
1235 human locus coeruleus 3-D stereotactic anatomy. *Surg. Radiol. Anat.* 34,
1236 879–885. doi: 10.1007/s00276-012-0979-y
- 1237 Fritz, T., Beigel, A., Müller, S. C., Yigit-Elliott, S., and Zuger, M. (2014).
1238 “Using psycho-physiological measures to assess task difficulty in software
1239 development,” in *Proceedings of the 36th ICSE 2014*, Hyderabad, 402–413. doi:
1240 10.1145/2568225.2568266
- 1241 German, D. C., Walker, B. S., Manaye, K., Smith, W. K., Woodward, D. J., and
1242 North, A. J. (1988). The human locus coeruleus: computer reconstruction of
1243 cellular distribution. *J. Neurosci.* 8, 1776–1788. doi: 10.1523/JNEUROSCI.08-
1244 05-01776.1988
- 1245 Glover, G. H., Li, T. Q., and Ress, D. (2000). Image-based method for retrospective
1246 correction of physiological motion effects in fMRI: retroicor. *Magn. Reson.*
1247 *Med.* 44, 162–167. doi: 10.1002/1522-2594(200007)44:1<162::AID-MRM23>
1248 3.0.CO;2-E
- 1249 Granholm, E., and Steinhauer, S. (2009). Introduction: pupillometric measures of
1250 cognitive and emotional processes. *Int. J. Psychophysiol.* 73, 88–94.
- 1251 Grant, S. J., Aston-Jones, G., and Redmond, D. E. (1988). Responses of primate
1252 locus coeruleus neurons to simple and complex sensory stimuli. *Brain Res. Bull.*
1253 21, 401–410. doi: 10.1016/0361-9230(88)90152-9
- 1254 Hämmerer, D., Callaghan, M. F., Hopkins, A., Kosciessa, J., and Betts, M. (2017).
1255 Locus coeruleus integrity in old age is selectively related to memories linked
1256 with salient negative events. *Proc. Natl. Acad. Sci. U.S.A.* 115, 2228–2233. doi:
1257 10.1073/pnas.1712268115
- 1258 Harvey, A. K., Pattinson, K. T. S., Brooks, J. C. W., Mayhew, S. D., Jenkinson, M.,
1259 and Wise, R. G. (2008). Brainstem functional magnetic resonance imaging:
1260 disentangling signal from physiological noise. *J. Magn. Reson. Imaging* 28,
1261 1337–1344. doi: 10.1002/jmri.21623
- 1262 Hogervorst, M. A., Brouwer, A. M., and van Erp, J. B. F. (2014). Combining
1263 and comparing EEG, peripheral physiology and eye-related measures for the
1264 assessment of mental workload. *Front. Neurosci.* 8:322. doi: 10.3389/fnins.2014.
1265 00322
- 1266 Jacobs, S. C., Friedman, R., Parker, J. D., Tofler, G. H., Jimenez, A. H., Muller, J. E.,
1267 et al. (1994). Use of skin conductance changes during mental stress testing as
1268 an index of autonomic arousal in cardiovascular research. *Am. Heart J.* 128,
1269 1170–1177. doi: 10.1016/0002-8703(94)90748-X
- 1270 Jo, H. J., Saad, Z. S., Simmons, W. K., Milbury, L. A., and Cox, R. W. (2010).
1271 Mapping sources of correlation in resting state fMRI, with artifact detection
1272 and removal. *Neuroimage* 52, 571–582. doi: 10.1016/j.neuroimage.2010.
1273 04.246
- 1274 Joshi, S., Li, Y., Kalwani, R. M., and Gold, J. I. (2016). Relationships between pupil
1275 diameter and neuronal activity in the locus coeruleus, colliculi, and cingulate
1276 cortex. *Neuron* 89, 221–234. doi: 10.1016/j.neuron.2015.11.028
- 1277

- 1255 Kahneman, D., Tursky, B., Shapiro, D., and Crider, A. (1969). Pupillary, heart rate,
1256 and skin resistance changes during a mental task. *J. Exp. Psychol.* 79, 164–167.
1257 doi: 10.1037/h0026952
- 1258 Keren, N. I., Lozar, C. T., Harris, K. C., Morgan, P. S., and Eckert, M. A. (2009).
1259 In vivo mapping of the human locus coeruleus. *Neuroimage* 47, 1261–1267.
1260 doi: 10.1016/j.neuroimage.2009.06.012
- 1261 Keren, N. I., Taheri, S., Vazey, E. M., Morgan, P. S., Granholm, A. C. E., Aston-
1262 Jones, G. S., et al. (2015). Histologic validation of locus coeruleus MRI contrast
1263 in post-mortem tissue. *Neuroimage* 113, 235–245. doi: 10.1016/j.neuroimage.
1264 2015.03.020
- 1265 Köhler, S., Bär, K. J., and Wagner, G. (2016). Differential involvement of brainstem
1266 noradrenergic and midbrain dopaminergic nuclei in cognitive control. *Hum.
1267 Brain Mapp.* 37, 2305–2318. doi: 10.1002/hbm.23173
- 1268 Köhler, S., Schumann, A., Cruz, F. D., Wagner, G., and Bär, K. (2018a). Towards
1269 response success prediction: an integrative approach using high-resolution
1270 fMRI and autonomic indices. *Neuropsychologia* 119, 182–190. doi: 10.1016/j.
1271 neuropsychologia.2018.08.003
- 1272 Köhler, S., Wagner, G., and Bär, K. (2018b). Activation of brainstem and midbrain
1273 nuclei during cognitive control in medicated patients with schizophrenia. *Hum.
1274 Brain Mapp.* doi: 10.1002/hbm.24365 [Epub ahead of print].
- 1275 Köhlich, O., and Schaefer, F. (1996). Physiological changes during computer tasks:
1276 responses to mental load or to motor demands? *Ergonomics* 39, 213–224.
- 1277 Laeng, B., Ørbo, M., Holmlund, T., and Miozzo, M. (2011). Pupillary stroop effects.
1278 *Cogn. Process.* 12, 13–21. doi: 10.1007/s10339-010-0370-z
- 1279 Laeng, B., Sirois, S., and Gredeback, G. (2012). Pupillometry: a window to the
1280 preconscious? *Perspect. Psychol. Sci.* 7, 18–27. doi: 10.1177/1745691611427305
- 1281 Lim, C. L., Rennie, C., Barry, R. J., Bahramali, H., Lazzaro, L., Manor, B., et al.
1282 (1997). Decomposing skin conductance into tonic and phasic components. *Int.
1283 J. Psychophysiol.* 25, 97–109. doi: 10.1016/S0167-8760(96)00713-1
- 1284 Linman, C., Zeidan, M. A., Pitman, R. K., and Milad, M. R. (2013). Resting
1285 cerebral metabolism correlates with skin conductance and functional brain
1286 activation during fear conditioning. *Biol. Psychol.* 92, 26–35. doi: 10.1016/j.
1287 biopsych.2012.03.002
- 1288 Mannella, F., Gurney, K., and Baldassarre, G. (2013). The nucleus accumbens as a
1289 nexus between values and goals in goal-directed behavior: a review and a new
1290 hypothesis. *Front. Behav. Neurosci.* 7, 135. doi: 10.3389/fnbeh.2013.00135
- 1291 Mehler, B., Reimer, B., Coughlin, J. F., and Dusek, J. A. (2009). Impact of
1292 incremental increases in cognitive workload on physiological arousal and
1293 performance in young adult drivers. *Transp. Res. Rec. J. Transp. Res. Board* 2138,
1294 6–12. doi: 10.3141/2138-02
- 1295 Miller, E. K., and Cohen, J. D. (2001). An integrative theory of prefrontal cortex
1296 function. *Neurosci. Res.* 24, 167–202.
- 1297 Murphy, P. R., O'Connell, R. G., O'Sullivan, M., Robertson, I. H., and Balsters, J. H.
1298 (2014). Pupil diameter covaries with BOLD activity in human locus coeruleus.
1299 *Hum. Brain Mapp.* 35, 4140–4154. doi: 10.1002/hbm.22466
- 1300 Patterson, J. (2002). Task-independent functional brain activity correlation with
1301 skin conductance changes: an fMRI study. *Neuroimage* 17, 1797–1806. doi:
1302 10.1006/nimg.2002.1306
- 1303 Querino, E., Dos Santos, L., Ginani, G., Nicolau, E., Miranda, D., Romano-
1304 Silva, M., et al. (2015). Cognitive effort and pupil dilation in controlled and
1305 automatic processes. *Transl. Neurosci.* 6, 168–173. doi: 10.1515/tnsci-2015-
1306 0017
- 1307 Rajkowski, J., Kubiak, P., and Aston-Jones, G. (1994). Locus coeruleus activity in
1308 monkey: phasic and tonic changes are associated with altered vigilance. *Brain
1309 Res. Bull.* 35, 607–616. doi: 10.1016/0361-9230(94)90175-9
- 1310 Reimer, B., and Mehler, B. (2011). The impact of cognitive workload
1311 on physiological arousal in young adult drivers: a field study and
1312 simulation validation. *Ergonomics* 54, 932–942. doi: 10.1080/00140139.2011.
1313 604431
- 1314 Rondeel, E. W. M., van Steenbergen, H., Holland, R. W., and van Knippenberg, A.
1315 (2015). A closer look at cognitive control: differences in resource allocation
1316 during updating, inhibition and switching as revealed by pupillometry. *Front.
1317 Hum. Neurosci.* 9:494. doi: 10.3389/fnhum.2015.00494
- 1318 Samuels, E. R., and Szabadi, E. (2008a). Functional neuroanatomy of the
1319 noradrenergic locus coeruleus: its roles in the regulation of arousal and
1320 autonomic function part I: principles of functional organisation. *Curr.
1321 Neuropharmacol.* 6, 235–253. doi: 10.2174/157015908785777229
- 1322 Samuels, E. R., and Szabadi, E. (2008b). Functional neuroanatomy of the
1323 noradrenergic locus coeruleus: its roles in the regulation of arousal
1324 and autonomic function part II: physiological and pharmacological
1325 manipulations and pathological alterations of locus coeruleus activity in
1326 humans. *Curr. Neuropharmacol.* 6, 254–285. doi: 10.2174/15701590878577
1327 7193
- 1328 Sequeira, H., and Roy, J.-C. (1993). "Cortical and hypothalamolimbic control of
1329 electrodermal responses progress," in *Electrodermal Research*, eds J. I. Roy, W.
1330 Boucsein, D. C. Fowles, and J. H. Gruzelier (New York, NY: Plenum Press),
1331 93–114.
- 1332 Sheehan, D. V., Lecrubier, Y., Sheehan, K. H., Amorim, P., Janavs, J., Weiller, E.,
1333 et al. (1998). The development and validation of a structured diagnostic
1334 psychiatric interview for DSM-IV and ICD-10. *J. Clin. Psychiatry* 59,
1335 22–33.
- 1336 Siegle, G. J., Steinhauer, S. R., and Thase, M. E. (2004). Pupillary assessment and
1337 computational modeling of the Stroop task in depression. *Int. J. Psychophysiol.*
1338 52, 63–76. doi: 10.1016/j.ijpsycho.2003.12.010
- 1339 Sirois, S., and Brisson, J. (2014). Pupillometry. *Wiley Interdiscip. Rev. Cogn. Sci.* 5,
1340 679–692. doi: 10.1002/wcs.1323
- 1341 Steinhauer, S. R., Siegle, G. J., Condray, R., and Pless, M. (2004). Sympathetic and
1342 parasympathetic innervation of pupillary dilation during sustained processing.
1343 *Int. J. Psychophysiol.* 52, 77–86. doi: 10.1016/j.ijpsycho.2003.12.005
- 1344 Stroop, J. R. (1935). Studies of interference in serial verbal reactions. *J. Exp. Physiol.*
1345 18, 643–662. doi: 10.1037/h0054651
- 1346 Urai, A. E., Braun, A., and Donner, T. H. (2017). Pupil-linked arousal is driven
1347 by decision uncertainty and alters serial choice bias. *Nat. Commun.* 8:14637.
1348 doi: 10.1038/ncomms14637
- 1349 Vö, M. L. H., Jacobs, A. M., Kuchinke, L., Hofmann, M., Conrad, M., Schacht, A.,
1350 et al. (2008). The coupling of emotion and cognition in the eye: introducing the
1351 pupil old/new effect. *Psychophysiology* 45, 130–140.
- 1352 Wager, T. D., Rilling, J. K., Smith, E. E., Sokolik, A., Casey, K. L., Davidson,
1353 R. J., et al. (2004). Placebo-Induced changes in fMRI in the anticipation and
1354 experience of pain. *Science* 303, 1162–1167. doi: 10.1126/science.1093065
- 1355 Wagner, G., De la Cruz, F., Schachtzabel, C., Güllmar, D., Schultz, C. C., Schlösser,
1356 R. G., et al. (2015). Structural and functional dysconnectivity of the fronto-
1357 thalamic system in schizophrenia: a DCM-DTI study. *Cortex* 66, 35–45.
1358 doi: 10.1016/j.cortex.2015.02.004
- 1359 Wagner, G., Sinsel, E., Sobanski, T., Köhler, S., Marinou, V., Mentzel, H. J., et al.
1360 (2006). Cortical Inefficiency in Patients with Unipolar depression: an event-
1361 related fMRI study with the stroop task. *Biol. Psychiatry* 59, 958–965. doi:
1362 10.1016/j.biopsych.2005.10.025
- 1363 Yamamoto, K., Arai, H., and Nakayama, S. (1990). Skin conductance response
1364 after 6-hydroxydopamine lesion of central noradrenergic system in rats. *Biol.
1365 Psychiatry* 28, 151–160. doi: 10.1016/0006-3223(90)90632-C
- 1366 Zekveld, A. A., Kramer, S. E., and Festen, J. M. (2010). Pupil response as an
1367 indication of effortful listening: the influence of sentence intelligibility. *Ear
1368 Hear.* 31, 480–490. doi: 10.1097/AUD.0b013e3181d4f251

Conflict of Interest Statement: The authors declare that the research was conducted in the absence of any commercial or financial relationships that could be construed as a potential conflict of interest.

Copyright © 2018 Schumann, Köhler, de la Cruz, Güllmar, Reichenbach, Wagner and Bär. This is an open-access article distributed under the terms of the Creative Commons Attribution License (CC BY). The use, distribution or reproduction in other forums is permitted, provided the original author(s) and the copyright owner(s) are credited and that the original publication in this journal is cited, in accordance with accepted academic practice. No use, distribution or reproduction is permitted which does not comply with these terms.



Towards response success prediction: An integrative approach using high-resolution fMRI and autonomic indices



Stefanie Köhler, Andy Schumann, Feliberto de la Cruz, Gerd Wagner, Karl-Jürgen Bär*

Psychiatric Brain and Body Research Group, Department of Psychiatry and Psychotherapy, Jena University Hospital, Jena, Germany

ARTICLE INFO

Keywords:

Response inhibition
Error processing
High-resolution functional imaging
Success prediction
Ventral tegmental area

ABSTRACT

Brainstem and midbrain nuclei are closely linked to effective cognitive performance and autonomic function. In the present study, we aimed to investigate indices of successful and unsuccessful response inhibition paying particular attention to the interplay between locus coeruleus (LC), ventral tegmental area (VTA)/substantia nigra (SN) and, most importantly, peripheral markers. We aimed to get insight in the predictive value of neural and physiological signals in response inhibition.

A total of 35 healthy controls were recruited from the local community and a typical task of behavioral response inhibition (Go/No-Go paradigm) was applied. We used high-resolution fMRI, advanced brainstem analyses and specifically corrected for respiratory signal and cardiac noise.

Our main results characterize specific neural activation patterns during successful and unsuccessful response inhibition especially comprising the anterior cingulate as well as the medial and lateral prefrontal cortex. A significant activation of the dopaminergic nuclei (VTA/SN) was found during error processing, but not during response inhibition. Most remarkably, specific neural activation patterns (i.e., dorsal anterior cingulate cortex) as well as accompanying autonomic indices (i.e., skin conductance response (SCR)) were identified to hold predictive information on an individual's performance.

In summary, the importance of the VTA/SN during error processing was shown. Furthermore, autonomic indices and specific neural activation patterns may contain valuable information to predict task performance.

1. Introduction

Spontaneous and rash behavior is characteristic for impulsive individuals and might frequently result in behavioral failures. Some psychiatric disorders (e.g., attention deficit hyperactivity disorder; Brewer and Potenza, 2008) are characterized by elevated impulsivity or diminished behavioral flexibility, which can result in adverse consequences for both the individual itself and the social environment. It is assumed that impulsivity might arise due to deficient inhibitory processes (Bari and Robbins, 2013). In order to improve the psychopharmacological as well as psychotherapeutic support regarding patients suffering from disorders associated with response inhibition deficits, a comprehensive understanding of its mechanisms is indispensable.

Inhibitory control can be subdivided into a cognitive and behavioral/motor domain (Bari and Robbins, 2013). In a recent study of our group (Köhler et al., 2016), we analyzed the former and showed the functional integration of the noradrenaline (NA) producing locus coeruleus (LC) and dopaminergic (DA) nuclei, i.e., the ventral

tegmental area (VTA) and substantia nigra (SN), in the cognitive control network in humans. In our present investigation, we aimed to study the behavioral/motor domain of cognitive control (i.e., response inhibition) and its neural correlates. A central component of this domain is action restraint, which represents the inhibition of a pre-potent response. Therefore, we aim to show whether the cognitive control network is activated during response inhibition integrating the LC and VTA/SN in the analysis. Differences in network composition depending on, for instance, cognitive domain and type of task are feasible. A typical task to measure the ability to inhibit a pre-potent response is the Go/No-Go paradigm (Bari and Robbins, 2013), in which subjects face categorical decisions requiring a response to the “Go” or to withhold a response to the “No-Go” type.

A successful inhibition of pre-potent motor responses (No-Go trials) depends on fronto-striatal loops including the inferior frontal gyrus, the (pre-) supplementary motor area (SMA) and the striatum (Alexander and Crutcher, 1990; Aron and Poldrack, 2006; Jentsch and Taylor, 1999; Simmonds et al., 2008). Deficits in the dorsomedial prefrontal cortex (DMPFC) were found to be responsible for impaired

* Correspondence to: Department of Psychiatry and Psychotherapy, University Hospital Jena, Philosophenweg 3, 07743 Jena, Germany.
E-mail address: Karl-Juergen.Baer@med.uni-jena.de (K.-J. Bär).

<https://doi.org/10.1016/j.neuropsychologia.2018.08.003>

Received 3 April 2018; Received in revised form 28 July 2018; Accepted 3 August 2018

Available online 06 August 2018

0028-3932/ © 2018 Elsevier Ltd. All rights reserved.

performances in Go/No-Go tasks (Godefroy et al., 1996). Patients with lesions including the (pre-)SMA and subdivisions of the anterior cingulate cortex (ACC) showed prolonged reaction times and increased error-rates (Picton et al., 2007; Stuss et al., 2002).

In our previous study, we were unable to study response failure and the possible involvement and predictive value of the LC and VTA/SN in error processing due to a very low number of error trials (Köhler et al., 2016). Thus, the activated whole-brain network during error processing as well as the integration of the LC and VTA/SN needs further clarification.

Error processing is a fundamental cognitive function for adaptive behavior (Lim et al., 2015). When performance errors occur, there is an increased need for behavioral monitoring and cognitive control (Botvinick et al., 2001; Cohen et al., 2000). Failures of response inhibition in No-Go trials usually result in behavioral adaption that can be observed immediately in terms of response slowing in following Go-trials. The brain's error processing network comprises the DMPFC, ACC and SMA (Garavan et al., 2002; van Noortd and Segalowitz, 2012). The error-related brain potential (ERP) induced by incorrect behavioral responses (Gehring et al., 1993; Gehring et al., 2000) was often linked to the ACC (Agam et al., 2014; Miltner et al., 1997; Miltner et al., 2003). The dorsal ACC (dACC) was also associated with attentional and performance monitoring (Shenhav et al., 2016). Error commission is also linked to significant autonomic responses that might facilitate a re-direction of attentional focus and performance adjustment (Bechara et al., 1997). The dACC seems to act as interface between cognitive, behavioral and autonomic regulation systems during of error processing (Critchley et al., 2005).

Human and non-human studies have indicated the importance of the dopaminergic system for inhibitory control. The main dopamine-producing regions VTA/SN are located in the midbrain. Both regions have strong projections to the prefrontal cortex (PFC), the ACC and to the striatum respectively, referred to as mesocortical and nigrostriatal dopaminergic pathways. Goschke and Bolte (2014) proposed that the nigrostriatal pathway modulates cognitive/behavioral control by integrating flexible and stimulus-dependent behavioral tendencies, mainly in the striatum. Goal persistence is modulated by the mesocortical pathway. The dopaminergic neurotransmitter system seems to modulate motor readiness for both response inhibition and activation (Bari et al., 2009). Moreover, dopamine was suggested to be an important neurotransmitter in error processing (Bari and Robbins, 2013; Nandam et al., 2013) and was implicated to impact on the autonomic nervous system (ANS) (Kur'yanova et al., 2017).

The locus coeruleus (LC) is a brainstem structure containing noradrenaline producing neurons. In their review, Aston-Jones and Cohen (2005) emphasized the specific role of the LC in cognitive flexibility. The authors proposed that enhanced LC activity produces a temporally specific release of noradrenaline, which increases the gain of specific task-associated cortical networks and optimizes task appropriate behavior. Besides, the noradrenergic neurotransmitter system seems to be critically involved in inhibiting an already initiated response (Eagle et al., 2008; Robbins and Arnsten, 2009). Thus, a decisive role of the dopaminergic and noradrenergic neurotransmitter systems in successful and unsuccessful response inhibition can be assumed (Claassen et al., 2017; Eagle et al., 2007; Kohno et al., 2016).

The brainstem, as a relay and processing station between the spinal cord, cerebellum and neocortex, contains vital nodes of various functional systems in the central nervous system (CNS) including the autonomic nervous system (ANS). The ANS regulates, for instance, the respiratory, cardiac, vasomotor, and endocrine system to adapt behavior to motor, emotional or cognitive challenges (Critchley et al., 2005; Thayer and Lane, 2000). A growing number of studies have investigated the role of different cortical and subcortical brain regions involved in autonomic control. Important brain regions associated with ANS regulation are the ACC, insula, amygdala, SMA, prefrontal cortices and the midbrain (i.e., VTA) (Beissner et al., 2013).

To gain a more comprehensive understanding of response inhibitory mechanisms, we aimed to combine information from relevant systems (e.g., CNS, ANS) involved (Critchley, 2009; Critchley et al., 2005). Some studies already suggested a close interaction between the peripheral ANS and the CNS in response inhibition and error processing (Critchley et al., 2003; Hajcak et al., 2003; Hofmann et al., 2009; Zhang et al., 2012, 2015). For instance, previous research showed enhanced skin conductance responses (SCRs) to errors in impulsive individuals (Zhang et al., 2012, 2015). Hajcak et al. (2003) applied electroencephalography and a modified Stroop task and found a fronto-centrally negative deflection in the ERP signal as well as an elevation in SCR in error trials. SCR is an important autonomic measure of psychophysiology research since it reflects sympathetic neural responses independently of direct parasympathetic control. SCR is suggested to be closely related to dACC activity (Critchley et al., 2001; Nagai et al., 2004; Zhang et al., 2014) and is used as an indirect measure of cognitive effort. For instance, healthy subjects were found to show increases in SCR prior decision making (Bechara et al., 1997) and the magnitude of ACC activity strongly reflected the degree of anticipatory arousal indexed by SCR (Critchley et al., 2001). Mehler et al. (2009) reported that SCR changes indicate cognitive workload already before the appearance of a clear decline in performance. Moreover, Zhang et al. (2012) applied a Stop-Signal Task and found that fluctuations in SCR during Go trials which followed another Go trial are driven by participants' effort in negotiating between speed and accuracy. In contrast, changes in SCR during trials following a Stop signal are in response to an antecedent response conflict. Thus, there is some evidence that the physiological state might influence successful response inhibition, behavioral monitoring and, remarkably, might already hold predictive information for performance accuracy.

In order to improve our understanding of human behavior and associated dysfunctions, we need to acquire a comprehensive understanding of the interplay between peripheral ANS and CNS in response inhibition focusing on the definite involvement of the dopaminergic and noradrenergic neurotransmitter systems. Here, we used high-resolution functional magnetic resonance imaging (fMRI) during a Go/No-Go task and an MRI-compatible multi-channel physiological recording system to answer the following questions: First, we aimed to identify the neural correlates of successful response inhibition in the Go/No-Go task. Based on our previous study (Köhler et al., 2016) and fMRI studies on response inhibition, we hypothesized increased BOLD activations in the cognitive control network accompanied by increased activation in dopaminergic (VTA/SN) and noradrenergic (LC) centers. Second, we aimed to analyze neural correlates of unsuccessful response inhibition. Based on findings regarding error processing (Shenhav et al., 2016), we assumed increased activation in the dACC and VTA/SN. Further, we want to explore the relationship between these structures and response monitoring, e. g. post-error slowing. Third, we focused on SCR to analyze correct and failed inhibitory responses. In particular, a larger SCR during failed compared to correct No-Go trials was assumed. Fourth, we wanted to get further insight in the predictive value of physiological and neural signals in response inhibition. We hypothesized that significant changes in SCR and neural activation (e.g., dACC) occur immediately before successful and unsuccessful response inhibition.

2. Materials and methods

2.1. Subjects

A total of 35 healthy controls were recruited from the local community. Two subjects were excluded from the final analysis because they reported forgotten task instructions. Thus, the final sample comprised 33 subjects (age $M = 26.8$ years; $SD = 5.2$ years; range: 20–40 years; 17 females). Individuals with past or current drug use, sleeping problems, excessive training, intermistic peculiarities, neurological or

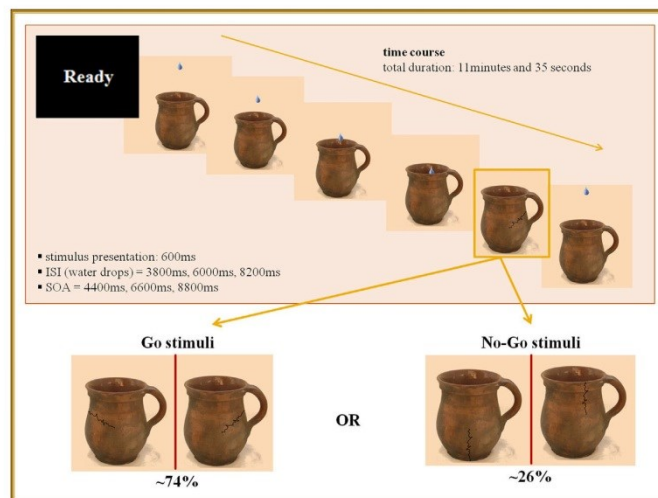


Fig. 1. Description of our Go/No-Go task: Before the experiment, the paradigm, i.e. the clay jug and the water drops falling into it, as well as the Go and No-Go stimulus types were explained to participants. They were instructed to respond as fast as possible on Go trials and to withhold their response on No-Go trials. The importance of response speed was particularly emphasized. To make sure the instructions were correctly understood, a short practice trial was run before the start of the experiment. At the beginning, people saw the word 'READY' in white capital letters in the middle of a black screen. Then, 'READY' was replaced by a clay jug, in which water was dropping much frequented representing our baseline measure. After varying time intervals a stimulus appeared which was either a Go or a No-Go trial. The Go stimuli are two kinds of transverse cracks either starting from the left handed side or from the right-handed side of the jug. The No-Go stimuli are two kinds of vertical cracks either starting from the upper end or from the bottom end of the jug. The stimuli were presented for 600 ms. The inter-stimulus-intervals (ISI) were 3800 ms, 6000 ms and 8200 ms which were presented one after the other and in equal parts, where the related stimulus-onset asynchronies (SOAs) were 4400 ms, 6600 ms and 8800 ms. Moreover, stimulus presentation onsets were jittered in order to prevent any signaling function of the water drops regarding the stimulus timing and to have a better time resolution of the hemodynamic

responses. All subjects were asked to indicate which type of crack was presented by either pressing a button (with the right index finger) as fast as possible when a Go stimulus appeared or by restraining their response when a No-Go stimulus appeared. Immediately after stimulus presentation water kept on dropping into the jug. To create a pre-potent response tendency, there were more Go stimuli (in ~ 74% of cases) than No-Go stimuli (in ~ 26% of cases). In sum, our Go/No-Go experiment lasted for 11 min and 35 s comprising 81 Go and 21 No-Go stimuli.

psychiatric diseases according to M.I.N.I (Sheehan et al., 1998) and/or first-degree relatives with Axis I psychiatric disorders were excluded. All subjects were German native speakers, right-handed according to the modified version of Annett's Handedness Inventory (Briggs and Nebes, 1975) and provided written informed consent prior to participating. The study protocol was approved by the Ethics Committee of the University of Jena. All subjects were paid 8 Euro per hour for their participation.

2.2. Experimental paradigm

The Go/No-Go paradigm is a commonly used task to measure the ability to inhibit a pre-potent response. The No-Go-signal, which triggers the inhibitory processes, is presented unexpectedly following a Go-signal, measuring the inhibition of a planned response (action restraint; Eagle et al., 2008). Our research group developed a modified version of the task which is described in detail in Fig. 1.

2.3. Trait Impulsivity

Impulsivity, as a personality trait, was assessed by the Barratt Impulsivity Scale 11 (BIS-11; Patton et al., 1995), which is a self-report questionnaire and consists of the attentional, motor and non-planning subscale.

2.4. MRI parameters

Functional data were collected on a 3 T Siemens TIM Trio whole body system (Siemens, Erlangen, Germany) equipped with a 64-element receive-only head matrix coil. T_2^* -weighted images were obtained using a gradient-echo EPI sequence (TR = 2120 ms, TE = 36 ms, TA = 2100 ms, FOV = 224 mm², acquisition matrix = 160 × 160 mm², flip angle = 90°) with 104 interleaved transverse slices of 1.4 mm thickness, a multi-band acceleration factor of 4 and with in-plane resolution of 1.4 × 1.4 mm². A series of 310 whole-brain volume sets were acquired in one session. High-resolution anatomical T1-weighted

images (MP-RAGE) were obtained with an isotropic resolution of 1 × 1 × 1 mm³ (TR = 2300 ms, TE = 2.07 ms, TA = 2288 ms, TI = 900 ms, flip angle = 9°, acquisition matrix = 256 × 256 mm², FOV = 256 mm, number of sagittal slices = 192).

2.5. Physiological recordings during fMRI

Photoplethysmogram (PPG), respiration and skin conductance (SC) were recorded throughout MR image acquisition using an MR-compatible polygraph MP150 (BIOPAC Systems Inc., Goleta, CA, USA). Respiratory activity was assessed by a strain gauge transducer incorporated in a belt that was tied around the chest, approximately at the level of the processus xiphoideus. The PPG sensor was attached to the proximal phalanx of the left index finger. SC was measured continuously (constant voltage technique) at the left hands' palm with Ag/AgCl electrodes placed at the thenar and hypothenar eminence. All signals were sampled at 500 Hz and amplified in a frequency range of 0.05–3 Hz for PPG, 0.05–10 Hz for respiration and 0–10 Hz for SC. Respiration and SC were offline median filtered (window of 250 samples) and smoothed (over 500 samples) to reduce MRI-related artifacts. The PPG signal was smoothed over 50 sample and differentiated. Pulse-wave onsets were automatically extracted by detecting peaks of the temporal derivative. The quality of the peak detection was visually inspected.

2.6. Physiological-noise correction

Prior to preprocessing, physiological fluctuations synchronized with cardiac and respiratory cycles were removed using the RETROICOR approach (Glover et al., 2000). To account for low frequency variations in the BOLD signal through slow blood oxygenation level fluctuations, five respiration volumes per time (RVT) regressors were additionally removed (Birn et al., 2008). The RVT regressors consisted of the RVT function and four delayed terms at 5, 10, 15, and 20 s (Birn et al., 2008; Jo et al., 2010), while 8 low-order Fourier time series (4 based on the cardiac phase and 4 on the respiratory phase) were created using the

RETROICOR algorithm. All regressors were generated on a slice-wise basis by AFNI's RetroTS.m script implemented in MATLAB 2016b, which takes the cardiac and respiratory time series synchronized with the fMRI acquisition as input. By combining the RETROICOR with RVT regressors, we ensured a “cleaned” BOLD signal from almost all respiratory-induced fluctuations.

2.7. Univariate functional data analyses

For image processing and statistical analyses, we used the SPM12 software (<http://www.fil.ion.ucl.ac.uk/spm>). After standard pre-processing steps using physiological-noise corrected data, the data were smoothed with a Gaussian filter of 4 mm FWHM, high-pass filtered (128 s) and corrected for serial correlations. Subsequently, data were analyzed voxel-wise within a general linear model (GLM) to calculate parametric maps of *t*-statistics for condition-specific effects and for each subject. In order to test our hypotheses regarding successful/unsuccessful response inhibition and its prediction, three different fixed-effects models were defined to create images of parameter estimates. Different models were computed, because the number of stimuli in each regressor of the respective model (successful/unsuccessful response inhibition and pre-error processing) was matched to either the number of correct or incorrect No-Go trials. The matching procedure happened in a randomized manner letting a MATLAB routine (based on the built-in function *randperm.m*) randomly select a matching number of events (either respecting the number of correct or incorrect No-Go events). The remaining stimuli, which were not used in the matching procedure, as well as the individual movement parameters were entered in the respective single-subject fixed-effects model as covariates of no interest. Parameter estimates were then entered into the particular second-level random-effects analyses. Thus, three ANOVAs were set up with each having the within-subjects factor TASK. In the first ANOVA (inhibitory control), we compared successful response inhibition (C No-Go) and successful responses (Go). In the second ANOVA (error processing), we compared unsuccessful response inhibition (IC No-Go) with successful response inhibition (C No-Go). In the third ANOVA (pre-error processing), we compared the Go stimuli preceding either another Go (with again two other Go's beforehand), a correct No-Go (pre-C) or an incorrect No-Go (pre-IC) event and finally contrasted pre-correct Go responses (pre-C) and pre-error Go responses (pre-IC). The statistical comparisons were thresholded on the voxel-level at $p < 0.001$ (uncorrected) and $p < 0.05$ FWE corrected at the cluster-level as recommended by Woo et al. (2014).

2.8. fMRI analysis of brainstem/cerebellum using SUIT toolbox

When whole-brain analyses revealed BOLD activation in the mid-brain/brainstem, we used the SUIT toolbox to conduct a more precise analysis. To improve the normalization procedure regarding the brainstem, the cropped brainstem/cerebellum data were normalized using a DARTEL engine to the spatially unbiased infra-tentorial template (SUIT, version 3.1; (Diedrichsen, 2006)) and smoothed with a Gaussian filter of 4 mm FWHM. The SUIT toolbox provides a new high-resolution atlas template of the human brainstem/cerebellum. After high-pass filtering and correction for serial correlations, a fixed-effects model (the same as at the whole-brain level) at the single-subject level was set-up with preprocessed functional brainstem/cerebellum images to create images of parameter estimates for the subsequent random-effects group analyses (RFX). The statistical comparison was thresholded on the voxel-level at $p < 0.001$ (uncorrected) and $p < 0.05$ FWE corrected at the cluster-level.

2.9. Physiological data analysis

Event-related SC responses were estimated on SC signals after removing the slowly varying component (SC smoothed over 10.000

samples). SC time courses at the onset of each Go/No-Go stimulus (reference time $t = 0$, lasting 6 s) were extracted and normalized to baseline (mean SC in 1 s before stimulus onset). We averaged responses per subject in C and IC, as well as in pre-IC and pre-C trials. Reactions of SC were quantified in terms of area under the curve by integrating subject-specific responses (Bach et al., 2010). SCR is given in normalized units (n.u.) and was compared between trials using the Wilcoxon signed-rank test (IC vs. C, pre-IC vs. pre-C).

2.10. Correlational analysis

Using SPSS Statistics V22, we conducted Spearman's correlational analyses including physiological parameters, self-ratings and behavioral performance scores, as well as the mean contrast estimates across all voxels within the significant VTA/SN cluster during error processing and the significant dACC cluster pre- and during response failure using SPM12. Because of the large extent of the cingular cluster activated during error processing, we created a sphere of 6 mm around the local maximum comprising dACC [centered at $x = 2$, $y = 20$, $z = 31$] and extracted the mean contrast estimates across all included voxels. All pairwise tests were FDR corrected to account for multiple comparison problems.

2.11. Behavioral data analysis

Behavioral data analyses were performed using SPSS Statistics V22 and paired *t*-tests. Potential differences in response accuracy were analyzed using the Wilcoxon signed-rank test.

3. Results

3.1. Behavioral performance

Subjects ($n = 33$) responded with a mean reaction time of $M = 450.57$ ms ($SD = 42.33$ ms) in the Go condition. Significantly slower responses were detected after error commissions comparing to correct responses ($\delta = 18.03$ ms ($SD = 50.04$ ms); $t(32) = -2.07$, $p = 0.047$). Accuracy in the Go condition was 99.89% ($SD = 0.48$), and in the No-Go condition 78.93% ($SD = 10.1$). The nonparametric Wilcoxon test revealed a significant accuracy difference between the Go and No-Go condition ($Z = -5.03$, $p < 0.001$).

Performance errors in the No-Go condition significantly correlated with overall impulsivity as assessed with the BIS-11 questionnaire (BIS total score; Spearman's $\rho = 0.450$, $p = 0.014$) and motor impulsivity (BIS motor subscale; $\rho = .404$, $p = 0.030$) indicating that the higher number of errors in the No-Go condition might be associated with higher degree of impulsivity.

3.2. Whole-brain high-resolution fMRI analysis: Inhibitory control

3.2.1. (Correct No-Go > Correct Go)

Contrasting successful behavioral inhibition (correct No-Go trials) to successful behavioral action (correct Go trials), we found increased bilateral BOLD activations within the cognitive control network, i.e. ventrolateral prefrontal cortex (VLPFC), anterior insula (AI), dorsolateral prefrontal cortex (DLPFC), and (pre-)SMA (Fig. 2; Table S1). This contrast was commonly used to reveal the brain network associated with response inhibition in the Go/No-Go task. No significant BOLD activations in the brainstem were detected in this contrast.

3.3. Whole-brain high-resolution fMRI analysis: error processing

3.3.1. (Incorrect No-Go > Correct No-Go)

Comparing unsuccessful to successful behavioral inhibition, we detected increased BOLD activations especially in the dorsal ACC, perigenual ACC (pgACC), DMPFC, SMA and occipital cortex (OCx)

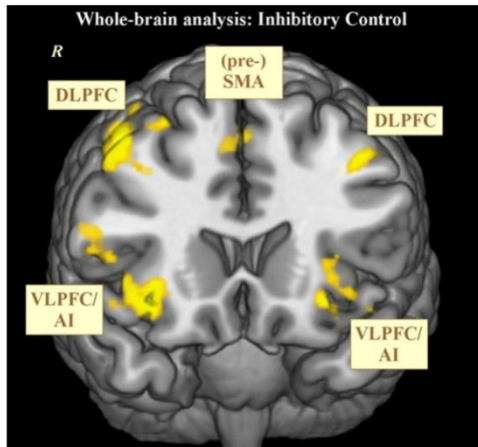


Fig. 2. Inhibitory control: Whole-brain fMRI analysis during successful response inhibition where the main effect of task (post-hoc *t*-test), i.e. correct No-Go vs. correct Go in the total group is illustrated (voxel-level $p < 0.001$ uncorr., cluster-level $p < 0.05$ FWE corr.). Abbreviations: DLPFC, dorsolateral prefrontal cortex; VLPFC, ventrolateral prefrontal cortex; AI, anterior insula; (pre-)SMA, (pre-)supplementary motor area.

(Table 1; Fig. 3A).

Brainstem/cerebellum high-resolution fMRI analysis using the SUI toolbox:

3.3.2. Error processing (Incorrect No-Go > Correct No-Go)

Applying advanced brainstem/cerebellum normalization, we observed increased BOLD activations in the cluster comprising VTA/SN ($x = 2, y = -18, z = -14, t = 5.03$; Fig. 3B) as well as in the right ($x = 10, y = -58, z = -14, t = 4.35, p < 0.001$) and left cerebellum ($x = -19, y = -61, z = -15, t = 4.14$). We created a mask image of the VTA/SN to verify the location of the cluster (Fig. S1). To obtain the anatomically most precise mask image, the VTA was manually traced based on the available atlases of the human brainstem (Naidich et al., 2009) as performed in our previous study (Bär et al., 2016). The boundaries of the VTA were defined laterally adjacent to the substantia nigra, and medially adjacent to the interpeduncular fossa. The SN was defined by means of the WFU Pickatlas (<http://fmri.wfubmc.edu/software/pickatlas>). VTA and SN were combined to one mask image.

3.3.3. Linking neural activation patterns to behavioral performance

In this analysis, we did not find a significant correlation between VTA/SN activation during error processing and the slowing of responding which was observed at the behavioral level. This might be caused by the low number of errors in the experiment. However, we found a significantly negative correlation between dACC activation during the occurrence of an error in the incorrect No-Go condition and response slowing post error ($\rho = -0.393, p = 0.024$). Thus, the more dACC involvement during response failure, the more behavioral control is present as adaptive response strategy after the occurrence of an error.

3.3.4. Linking physiological indices to behavioral performance

As shown in Fig. 4, we observed stronger skin conductance responses to incorrect ($SCR = 4949 \pm 2963$ in normalized units (n.u.)) than to correct ($SCR = 3299 \pm 642$ n.u., $p < 0.001$) No-Go stimuli. Thus, the SCR is higher during failed behavioral control when compared to successful inhibition.

Table 1
Whole-brain analysis: Error processing.

Region of activation	Right/Left	Brodmann's Area	Cluster size ^a	MNI coordinate			T value
				x	y	z	
Anterior Cingulate Gyrus	R	32	6629	2	20	31	7.71
Supplementary Motor Area	R	6		5	10	71	7.59
Inferior Frontal Gyrus	L	47	2070	-30	20	-15	6.44
Insula	L	13		-38	10	5	5.50
Supplementary Motor Area	R	6	3916	51	-9	40	5.87
Inferior Frontal Gyrus	R	47		32	19	-18	5.62
Precentral Gyrus	R	4		44	-15	40	5.61
Middle Frontal Gyrus	R	9	77	41	19	26	4.91
Postcentral Gyrus	L	40	2119	-60	-21	19	5.36
Insula	L	13		-38	-10	13	5.27
Precentral Gyrus	L	4	1444	-44	-15	46	6.02
Occipital Lobe	L	18/19	10290	-17	-58	2	7.45
Posterior Cingulate Gyrus	R	30		24	-60	8	6.60
Caudate Nucleus	R		252	11	1	13	5.56
Parahippocampal Gyrus	L	34	86	-12	-13	-16	4.94
Subthalamic Nucleus	L			-12	-10	-6	4.66
Caudate Nucleus	L		199	-14	4	13	4.90
Thalamus	L			-8	-4	7	4.36
Lentiform Nucleus	L			-8	1	-1	3.59
Superior Temporal Gyrus	R	38	74	53	10	-19	4.88
Middle Temporal Gyrus	R	21		56	2	-16	3.44
Cerebellum	R		231	5	-39	4	4.88
Thalamus	L			-5	-22	5	4.84
Middle Temporal Gyrus	R	22	173	51	-42	7	4.85
Superior Temporal Gyrus	R	21		50	-24	-6	4.22
Inferior Parietal Lobule	R	40	827	50	-31	29	4.64
Postcentral Gyrus	R	43		56	-18	16	4.45
Superior Temporal Gyrus	R	22		65	-40	22	4.43
Cerebellum	L		141	-20	-63	-19	4.57
Thalamus	R		74	14	-10	4	4.51
Paracentral Lobule	L/R	5	115	5	-39	53	3.49

^a $p < 0.05$ FWE corrected; R = right; L = left.

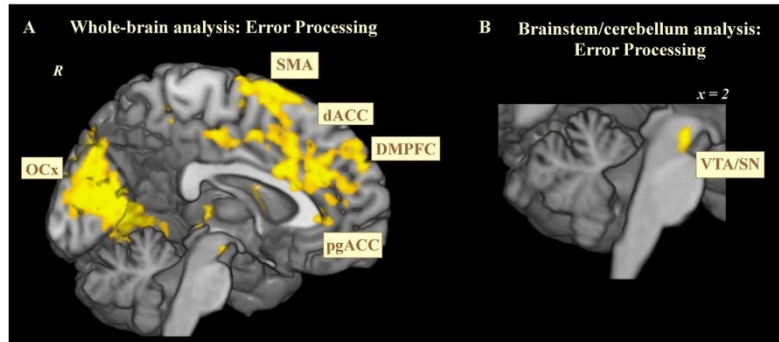


Fig. 3. Error processing: **A.** Whole-brain fMRI analysis during error processing where the main effect of task (post-hoc *t*-test), i.e. incorrect No-Go vs. correct No-Go in the total group is illustrated (voxel-level $p < 0.001$ uncorr., cluster-level, $p < 0.05$, FWE corr.); **B.** Brainstem/cerebellum fMRI analysis during error processing where the main effect of task (post-hoc *t*-test), i.e. incorrect No-Go vs. correct No-Go in the total group is illustrated (voxel-level $p < 0.001$ uncorr., cluster-level, $p < 0.05$ FWE corr.). Abbreviations: dACC, dorsal anterior cingulate cortex; pgACC, perigenual anterior cingulate cortex; DMPFC dorsomedial prefrontal cortex; SMA, supplementary motor area; OCx, occipital cortex; VTA/SN,

ventral tegmental area/substantia nigra; ρ , Greek small letter 'Rho'(Spearman's rho).

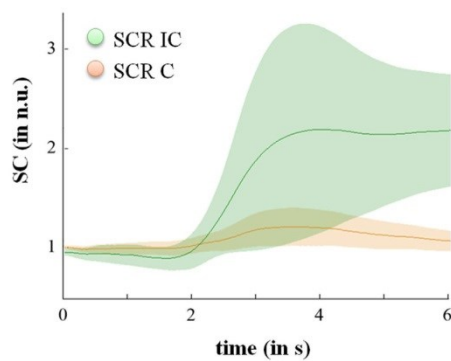


Fig. 4. Linking physiological indices to behavioral performance: Mean SCRs in the incorrect No-Go (green) and correct No-Go (orange) trials are shown (areas under the curve indicate standard deviations). Abbreviations: C; correct; IC, incorrect; SC, skin conductance; SCR, skin conductance response; n. u., normalized units; ρ , Greek small letter 'Rho'(Spearman's rho).

3.3.5. Pre-error processing (pre-correct No-Go > pre-incorrect No-Go)

In case of the pre-error analysis, we finally contrasted Go stimuli immediately preceding correct No-Go (pre-C) events with Go stimuli immediately preceding incorrect No-Go (pre-IC) events. The time intervals (ISI) between a Go trial and a following No-Go trial ranged from 3800 ms to 8200 ms. We detected increased BOLD activations in the right VLPFC (BA 47; $x = -37.5$, $y = 21.5$, $z = -11.5$, $t = 4.13$) and dACC (BA 32; $x = -8$, $y = 38$, $z = 11$, $t = 4.44$) as well as in the right cerebellum ($x = 2$, $y = -64$, $z = -30$, $t = 6.12$), which indicates elevated BOLD activation in central regions of the cognitive control network prior to trials associated with successful behavioral inhibition (Fig. 5B).

3.3.6. Linking physiological indices to pre-error fMRI activation

When analyzing physiological responses before error occurrence, we found that pre-incorrect No-Go trials elicited weaker SC responses ($SCR = 2865 \pm 347$ n.u.) compared to pre-correct No-Go trials ($SCR = 3237 \pm 448$ n.u.; $p < 0.001$, Fig. 5A). Thus, weaker SCRs prior to events requiring action restraint were associated with an increased probability of impulsive behavior.

Interestingly, SCR in pre-incorrect No-Go trials was positively correlated to parameter estimates from the dACC in pre-incorrect No-Go trials ($\rho = .443$, $p = 0.010$). This means that weaker SCRs go also along

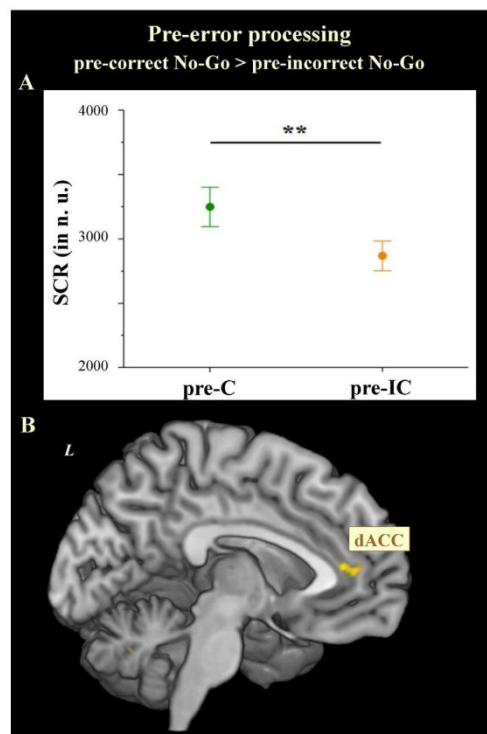


Fig. 5. Pre-error processing: **A.** Skin conductance responses to pre-correct and pre-incorrect No-Go trials; **B.** Whole-brain fMRI analysis during pre-error processing where the main effect of task (post-hoc *t*-test), i.e. pre-correct No-Go vs. pre-incorrect No-Go in the total group is illustrated (voxel-level $p < 0.001$ uncorr., cluster-level $p < 0.05$ FWE corr.). Abbreviations: dACC, dorsal anterior cingulate cortex; C; correct; IC, incorrect; SCR, skin conductance response; n. u., normalized units; ** $p < 0.01$.

with weaker dACC activation prior to trials requiring action restraint.

4. Discussion

The present investigation was performed to identify the significance of central activation patterns and peripheral autonomic regulation indicating the degree of arousal during successful and unsuccessful response inhibition. Here, we describe the putative involvement of the dopaminergic neurotransmitter system in error processing. Most remarkably, specific autonomic parameters were identified containing predictive information on an individual's performance and correlating with BOLD activation in brain regions of response inhibition and behavioral monitoring.

In our present study, we found core regions of the cognitive control network, i.e., DLPFC and VLPFC activated during action restraint. Surprisingly, no BOLD activations were found in the VTA/SN and LC during successful response inhibition. This difference to our previous results (Köhler et al., 2016) might be due to the type of inhibitory control addressed by the present task. In our former study, we focused on the cognitive domain of inhibitory control and individuals were asked to decide between two answers indicating either decision by pressing the button. However, in the present analysis, we addressed the behavioral/motor domain of response inhibition and individuals were asked to either press a button or to withhold their response. Therefore, two different domains of inhibitory control were investigated indicating that the VTA/SN and LC are not as decisive in action restraint as in a more cognitive focus of inhibitory control (Nandam et al., 2013).

During failed response inhibition, we found increased activations in the dACC and DMPPFC, which is also known to be important in performance monitoring and error processing (Soshi et al., 2014; Vila-Ballo et al., 2014). Increased BOLD activation in the VTA/SN was also detected, emphasizing the potential role of dopamine during error monitoring and performance adjustment (Bari et al., 2009; Bari and Robbins, 2013).

Previous studies indicated that the early stages of error processing might also be preconscious and independent of any awareness of errors (O'Connell et al., 2007). This stage has a characteristic ERP, the error-related negativity, which may arise from the ACC via signaling from the VTA/SN (Holroyd and Coles, 2002). Thus, a decisive role of the dACC was emphasized in goal-directed behavior (Jahn et al., 2014; Miller and Cohen, 2001), which requires the capability to make predictions. The dACC was supposed to formulate predictions and to compute a signal termed prediction error, which scales the discrepancy between a predicted and an actual outcome (Alexander and Brown, 2011). This allows rapid prediction updating according to, e.g., an error. Adequate dopaminergic function is critical for adaptive prediction error coding (Diederer et al., 2016), which again emphasizes the essential role of dopamine in error processing.

In the present study, we found increased activation in the dACC as well as in the VTA/SN during failed response inhibition. We did not find a correlation between VTA/SN activation and the slowing of responding which was observed at the behavioral level. However, a close interplay between the dACC and VTA/SN was previously suggested (Holroyd and Coles, 2002). Thus, we investigated, if dACC activation during the occurrence of an error might be related to the slowing of responding after response failure. We found a significant negative correlation between dACC activation during the occurrence of an error in the incorrect No-Go condition and response slowing post error. In a broader sense it might be possible that the potential role of the VTA/SN in the modulation of behavior in a Go/No-Go task might arise via its modulating effect on the dACC. However, the described association needs further investigation as well as replication.

In sum, our present findings support recent research results, especially the potential involvement of the midbrain dopaminergic systems during error processing (Di Domenico and Ryan, 2017; Howard et al., 2017; Kasanova et al., 2017). The pivotal role of the VTA in predicting

behavioral outcomes was demonstrated by Redila et al. (2015). In the used paradigm subjects had to retain information until the outcome occurred. The ability of the brain to accurately predict behavioral outcomes has been extensively studied in the context of the role of dopamine in reinforcement - based learning. VTA dopamine neurons appear to be involved in the regulation of motivation and learning by signaling the subjective value of the outcomes of behavioral actions (Arnstén et al., 2012; Bromberg-Martin et al., 2010; Schultz, 2010). Moreover, dopaminergic neurons can promptly signal a reward prediction error input from the lateral habenula (Hong et al., 2011), which is transmitted to the cortex, and may in turn destabilize spatial representations in the hippocampus so that new information may be incorporated (Mizumori, 2013) and behavioral strategies can be changed.

A study by Düzel et al. (2009) summarized that several findings support the possibility of a quantitative relationship between the magnitude of the fMRI VTA/SN signal and the magnitude of dopamine release. However, there are some methodological and conceptual caveats. The VTA contains three types of neurons. The most abundant are dopaminergic neurons which make up 60–65% of the total number of neurons, followed by gamma-amino-butyric-acid (GABA) neurons which make up about 30–35% of total neurons, and a small number of glutamatergic neurons comprising approximately 2–3% of the total amount (Sesack and Grace, 2010). Brocka et al. (2018) investigated the contribution of dopaminergic and non-dopaminergic neurons to VTA-stimulation induced neurovascular responses in brain reward circuits. The authors concluded that canonical BOLD responses in the reward system are mainly represented by the activity of non-dopaminergic neurons. Therefore, it is important to understand that glutamate and GABA regulate dopamine signaling (Dandash et al., 2017). Therefore, caution is required when linking the BOLD signal in the VTA/SN to the release of dopamine. Because the brain functions through highly complex simultaneous interactions of different neurotransmitter systems, an interesting future direction might be the combination of multiple neurotransmitter measures with functional brain responses to better characterize these interactions (Duncan et al., 2014).

Remarkably, an increased BOLD activation prior to a correct No-Go response was mainly found in the dACC indicating proper performance monitoring (Luks et al., 2002; Shenhav et al., 2013). This finding accords well with the result of reduced phasic SC responses prior to unsuccessful (pre-incorrect No-Go trials) compared to successful (pre-correct No-Go trials) behavioral inhibition and strengthens the interpretation of a beneficial effect of an elevated SCR before the occurrence of a more cognitively demanding event. Additionally, when analyzing events preceding a failed stop, a decline in SCRs was associated with an activation decline in dACC. The dACC is critically involved in top-down control and conflict monitoring (Botvinick et al., 2001; Kerns et al., 2004; Shenhav et al., 2016). Consequently, reduced attentional control, as characterized by reduced SCRs, seems to be associated with diminished dACC activations leading to performance errors (Critchley et al., 2000). According to the title of our approach *Towards response success prediction*, we found that neural activation and peripheral indices seem to be indicators of successful and unsuccessful response inhibition.

A number of limitations should be noted. The nuclei within the brainstem/midbrain are small compared to the cortical regions activated during error processing, and are more susceptible to signal distortion and artifacts arising from local tissue interfaces and physiological noise. However, we addressed this issue by using high-resolution fMRI, advanced brainstem methods using the SUIT toolbox as well as a method which corrects for respiratory and cardiac noise before analyzing the brainstem/midbrain fMRI images. The improved normalization of the brainstem/cerebellum using the SUIT toolbox was originally validated for the cerebellum (Diedrichsen, 2006), but not for the brainstem and midbrain. However, by creating a high-resolution atlas template of both, cerebellum and brainstem, the normalization of brainstem and midbrain structures is assumed to be improved as well. Still, a certain degree of uncertainty remains when assigning an

activation cluster to a specific nucleus. Although an anatomically defined mask image of the VTA/SN was used, future studies might make use of applying structural neuromelanin-sensitive MRI scans to improve detection of some brainstem/midbrain nuclei. Moreover, there were 21 No-Go trials with an obtained accuracy of around 80%. Thus, on average only four to five incorrect No-Go trials were recorded which reduces the power of the error-analysis. We tried to comply with this limitation by matching the number of events. Nevertheless, results should be interpreted with caution and a follow-up project is needed with an increased number of Go and No-Go trials to validate the reliability of the present results.

In summary, our study shows the paramount importance of the dopaminergic regions VTA/SN during error processing. Since catecholaminergic neurotransmission is essential to neocortical and subcortical functions, our findings contribute to a comprehensive understanding of the functional organization of the human brain. Moreover, the results of our study provide further insight into the interplay between the peripheral ANS and CNS in response inhibition, i.e. the Go/No-Go task. Importantly, predictive information regarding response inhibition capabilities were held by the ANS via SCR as well as by the CNS via dACC activations tentatively. Nevertheless, more precise explorations of the exact interrelations between the CNS and ANS in impulsivity-related disorders are needed.

Acknowledgements

The authors have declared that there are no conflicts of interest in relation to the subject of this study.

Appendix A. Supplementary material

Supplementary data associated with this article can be found in the online version at doi:10.1016/j.neuropsychologia.2018.08.003.

References

- Agam, Y., Vangel, M., Roffman, J.L., Gallagher, P.J., Chaponis, J., Haddad, S., Manoach, D.S., 2014. Dissociable genetic contributions to error processing: a multimodal neuroimaging study. *PLoS One* 9 (7), e101784. <https://doi.org/10.1371/journal.pone.0101784>.
- Alexander, G.E., Crutcher, M.D., 1990. Functional architecture of basal ganglia circuits: neural substrates of parallel processing. *Trends Neurosci.* 13 (7), 266–271.
- Alexander, W.H., Brown, J.W., 2011. Medial prefrontal cortex as an action-outcome predictor. *Nat. Neurosci.* 14 (10), 1338–1344. <https://doi.org/10.1038/nn.2921>.
- Aron, A.R., Poldrack, R.A., 2006. Cortical and subcortical contributions to Stop signal response inhibition: role of the subthalamic nucleus. *J. Neurosci.* 26 (9), 2424–2433. <https://doi.org/10.1523/jneurosci.4682-05.2006>.
- Arnsen, A.F., Wang, M.J., Paspalas, C.D., 2012. Neuromodulation of thought: flexibilities and vulnerabilities in prefrontal cortical network synapses. *Neuron* 76 (1), 223–239. <https://doi.org/10.1016/j.neuron.2012.08.038>.
- Aston-Jones, G., Cohen, J.D., 2005. An integrative theory of locus coeruleus-nor-epinephrine function: adaptive gain and optimal performance. *Annu. Rev. Neurosci.* 28, 403–450. <https://doi.org/10.1146/annurev.neuro.28.061604.135709>.
- Bach, D.R., Friston, K.J., Dolan, R.J., 2010. Analytic measures for quantification of arousal from spontaneous skin conductance fluctuations. *Int. J. Psychophysiol.* 76 (1), 52–55. <https://doi.org/10.1016/j.ijpsycho.2010.01.011>.
- Bär, K.J., de la Cruz, F., Schumann, A., Koehler, S., Sauer, H., Critchley, H., Wagner, G., 2016. Functional connectivity and network analysis of midbrain and brainstem nuclei. *NeuroImage* 134, 53–63. <https://doi.org/10.1016/j.neuroimage.2016.03.071>.
- Bari, A., Eagle, D.M., Mar, A.C., Robinson, E.S., Robbins, T.W., 2009. Dissociable effects of noradrenaline, dopamine, and serotonin uptake blockade on stop task performance in rats. *Psychopharmacology (Berl)* 205 (2), 273–283. <https://doi.org/10.1007/s00213-009-1537-0>.
- Bari, A., Robbins, T.W., 2013. Inhibition and impulsivity: behavioral and neural basis of response control. *Prog. Neurobiol.* 108, 44–79. <https://doi.org/10.1016/j.pneurobio.2013.06.005>.
- Bechara, A., Damasio, H., Tranel, D., Damasio, A.R., 1997. Deciding advantageously before knowing the advantageous strategy. *Science* 275 (5304), 1293–1295.
- Beissner, F., Meissner, K., Bar, K.J., Napadow, V., 2013. The autonomic brain: an activation likelihood estimation meta-analysis for central processing of autonomic function. *J. Neurosci.* 33 (25), 10503–10511. <https://doi.org/10.1523/jneurosci.1103-13.2013>.
- Birn, R.M., Smith, M.A., Jones, T.B., Bandettini, P.A., 2008. The respiration response function: the temporal dynamics of fMRI signal fluctuations related to changes in respiration. *NeuroImage* 40 (2), 644–654. <https://doi.org/10.1016/j.neuroimage.2007.11.059>.
- Botvinick, M.M., Braver, T.S., Barch, D.M., Carter, C.S., Cohen, J.D., 2001. Conflict monitoring and cognitive control. *Psychol. Rev.* 108 (3), 624–652.
- Brewer, J.A., Potenza, M.N., 2008. The neurobiology and genetics of impulse control disorders: relationships to drug addictions. *Biochem. Pharmacol.* 75 (1), 63–75. <https://doi.org/10.1016/j.bcp.2007.06.043>.
- Briggs, G.G., Nebes, R.D., 1975. Patterns of hand preference in a student population. *Cortex* 11 (3), 230–238.
- Bromberg-Martin, E.S., Matsumoto, M., Hikosaka, O., 2010. Dopamine in motivational control: rewarding, aversive, and alerting. *Neuron* 68, 815–834.
- Brocka, M., Helbing, C., Vincenz, D., Scherf, T., Montag, D., Goldschmidt, J., Lippert, M., 2018. Contributions of dopaminergic and non-dopaminergic neurons to VTA-stimulation induced neurovascular responses in brain reward circuits. *NeuroImage* 177, 88–97. <https://doi.org/10.1016/j.neuroimage.2018.04.059>.
- Claassen, D.O., Stark, A.J., Spears, C.A., Petersen, K.J., van Wouwe, N.C., Kessler, R.M., Donahue, M.J., 2017. Mesocorticolimbic hemodynamic response in Parkinson's disease patients with compulsive behaviors. *Mov. Disord.* <https://doi.org/10.1002/mds.27047>.
- Cohen, J.D., Botvinick, M., Carter, C.S., 2000. Anterior cingulate and prefrontal cortex: who's in control? *Nat. Neurosci.* 3 (5), 421–423. <https://doi.org/10.1038/74783>.
- Critchley, H.D., 2009. Psychophysiology of neural, cognitive and affective integration: fMRI and autonomic indicators. *Int. J. Psychophysiol.* 73 (2), 88–94. <https://doi.org/10.1016/j.ijpsycho.2009.01.012>.
- Critchley, H.D., Elliott, R., Mathias, C.J., Dolan, R.J., 2000. Neural activity relating to generation and representation of galvanic skin conductance responses: a functional magnetic resonance imaging study. *J. Neurosci.* 20 (8), 3033–3040.
- Critchley, H.D., Mathias, C.J., Dolan, R.J., 2001. Neural activity in the human brain relating to uncertainty and arousal during anticipation. *Neuron* 29 (2), 537–545.
- Critchley, H.D., Mathias, C.J., Josephs, O., O'Doherty, J., Zanini, S., Dewar, B.K., Dolan, R.J., 2003. Human cingulate cortex and autonomic control: converging neuroimaging and clinical evidence. *Brain* 126 (Pt 10), 2139–2152. <https://doi.org/10.1093/brain/awg216>.
- Critchley, H.D., Rotshtein, P., Nagai, Y., O'Doherty, J., Mathias, C.J., Dolan, R.J., 2005. Activity in the human brain predicting heartbeat rate responses to emotional facial expressions. *NeuroImage* 24 (3), 751–762. <https://doi.org/10.1016/j.neuroimage.2004.10.013>.
- Dandash, O., Pantelis, C., Fornito, A., 2017. Dopamine, fronto-striato-thalamic circuits and risk for psychosis. *Schizophr Res.* 180, 48–57. <https://doi.org/10.1016/j.schres.2016.08.020>.
- Di Domenico, S.L., Ryan, R.M., 2017. The emerging neuroscience of intrinsic motivation: a new frontier in self-determination research. *Front. Hum. Neurosci.* 11, 145. <https://doi.org/10.3389/fnhum.2017.00145>.
- Diederen, K.M., Spencer, T., Vestergaard, M.D., Fletcher, P.C., Schultz, W., 2016. Adaptive prediction error coding in the human midbrain and striatum facilitates behavioral adaptation and learning efficiency. *Neuron* 90 (5), 1127–1138. <https://doi.org/10.1016/j.neuron.2016.04.019>.
- Diedrichsen, J., 2006. A spatially unbiased atlas template of the human cerebellum. *NeuroImage* 33 (1), 127–138. <https://doi.org/10.1016/j.neuroimage.2006.05.056>.
- Duncan, N.W., Wiebking, C., Northoff, G., 2014. Associations of regional GABA and glutamate with intrinsic and extrinsic neural activity in humans—a review of multimodal imaging studies. *Neurosci. Biobehav. Rev.* 47, 36–52. <https://doi.org/10.1016/j.neubiorev.2014.07.016>.
- Düzel, E., Bunzeck, N., Guitart-Masip, M., Wittmann, B., Schott, B.H., Tobler, P.N., 2009. Functional imaging of the human dopaminergic midbrain. *Trends Neurosci.* 32 (6), 321–328. <https://doi.org/10.1016/j.tins.2009.02.005>.
- Eagle, D.M., Bari, A., Robbins, T.W., 2008. The neuropharmacology of action inhibition: cross-species translation of the stop-signal and go/no-go tasks. *Psychopharmacology (Berl)* 199 (3), 439–456. <https://doi.org/10.1007/s00213-008-1127-6>.
- Eagle, D.M., Tufft, M.R., Goodchild, H.L., Robbins, T.W., 2007. Differential effects of modafinil and methylphenidate on stop-signal reaction time task performance in the rat, and interactions with the dopamine receptor antagonist cis-flupenthixol. *Psychopharmacol. (Berl)* 192 (2), 193–206. <https://doi.org/10.1007/s00213-007-0701-7>.
- Garavan, H., Ross, T.J., Murphy, K., Roche, R.A., Stein, E.A., 2002. Dissociable executive functions in the dynamic control of behavior: inhibition, error detection, and correction. *NeuroImage* 17 (4), 1820–1829.
- Gehring, W.J., Goss, B., Coles, M.G.H., Meyer, D.E., Donchin, E., 1993. A neural system for error detection and compensation. *Psychol. Sci.* 4 (6).
- Gehring, W.J., Himle, J., Nisenson, L.G., 2000. Action-monitoring dysfunction in obsessive-compulsive disorder. *Psychol. Sci.* 11 (1), 1–6. <https://doi.org/10.1111/1467-9280.00206>.
- Glover, G.H., Li, T.Q., Ress, D., 2000. Image-based method for retrospective correction of physiological motion effects in fMRI: retroicor. *Magn. Reson. Med.* 44 (1), 162–167.
- Godefroy, O., Lhullier, C., Rousseaux, M., 1996. Non-spatial attention disorders in patients with frontal or posterior brain damage. *Brain* 119 (Pt 1), 191–202.
- Goschke, T., Bolte, A., 2014. Emotional modulation of control dilemmas: the role of positive affect, reward, and dopamine in cognitive stability and flexibility. *Neuropsychologia* 62, 403–423. <https://doi.org/10.1016/j.neuropsychologia.2014.07.015>.
- Hajcak, G., McDonald, N., Simons, R.F., 2003. To err is autonomic: error-related brain potentials, ANS activity, and post-error compensatory behavior. *Psychophysiology* 40 (6), 895–903.
- Hofmann, W., Friese, M., Strack, F., 2009. Impulse and self-control from a dual-systems perspective. *Perspect. Psychol. Sci.* 4 (2), 162–176. <https://doi.org/10.1111/j.1745-6924.2009.01116.x>.

- Holroyd, C.B., Coles, M.G., 2002. The neural basis of human error processing: reinforcement learning, dopamine, and the error-related negativity. *Psychol. Rev.* 109 (4), 679–709.
- Howard, C.D., Li, H., Geddes, C.E., Jin, X., 2017. Dynamic nigrostriatal dopamine biases action selection (e1438). *Neuron* 93 (6), 1436–1450. <https://doi.org/10.1016/j.neuron.2017.02.029>.
- Jahn, A., Nee, D.E., Alexander, W.H., Brown, J.W., 2014. Distinct regions of anterior cingulate cortex signal prediction and outcome evaluation. *NeuroImage* 95, 80–89. <https://doi.org/10.1016/j.neuroimage.2014.03.050>.
- Jentsch, J.D., Taylor, J.R., 1999. Impulsivity resulting from frontostriatal dysfunction in drug abuse: implications for the control of behavior by reward-related stimuli. *Psychopharmacology (Berl)* 146 (4), 373–390.
- Jo, H.J., Saad, Z.S., Simmons, W.K., Milbury, L.A., Cox, R.W., 2010. Mapping sources of correlation in resting state fMRI, with artifact detection and removal. *NeuroImage* 52 (2), 571–582. <https://doi.org/10.1016/j.neuroimage.2010.04.246>.
- Kasanova, Z., Ceccarini, J., Frank, M.J., Amelvoort, T.V., Booij, J., Heinz, A., Myin-Zemels, I., 2017. Striatal dopaminergic modulation of reinforcement learning predicts reward-oriented behavior in daily life. *Biol. Psychol.* 127, 1–9. <https://doi.org/10.1016/j.biopsycho.2017.04.014>.
- Kerns, J.G., Cohen, J.D., MacDonald 3rd, A.W., Cho, R.Y., Stenger, V.A., Carter, C.S., 2004. Anterior cingulate conflict monitoring and adjustments in control. *Science* 303 (5660), 1023–1026. <https://doi.org/10.1126/science.1089910>.
- Köhler, S., Bär, K.J., Wagner, G., 2016. Differential involvement of brainstem noradrenergic and midbrain dopaminergic nuclei in cognitive control. *Hum. Brain Mapp.* 37 (6), 2305–2318. <https://doi.org/10.1002/hbm.23173>.
- Kohno, M., Okita, K., Morales, A.M., Robertson, C.L., Dean, A.C., Ghahremani, D.G., London, E.D., 2016. Midbrain functional connectivity and ventral striatal dopamine D2-type receptors: link to impulsivity in methamphetamine users. *Mol. Psychiatry* 21 (11), 1554–1560. <https://doi.org/10.1038/mp.2015.223>.
- Kuryanova, E.V., Tryaschev, A.V., Stupin, V.O., Teply, D.L., 2017. Effect of stimulation of neurotransmitter systems on heart rate variability and beta-adrenergic responsiveness of erythrocytes in outbred rats. *Bull. Exp. Biol. Med.* 163 (1), 31–36. <https://doi.org/10.1007/s10517-017-3731-0>.
- Lim, L., Hart, H., Mehta, M.A., Simmons, A., Mirza, K., Rubia, K., 2015. Neural correlates of error processing in young people with a history of severe childhood abuse: an fMRI study. *Am. J. Psychiatry* 172 (9), 892–900. <https://doi.org/10.1176/appi.ajp.2015.14081042>.
- Luks, T.L., Simpson, G.V., Feiwel, R.J., Miller, W.L., 2002. Evidence for anterior cingulate cortex involvement in monitoring preparatory attentional set. *NeuroImage* 17 (2), 792–802.
- Mehler, B., Reimer, B., Coughlin, J.F., Dusek, J., 2009. Impact of incremental increases in cognitive workload on physiological arousal and performance in young adult drivers. *J. Transp. Res. Rec.: Transp. Res. Board* 2138 (1), 6–12.
- Miller, E.K., Cohen, J.D., 2001. An integrative theory of prefrontal cortex function. *Annu. Rev. Neurosci.* 24, 167–202. <https://doi.org/10.1146/annurev.neuro.24.1.167>.
- Miltner, W.H., Braun, C.H., Coles, M.G., 1997. Event-related brain potentials following incorrect feedback in a time-estimation task: evidence for a “generic” neural system for error detection. *J. Cogn. Neurosci.* 9 (6), 788–798. <https://doi.org/10.1162/jocn.1997.9.6.788>.
- Miltner, W.H., Lemke, U., Weiss, T., Holroyd, C., Scheffers, M.K., Coles, M.G., 2003. Implementation of error-processing in the human anterior cingulate cortex: a source analysis of the magnetic equivalent of the error-related negativity. *Biol. Psychol.* 64 (1–2), 157–166.
- Mizumori, S.J., Jo, Y.S., 2013. Homeostatic regulation of memory systems and adaptive decisions. *Hippocampus* 23 (11), 1103–1124. <https://doi.org/10.1002/hipo.22176>.
- Nagai, Y., Critchley, H.D., Featherstone, E., Trimble, M.R., Dolan, R.J., 2004. Activity in ventromedial prefrontal cortex covaries with sympathetic skin conductance level: a physiological account of a “default mode” of brain function. *NeuroImage* 22 (1), 243–251. <https://doi.org/10.1016/j.neuroimage.2004.01.019>.
- Naidich, T.P., Duvernoy, H.M., Delman, B.N., Sorensen, A.G., Kollias, S.S., Haacke, E.M., 2009. *Duvernoy's Atlas of the Human Brain Stem and Cerebellum*. Springer, Wien.
- Nandam, L.S., Hester, R., Wagner, J., Dean, A.J., Messer, C., Honeysett, A., Bellgrove, M.A., 2013. Dopamine D(2) receptor modulation of human response inhibition and error awareness. *J. Cogn. Neurosci.* 25 (4), 649–656. <https://doi.org/10.1162/jocn.a.00327>.
- O'Connell, R.G., Dockree, P.M., Bellgrove, M.A., Kelly, S.P., Hester, R., Garavan, H., Foxe, J.J., 2007. The role of cingulate cortex in the detection of errors with and without awareness: a high-density electrical mapping study. *Eur. J. Neurosci.* 25 (8), 2571–2579. <https://doi.org/10.1111/j.1460-9568.2007.05477.x>.
- Patton, J.H., Stanford, M.S., Barratt, E.S., 1995. Factor structure of the Barratt impulsiveness scale. *J. Clin. Psychol.* 51 (6), 768–774.
- Picton, T.W., Stuss, D.T., Alexander, M.P., Shallice, T., Binns, M.A., Gillingham, S., 2007. Effects of focal frontal lesions on response inhibition. *Cereb. Cortex* 17 (4), 826–838. <https://doi.org/10.1093/cercor/bhk031>.
- Redila, V., Kinzel, C., Jo, Y.S., Puryear, C.B., Mizumori, S.J., 2015. A role for the lateral dorsal tegmentum in memory and decision neural circuitry. *Neurobiol. Learn Mem.* 117, 93–108. <https://doi.org/10.1016/j.nlm.2014.05.009>.
- Robbins, T.W., Arnsten, A.F., 2009. The neuropsychopharmacology of fronto-executive function: monoaminergic modulation. *Annu. Rev. Neurosci.* 32, 267–287. <https://doi.org/10.1146/annurev.neuro.051508.135535>.
- Schultz, W., 2010. Dopamine signals for reward value and risk: basic and recent data. *Behav. Brain Funct.* 6 (24). <https://doi.org/10.1186/1744-9081-6-24>.
- Sesack, S.R., Grace, A.A., 2010. Cortico-Basal Ganglia reward network microcircuitry. *Neuropsychopharmacology* 35 (1), 27–47. <https://doi.org/10.1038/npp.2009.93>.
- Sheehan, D.V., Lecrubier, Y., Sheehan, K.H., Amorim, P., Janavs, J., Weiller, E., Dunbar, G.C., 1998. The Mini-International neuropsychiatric Interview (M.I.N.I.): the development and validation of a structured diagnostic psychiatric interview for DSM-IV and ICD-10. *J. Clin. Psychiatry* 59 (Suppl 20), 22–33 (quiz34–57).
- Shenhav, A., Botvinick, M.M., Cohen, J.D., 2013. The expected value of control: an integrative theory of anterior cingulate cortex function. *Neuron* 79 (2), 217–240. <https://doi.org/10.1016/j.neuron.2013.07.007>.
- Shenhav, A., Cohen, J.D., Botvinick, M.M., 2016. Dorsal anterior cingulate cortex and the value of control. *Nat. Neurosci.* 19 (10), 1286–1291. <https://doi.org/10.1038/nn.4384>.
- Simmonds, D.J., Pekar, J.J., Mostofsky, S.H., 2008. Meta-analysis of Go/No-go tasks demonstrating that fMRI activation associated with response inhibition is task-dependent. *Neuropsychologia* 46 (1), 224–232. <https://doi.org/10.1016/j.neuropsychologia.2007.07.015>.
- Soshi, T., Ando, K., Noda, T., Nakazawa, K., Tsumura, H., Okada, T., 2014. Post-error action control is neurobehaviorally modulated under conditions of constant speeded response. *Front Hum. Neurosci.* 8, 1072. <https://doi.org/10.3389/fnhum.2014.01072>.
- Stuss, D.T., Binns, M.A., Murphy, K.J., Alexander, M.P., 2002. Dissociations within the anterior attentional system: effects of task complexity and irrelevant information on reaction time speed and accuracy. *Neuropsychologia* 16 (4), 500–513.
- Thayer, J.F., Lane, R.D., 2000. A model of neurovisceral integration in emotion regulation and dysregulation. *J. Affect. Disord.* 61 (3), 201–216.
- van Noordt, S.J., Segalowitz, S.J., 2012. Performance monitoring and the medial prefrontal cortex: a review of individual differences and context effects as a window on self-regulation. *Front. Hum. Neurosci.* 6, 197. <https://doi.org/10.3389/fnhum.2012.00197>.
- Vila-Ballo, A., Hdez-Lafuente, P., Rostan, C., Cunillera, T., Rodriguez-Fornells, A., 2014. Neurophysiological correlates of error monitoring and inhibitory processing in juvenile violent offenders. *Biol. Psychol.* 102, 141–152. <https://doi.org/10.1016/j.biopsycho.2014.07.021>.
- Woo, C.W., Krishnan, A., Wager, T.D., 2014. Cluster-extent based thresholding in fMRI analyses: pitfalls and recommendations. *NeuroImage* 91, 412–419. <https://doi.org/10.1016/j.neuroimage.2013.12.058>.
- Zhang, S., Hu, S., Chao, H.H., Ide, J.S., Luo, X., Farr, O.M., Li, C.S., 2014. Ventromedial prefrontal cortex and the regulation of physiological arousal. *Soc. Cogn. Affect. Neurosci.* 9 (7), 900–908. <https://doi.org/10.1093/scan/nst064>.
- Zhang, S., Hu, S., Chao, H.H., Luo, X., Farr, O.M., Li, C.S., 2012. Cerebral correlates of skin conductance responses in a cognitive task. *NeuroImage* 62 (3), 1489–1498. <https://doi.org/10.1016/j.neuroimage.2012.05.036>.
- Zhang, S., Hu, S., Hu, J., Wu, P.L., Chao, H.H., Li, C.S., 2015. Barratt impulsivity and neural regulation of physiological arousal. *PLoS One* 10 (6), e0129139. <https://doi.org/10.1371/journal.pone.0129139>.

REFERENCES

- Alexander, G. E., & Crutcher, M. D. (1990). Functional architecture of basal ganglia circuits: neural substrates of parallel processing. *Trends Neurosci*, *13*(7), 266-271.
- Amat, J., Baratta, M. V., Paul, E., Bland, S. T., Watkins, L. R., & Maier, S. F. (2005). Medial prefrontal cortex determines how stressor controllability affects behavior and dorsal raphe nucleus. *Nat Neurosci*, *8*(3), 365-371. doi:10.1038/nm1399
- Aron, A. R., & Poldrack, R. A. (2006). Cortical and subcortical contributions to Stop signal response inhibition: role of the subthalamic nucleus. *J Neurosci*, *26*(9), 2424-2433. doi:10.1523/jneurosci.4682-05.2006
- Aston-Jones, G., & Bloom, F. E. (1981). Norepinephrine-containing locus coeruleus neurons in behaving rats exhibit pronounced responses to non-noxious environmental stimuli. *J Neurosci*, *1*(8), 887-900.
- Aston-Jones, G., & Cohen, J. D. (2005). An integrative theory of locus coeruleus-norepinephrine function: adaptive gain and optimal performance. *Annu Rev Neurosci*, *28*, 403-450. doi:10.1146/annurev.neuro.28.061604.135709
- Aston-Jones, G., Rajkowski, J., & Cohen, J. (1999). Role of locus coeruleus in attention and behavioral flexibility. *Biol Psychiatry*, *46*(9), 1309-1320.
- Bär, K.-J., Letsch, A., Jochum, T., Wagner, G., Greiner, W., & Sauer, H. (2005). Loss of efferent vagal activity in acute schizophrenia. *J Psychiatr Res*, *39*(5), 519-527. doi:<https://doi.org/10.1016/j.jpsychires.2004.12.007>
- Bari, A., & Robbins, T. W. (2013). Inhibition and impulsivity: behavioral and neural basis of response control. *Prog Neurobiol*, *108*, 44-79. doi:10.1016/j.pneurobio.2013.06.005
- Bechara, A., Damasio, H., Tranel, D., & Damasio, A. R. (1997). Deciding advantageously before knowing the advantageous strategy. *Science*, *275*(5304), 1293-1295.

- Beissner, F., & Baudrexel, S. (2014). Investigating the human brainstem with structural and functional MRI. *Front Hum Neurosci*, 8, 116. doi:10.3389/fnhum.2014.00116
- Beissner, F., Meissner, K., Bar, K. J., & Napadow, V. (2013). The autonomic brain: an activation likelihood estimation meta-analysis for central processing of autonomic function. *J Neurosci*, 33(25), 10503-10511. doi:10.1523/jneurosci.1103-13.2013
- Beissner, F., Schumann, A., Brunn, F., Eisentrager, D., & Bar, K. J. (2014). Advances in functional magnetic resonance imaging of the human brainstem. *Neuroimage*, 86, 91-98. doi:10.1016/j.neuroimage.2013.07.081
- Benarroch, E. E. (1993). The central autonomic network: functional organization, dysfunction, and perspective. *Mayo Clin Proc*, 68(10), 988-1001.
- Botvinick, M. M., Braver, T. S., Barch, D. M., Carter, C. S., & Cohen, J. D. (2001). Conflict monitoring and cognitive control. *Psychol Rev*, 108(3), 624-652.
- Boucsein, W. (1992). *Electrodermal Activity*: Plenum Press.
- Brewer, J. A., & Potenza, M. N. (2008). The Neurobiology and Genetics of Impulse Control Disorders: Relationships to Drug Addictions. *Biochemical pharmacology*, 75(1), 63-75. doi:10.1016/j.bcp.2007.06.043
- Brooks, J. C., Faull, O. K., Pattinson, K. T., & Jenkinson, M. (2013). Physiological noise in brainstem fMRI. *Front Hum Neurosci*, 7, 623. doi:10.3389/fnhum.2013.00623
- Brown, J. W., & Braver, T. S. (2005). Learned predictions of error likelihood in the anterior cingulate cortex. *Science*, 307(5712), 1118-1121. doi:10.1126/science.1105783
- Callicott, J. H., Bertolino, A., Mattay, V. S., Langheim, F. J., Duyn, J., Coppola, R., . . . Weinberger, D. R. (2000). Physiological dysfunction of the dorsolateral prefrontal cortex in schizophrenia revisited. *Cereb Cortex*, 10(11), 1078-1092.
- Claassen, D. O., Stark, A. J., Spears, C. A., Petersen, K. J., van Wouwe, N. C., Kessler, R. M., . . . Donahue, M. J. (2017). Mesocorticolimbic hemodynamic response in Parkinson's disease patients with compulsive behaviors. *Mov Disord*. doi:10.1002/mds.27047

- Clamor, A., Schlier, B., Kother, U., Hartmann, M. M., Moritz, S., & Lincoln, T. M. (2015). Bridging psychophysiological and phenomenological characteristics of psychosis-- Preliminary evidence for the relevance of emotion regulation. *Schizophr Res*, *169*(1-3), 346-350. doi:10.1016/j.schres.2015.10.035
- Clayton, E. C., Rajkowski, J., Cohen, J. D., & Aston-Jones, G. (2004). Phasic activation of monkey locus ceruleus neurons by simple decisions in a forced-choice task. *J Neurosci*, *24*(44), 9914-9920. doi:10.1523/jneurosci.2446-04.2004
- Corbetta, M., Patel, G., & Shulman, G. L. (2008). The Reorienting System of the Human Brain: From Environment to Theory of Mind. *Neuron*, *58*(3), 306-324. doi:<http://dx.doi.org/10.1016/j.neuron.2008.04.017>
- Coull, J. T., Buchel, C., Friston, K. J., & Frith, C. D. (1999). Noradrenergically mediated plasticity in a human attentional neuronal network. *Neuroimage*, *10*(6), 705-715. doi:10.1006/nimg.1999.0513
- Critchley, H. D. (2009). Psychophysiology of neural, cognitive and affective integration: fMRI and autonomic indicants. *Int J Psychophysiol*, *73*(2), 88-94. doi:10.1016/j.ijpsycho.2009.01.012
- Critchley, H. D., Elliott, R., Mathias, C. J., & Dolan, R. J. (2000). Neural activity relating to generation and representation of galvanic skin conductance responses: a functional magnetic resonance imaging study. *J Neurosci*, *20*(8), 3033-3040.
- Critchley, H. D., Mathias, C. J., & Dolan, R. J. (2001). Neural activity in the human brain relating to uncertainty and arousal during anticipation. *Neuron*, *29*(2), 537-545.
- Critchley, H. D., Mathias, C. J., Josephs, O., O'Doherty, J., Zanini, S., Dewar, B. K., . . . Dolan, R. J. (2003). Human cingulate cortex and autonomic control: converging neuroimaging and clinical evidence. *Brain*, *126*(Pt 10), 2139-2152. doi:10.1093/brain/awg216

- Critchley, H. D., Rotshtein, P., Nagai, Y., O'Doherty, J., Mathias, C. J., & Dolan, R. J. (2005). Activity in the human brain predicting differential heart rate responses to emotional facial expressions. *Neuroimage*, 24(3), 751-762. doi:10.1016/j.neuroimage.2004.10.013
- Davidson, R. J. (2000). *The functional neuroanatomy of affective style*. New York: Oxford University Press.
- Eagle, D. M., Bari, A., & Robbins, T. W. (2008). The neuropsychopharmacology of action inhibition: cross-species translation of the stop-signal and go/no-go tasks. *Psychopharmacology (Berl)*, 199(3), 439-456. doi:10.1007/s00213-008-1127-6
- Eagle, D. M., Tufft, M. R., Goodchild, H. L., & Robbins, T. W. (2007). Differential effects of modafinil and methylphenidate on stop-signal reaction time task performance in the rat, and interactions with the dopamine receptor antagonist cis-flupenthixol. *Psychopharmacology (Berl)*, 192(2), 193-206. doi:10.1007/s00213-007-0701-7
- Ettinger, U., Aichert, D. S., Wostmann, N., Dehning, S., Riedel, M., & Kumari, V. (2017). Response inhibition and interference control: Effects of schizophrenia, genetic risk, and schizotypy. *J Neuropsychol*. doi:10.1111/jnp.12126
- Fields, R. B., Van Kammen, D. P., Peters, J. L., Rosen, J., Van Kammen, W. B., Nugent, A., . . . Linnoila, M. (1988). Clonidine improves memory function in schizophrenia independently from change in psychosis. Preliminary findings. *Schizophr Res*, 1(6), 417-423.
- Friedman, J. I., Adler, D. N., & Davis, K. L. (1999). The role of norepinephrine in the pathophysiology of cognitive disorders: potential applications to the treatment of cognitive dysfunction in schizophrenia and Alzheimer's disease. *Biol Psychiatry*, 46(9), 1243-1252.

- Friedman, N. P., & Miyake, A. (2004). The relations among inhibition and interference control functions: a latent-variable analysis. *J Exp Psychol Gen*, *133*(1), 101-135. doi:10.1037/0096-3445.133.1.101
- Fuxe, K., Hamberger, B., & Hokfelt, T. (1968). Distribution of noradrenaline nerve terminals in cortical areas of the rat. *Brain Res*, *8*(1), 125-131.
- Godefroy, O., Lhullier, C., & Rousseaux, M. (1996). Non-spatial attention disorders in patients with frontal or posterior brain damage. *Brain*, *119* (Pt 1), 191-202.
- Hajcak, G., McDonald, N., & Simons, R. F. (2003). To err is autonomic: error-related brain potentials, ANS activity, and post-error compensatory behavior. *Psychophysiology*, *40*(6), 895-903.
- Hofmann, W., Friese, M., & Strack, F. (2009). Impulse and Self-Control From a Dual-Systems Perspective. *Perspect Psychol Sci*, *4*(2), 162-176. doi:10.1111/j.1745-6924.2009.01116.x
- Jacobs, S. C., Friedman, R., Parker, J. D., Tofler, G. H., Jimenez, A. H., Muller, J. E., . . . Stone, P. H. (1994). Use of skin conductance changes during mental stress testing as an index of autonomic arousal in cardiovascular research. *Am Heart J*, *128*(6 Pt 1), 1170-1177.
- Jentsch, J. D., & Taylor, J. R. (1999). Impulsivity resulting from frontostriatal dysfunction in drug abuse: implications for the control of behavior by reward-related stimuli. *Psychopharmacology (Berl)*, *146*(4), 373-390.
- Koch, K., Schachtzabel, C., Wagner, G., Schikora, J., Schultz, C., Reichenbach, J. R., . . . Schlosser, R. G. (2010). Altered activation in association with reward-related trial-and-error learning in patients with schizophrenia. *Neuroimage*, *50*(1), 223-232. doi:10.1016/j.neuroimage.2009.12.031

- Köhler, S., Bär, K.-J., & Wagner, G. (2016). Differential involvement of brainstem noradrenergic and midbrain dopaminergic nuclei in cognitive control. *Hum Brain Mapp*, *37*(6), 2305-2318. doi:10.1002/hbm.23173
- Kohlisch, O., & Schaefer, F. (1996). Physiological changes during computer tasks: responses to mental load or to motor demands? *Ergonomics*, *39*(2), 213-224. doi:10.1080/00140139608964452
- Kohno, M., Okita, K., Morales, A. M., Robertson, C. L., Dean, A. C., Ghahremani, D. G., . . . London, E. D. (2016). Midbrain functional connectivity and ventral striatal dopamine D2-type receptors: link to impulsivity in methamphetamine users. *Mol Psychiatry*, *21*(11), 1554-1560. doi:10.1038/mp.2015.223
- Laeng, B., Orbo, M., Holmlund, T., & Miozzo, M. (2011). Pupillary Stroop effects. *Cogn Process*, *12*(1), 13-21. doi:10.1007/s10339-010-0370-z
- Lane, R. D., McRae, K., Reiman, E. M., Chen, K., Ahern, G. L., & Thayer, J. F. (2009). Neural correlates of heart rate variability during emotion. *Neuroimage*, *44*(1), 213-222. doi:10.1016/j.neuroimage.2008.07.056
- Lapiz, M. D., & Morilak, D. A. (2006). Noradrenergic modulation of cognitive function in rat medial prefrontal cortex as measured by attentional set shifting capability. *Neuroscience*, *137*(3), 1039-1049. doi:10.1016/j.neuroscience.2005.09.031
- LeDoux, J. (1996). *The Emotional Brain*. New York: Simon and Schuster.
- Lim, C. L., Rennie, C., Barry, R. J., Bahramali, H., Lazzaro, I., Manor, B., & Gordon, E. (1997). Decomposing skin conductance into tonic and phasic components. *Int J Psychophysiol*, *25*(2), 97-109.
- Logan, G. D. (1985). EXECUTIVE CONTROL OF THOUGHT AND ACTION. *Acata Psychologia*, *60*, 193-210.
- Lohr, J. B., & Jeste, D. V. (1988). Locus ceruleus morphometry in aging and schizophrenia. *Acta Psychiatr Scand*, *77*(6), 689-697.

- M'Hamed, S. B., Sequeira, H., & Roy, J. C. (1993). Bilateral electrodermal activity during sleep and waking in the cat. *Sleep, 16*(8), 695-701.
- Mansouri, F. A., Tanaka, K., & Buckley, M. J. (2009). Conflict-induced behavioural adjustment: a clue to the executive functions of the prefrontal cortex. *Nat Rev Neurosci, 10*(2), 141-152. doi:10.1038/nrn2538
- Mather, M., Joo Yoo, H., Clewett, D. V., Lee, T. H., Greening, S. G., Ponzio, A., . . . Thayer, J. F. (2017). Higher locus coeruleus MRI contrast is associated with lower parasympathetic influence over heart rate variability. *Neuroimage, 150*, 329-335. doi:10.1016/j.neuroimage.2017.02.025
- Mathewson, K. J., Jetha, M. K., Goldberg, J. O., & Schmidt, L. A. (2012). Autonomic regulation predicts performance on Wisconsin Card Sorting Test (WCST) in adults with schizophrenia. *Biol Psychol, 91*(3), 389-399. doi:10.1016/j.biopsycho.2012.09.002
- McEwen, B. S. (1998). Protective and damaging effects of stress mediators. *N Engl J Med, 338*(3), 171-179. doi:10.1056/nejm199801153380307
- Mehler, B., Reimer, B., Coughlin, J. F., & Dusek, J. (2009). Impact of incremental increases in cognitive workload on physiological arousal and performance in young adult drivers. *J. Transp. Res. Rec.: Transp. Res. Board, 2138*(1), 6-12.
- Miller, E. K., & Cohen, J. D. (2001). An integrative theory of prefrontal cortex function. *Annu Rev Neurosci, 24*, 167-202. doi:10.1146/annurev.neuro.24.1.167
- Murphy, P. R., O'Connell, R. G., O'Sullivan, M., Robertson, I. H., & Balsters, J. H. (2014). Pupil diameter covaries with BOLD activity in human locus coeruleus. *Hum Brain Mapp, 35*(8), 4140-4154. doi:10.1002/hbm.22466
- Nagai, Y., Critchley, H. D., Featherstone, E., Trimble, M. R., & Dolan, R. J. (2004). Activity in ventromedial prefrontal cortex covaries with sympathetic skin conductance level: a

- physiological account of a "default mode" of brain function. *Neuroimage*, 22(1), 243-251. doi:10.1016/j.neuroimage.2004.01.019
- Nandam, L. S., Hester, R., Wagner, J., Dean, A. J., Messer, C., Honeysett, A., . . . Bellgrove, M. A. (2013). Dopamine D(2) receptor modulation of human response inhibition and error awareness. *J Cogn Neurosci*, 25(4), 649-656. doi:10.1162/jocn_a_00327
- Nikolin, S., Boonstra, T. W., Loo, C. K., & Martin, D. (2017). Combined effect of prefrontal transcranial direct current stimulation and a working memory task on heart rate variability. *PLoS One*, 12(8), e0181833. doi:10.1371/journal.pone.0181833
- Northoff, G. (2015). Resting state activity and the "stream of consciousness" in schizophrenia--neurophenomenal hypotheses. *Schizophr Bull*, 41(1), 280-290. doi:10.1093/schbul/sbu116
- Patterson, J. C., 2nd, Ungerleider, L. G., & Bandettini, P. A. (2002). Task-independent functional brain activity correlation with skin conductance changes: an fMRI study. *Neuroimage*, 17(4), 1797-1806.
- Picton, T. W., Stuss, D. T., Alexander, M. P., Shallice, T., Binns, M. A., & Gillingham, S. (2007). Effects of focal frontal lesions on response inhibition. *Cereb Cortex*, 17(4), 826-838. doi:10.1093/cercor/bhk031
- Posner, M. I., & Snyder, C. R. R. (1975). Attention and cognitive control. In R. L. Solso (Ed.), *Information Processing and Cognition: The Loyola Symposium*: Lawrence Erlbaum.
- Reimer, B., & Mehler, B. (2011). The impact of cognitive workload on physiological arousal in young adult drivers: a field study and simulation validation. *Ergonomics*, 54(10), 932-942. doi:10.1080/00140139.2011.604431
- Robbins, T. W., & Arnsten, A. F. (2009). The neuropsychopharmacology of fronto-executive function: monoaminergic modulation. *Annu Rev Neurosci*, 32, 267-287. doi:10.1146/annurev.neuro.051508.135535

- Rondeel, E. W., van Steenbergen, H., Holland, R. W., & van Knippenberg, A. (2015). A closer look at cognitive control: differences in resource allocation during updating, inhibition and switching as revealed by pupillometry. *Front Hum Neurosci*, *9*, 494. doi:10.3389/fnhum.2015.00494
- Samuels, E. R., & Szabadi, E. (2008). Functional neuroanatomy of the noradrenergic locus coeruleus: its roles in the regulation of arousal and autonomic function part I: principles of functional organisation. *Curr Neuropharmacol*, *6*(3), 235-253. doi:10.2174/157015908785777229
- Sara, S. J., & Bouret, S. (2012). Orienting and reorienting: the locus coeruleus mediates cognition through arousal. *Neuron*, *76*(1), 130-141. doi:10.1016/j.neuron.2012.09.011
- Sara, S. J., & Herve-Minvielle, A. (1995). Inhibitory influence of frontal cortex on locus coeruleus neurons. *Proc Natl Acad Sci U S A*, *92*(13), 6032-6036.
- Schlosser, R. G., Koch, K., Wagner, G., Nenadic, I., Roebel, M., Schachtzabel, C., . . . Sauer, H. (2008). Inefficient executive cognitive control in schizophrenia is preceded by altered functional activation during information encoding: an fMRI study. *Neuropsychologia*, *46*(1), 336-347. doi:10.1016/j.neuropsychologia.2007.07.006
- Schmidt, R. F., & Thews, G. (1983). *Human Physiology*.
- Sheehan, D. V., Lecrubier, Y., Sheehan, K. H., Amorim, P., Janavs, J., Weiller, E., . . . Dunbar, G. C. (1998). The Mini-International Neuropsychiatric Interview (M.I.N.I.): the development and validation of a structured diagnostic psychiatric interview for DSM-IV and ICD-10. *J Clin Psychiatry*, *59 Suppl 20*, 22-33;quiz 34-57.
- Shibata, E., Sasaki, M., Tohyama, K., Otsuka, K., Endoh, J., Terayama, Y., & Sakai, A. (2008). Use of neuromelanin-sensitive MRI to distinguish schizophrenic and depressive patients and healthy individuals based on signal alterations in the substantia nigra and locus ceruleus. *Biol Psychiatry*, *64*(5), 401-406. doi:10.1016/j.biopsych.2008.03.021

- Shields, S. A., MacDowell, K. A., Fairchild, S. B., & Campbell, M. L. (1987). Is mediation of sweating cholinergic, adrenergic, or both? A comment on the literature. *Psychophysiology*, *24*(3), 312-319.
- Siegle, G. J., Steinhauer, S. R., & Thase, M. E. (2004). Pupillary assessment and computational modeling of the Stroop task in depression. *Int J Psychophysiol*, *52*(1), 63-76. doi:10.1016/j.ijpsycho.2003.12.010
- Simmonds, D. J., Pekar, J. J., & Mostofsky, S. H. (2008). Meta-analysis of Go/No-go tasks demonstrating that fMRI activation associated with response inhibition is task-dependent. *Neuropsychologia*, *46*(1), 224-232. doi:10.1016/j.neuropsychologia.2007.07.015
- Stroop, J. R. (1935). Studies of interference in serial verbal reactions. *Journal of Experimental Psychology*, *18*(6), 643-662. doi:10.1037/h0054651
- Stuss, D. T., Binns, M. A., Murphy, K. J., & Alexander, M. P. (2002). Dissociations within the anterior attentional system: effects of task complexity and irrelevant information on reaction time speed and accuracy. *Neuropsychology*, *16*(4), 500-513.
- Thayer, J. F. (2006). On the Importance of Inhibition: Central and Peripheral Manifestations of Nonlinear Inhibitory Processes in Neural Systems. *Dose-Response*, *4*(1), 2-21. doi:10.2203/dose-response.004.01.002.Thayer
- Thayer, J. F., Ahs, F., Fredrikson, M., Sollers, J. J., 3rd, & Wager, T. D. (2012). A meta-analysis of heart rate variability and neuroimaging studies: implications for heart rate variability as a marker of stress and health. *Neurosci Biobehav Rev*, *36*(2), 747-756. doi:10.1016/j.neubiorev.2011.11.009
- Thayer, J. F., & Brosschot, J. F. (2005). Psychosomatics and psychopathology: looking up and down from the brain. *Psychoneuroendocrinology*, *30*(10), 1050-1058. doi:10.1016/j.psyneuen.2005.04.014

- Thayer, J. F., & Lane, R. D. (2000). A model of neurovisceral integration in emotion regulation and dysregulation. *J Affect Disord*, *61*(3), 201-216.
- Thayer, J. F., & Lane, R. D. (2009). Claude Bernard and the heart-brain connection: further elaboration of a model of neurovisceral integration. *Neurosci Biobehav Rev*, *33*(2), 81-88. doi:10.1016/j.neubiorev.2008.08.004
- Urai, A. E., Braun, A., & Donner, T. H. (2017). Pupil-linked arousal is driven by decision uncertainty and alters serial choice bias. *Nat Commun*, *8*, 14637. doi:10.1038/ncomms14637
- van Kammen, D. P., Peters, J. L., van Kammen, W. B., Rosen, J., Yao, J. K., McAdam, D., & Linnoila, M. (1989). Clonidine treatment of schizophrenia: can we predict treatment response? *Psychiatry Res*, *27*(3), 297-311.
- van Os, J., & Kapur, S. (2009). Schizophrenia. *Lancet*, *374*(9690), 635-645. doi:10.1016/S0140-6736(09)60995-8
- Verbruggen, F., & Logan, G. D. (2008). Automatic and controlled response inhibition: associative learning in the go/no-go and stop-signal paradigms. *J Exp Psychol Gen*, *137*(4), 649-672. doi:10.1037/a0013170
- Waford, R. N., & Lewine, R. (2010). Is perseveration uniquely characteristic of schizophrenia? *Schizophr Res*, *118*(1), 128-133. doi:<https://doi.org/10.1016/j.schres.2010.01.031>
- Wagner, G., De la Cruz, F., Schachtzabel, C., Gullmar, D., Schultz, C. C., Schlosser, R. G., . . . Koch, K. (2015). Structural and functional dysconnectivity of the fronto-thalamic system in schizophrenia: a DCM-DTI study. *Cortex*, *66*, 35-45. doi:10.1016/j.cortex.2015.02.004
- Wagner, G., Koch, K., Schachtzabel, C., Schultz, C. C., Gaser, C., Reichenbach, J. R., . . . Schlosser, R. G. (2013). Structural basis of the fronto-thalamic dysconnectivity in

- schizophrenia: A combined DCM-VBM study. *Neuroimage Clin*, 3, 95-105.
doi:10.1016/j.nicl.2013.07.010
- Wilson, R. S., Nag, S., Boyle, P. A., Hizel, L. P., Yu, L., Buchman, A. S., . . . Bennett, D. A. (2013). Neural reserve, neuronal density in the locus ceruleus, and cognitive decline. *Neurology*, 80(13), 1202-1208. doi:10.1212/WNL.0b013e3182897103
- Yamamoto, K., Arai, H., & Nakayama, S. (1990). Skin conductance response after 6-hydroxydopamine lesion of central noradrenaline system in cats. *Biol Psychiatry*, 28(2), 151-160.
- Yamamoto, K., & Hornykiewicz, O. (2004). Proposal for a noradrenaline hypothesis of schizophrenia. *Prog Neuropsychopharmacol Biol Psychiatry*, 28(5), 913-922.
doi:10.1016/j.pnpbp.2004.05.033
- Zhang, S., Hu, S., Chao, H. H., Ide, J. S., Luo, X., Farr, O. M., & Li, C. S. (2014). Ventromedial prefrontal cortex and the regulation of physiological arousal. *Soc Cogn Affect Neurosci*, 9(7), 900-908. doi:10.1093/scan/nst064
- Zhang, S., Hu, S., Chao, H. H., Luo, X., Farr, O. M., & Li, C. S. (2012). Cerebral correlates of skin conductance responses in a cognitive task. *Neuroimage*, 62(3), 1489-1498.
doi:10.1016/j.neuroimage.2012.05.036
- Zhang, S., Hu, S., Hu, J., Wu, P. L., Chao, H. H., & Li, C. S. (2015). Barratt Impulsivity and Neural Regulation of Physiological Arousal. *PLoS One*, 10(6), e0129139.
doi:10.1371/journal.pone.0129139

APPENDIX A

Stefanie M. Köhler

Curriculum Vitae

Persönliche Daten

Name: Stefanie Marion Köhler
Geburtsdatum: 24. Juni 1988
Geburtsort: Meerane
Adresse: Mühlenweg 49
07751 Jena
E-Mail: Stefanie.Koehler@med.uni-jena.de
Familienstand: ledig, keine Kinder
Nationalität: Deutsch

Werdegang

Beruflicher Werdegang

seit Februar 2017 Tätigkeit als Psychologin im Rahmen der Weiterbildung zur Psychologischen Psychotherapeutin in der Ambulanz für Forschung und Lehre (WPP Jena)
seit April 2014 Tätigkeit als wissenschaftliche Mitarbeiterin an der Klinik für Psychiatrie und Psychotherapie des Universitätsklinikums Jena (20-40 Stunden/Woche)
August 2014 - Juli 2016 Tätigkeit als Psychologin an der Klinik für Psychiatrie und Psychotherapie des Universitätsklinikums Jena (20 Stunden/Woche; Kriseninterventionsstation sowie Verhaltenstherapiestation für Angst- und Zwangserkrankungen)

Studium

Oktober 2011 - März 2014 Masterstudiums an der Friedrich-Schiller-Universität Jena (Hauptfach: Psychologie)
Schwerpunkt: Klinische Psychologie, Psychotherapie und Gesundheit
Abschluss: Master of Science (Note 1,5)
2008 - 2011 Bachelorstudium an der Friedrich-Schiller-Universität Jena (Hauptfach: Psychologie)
Abschluss: Bachelor of Science (Note 2,0)

Universitäres Engagement und Nebentätigkeiten

Oktober 2013 - März 2014 Tätigkeit als wissenschaftliche Hilfskraft an der Fakultät für Sozial- und Verhaltenswissenschaften (Abteilung für Klinisch-psychologische Intervention) der FSU Jena
Oktober 2013 - März 2014 Tätigkeit als wissenschaftliche Hilfskraft an der Klinik für Psychiatrie und Psychotherapie des Universitätsklinikums Jena
Oktober 2011 - September 2013 Tätigkeit als studentische Hilfskraft für pflegerische und wirtschaftliche Tätigkeiten in Pflege- und Funktionsbereichen des Universitätsklinikums Jena
2010-2011 Arbeit als studentische Hilfskraft an der Fakultät für Sozial- und Verhaltenswissenschaften (Abteilung für Differentielle Psychologie, Persönlichkeitspsychologie und Psychologische Diagnostik) der FSU Jena

Sonstiger Werdegang

2007-2008 14-monatiger Aufenthalt in England, dabei Tätigkeit als Au-Pair

Schule

1999-2007 Georgius-Agricola-Gymnasium Glauchau, Abschluss: Abitur (Note: 1,2)
1995-1999 Grundschule am Rosarium Glauchau

APPENDIX B

Erklärung über den Eigenanteil

Erklärung über den Eigenanteil sowie über den Anteil weiterer Autoren an den veröffentlichten wissenschaftlichen Schriften, die in der Dissertationsschrift verwendet wurden, gemäß §7 Abs. 3 Satz 3 der Promotionsordnung.

Persönliche Angaben des Antragstellers

Köhler, Stefanie

Einrichtung: Klinik für Psychiatrie und Psychotherapie Jena

Promotionsfach: Psychologie

Thema der Dissertation: The locus coeruleus: The central relay between neuronal network activation and sympathetic responses in cognitive control

Nummerierte Aufstellung der eingereichten Schriften

1. Titel: **Differential involvement of brainstem noradrenergic and midbrain dopaminergic nuclei in cognitive control.**

Autoren: Stefanie Köhler, Karl-Jürgen Bär, Gerd Wagner

Zeitschrift: Human Brain Mapping

Stand: **veröffentlicht**

Jahr: 2016

2. Titel: **Activation of brainstem and midbrain nuclei during cognitive control in medicated patients with schizophrenia.**

Autoren: Stefanie Köhler, Gerd Wagner, Karl-Jürgen Bär

Zeitschrift: Human Brain Mapping

Stand: **veröffentlicht**

Jahr: 2018

3. Titel: **The use of physiological signals in brainstem/midbrain fMRI.**

Autoren: Andy Schumann, Stefanie Köhler, Feliberto de la Cruz, Daniel Güllmar, Jürgen R. Reichenbach, Gerd Wagner, Karl-Jürgen Bär

Zeitschrift: Frontiers in Neuroscience

Stand: **veröffentlicht**

Jahr: 2018

4. Titel: **Towards response success prediction: An integrative approach using high-resolution fMRI and autonomic indices.**

Autoren: Stefanie Köhler, Andy Schumann, Feliberto de la Cruz, Gerd Wagner, Karl-Jürgen Bär

Zeitschrift: Neuropsychologia

Stand: **veröffentlicht**

Jahr: 2018

Darlegung des Anteils aller Autoren sowie des Eigenanteils an diesen Schriften zu:

Nr. 1 - Differential involvement of brainstem noradrenergic and midbrain dopaminergic nuclei in cognitive control

Konzeption (G. W., K.-J. B., S. K. [in Teilen]), Literaturrecherche (G. W., S. K. [in Teilen]), Versuchsdesign (G. W., S. K. [in Teilen]), Datenerhebung (S. K. [vollständig]), Datenauswertung (G. W., S. K. [in Teilen]), Ergebnisdiskussion (G. W., K.-J. B., S. K. [in Teilen]), Erstellen und Revision des Manuskripts (G. W., K.-J. B., S. K. [in Teilen]).

Nr. 2 - Activation of brainstem and midbrain nuclei during cognitive control in medicated patients with schizophrenia

Konzeption (G. W., K.-J. B., S. K. [in Teilen]), Literaturrecherche (G. W., S. K. [mehrheitlich]), Versuchsdesign (G. W., S. K. [in Teilen]), Datenerhebung (S. K. [vollständig]), Datenauswertung (G. W., S. K. [überwiegend]), Ergebnisdiskussion (G. W., K.-J. B., S. K. [überwiegend]), Erstellen und Revision des Manuskripts (G. W., K.-J. B., S. K. [überwiegend]).

Nr. 3 - The use of physiological signals in brainstem/midbrain fMRI

Konzeption (G. W., A. S., S. K. [in Teilen]), Literaturrecherche (A. S., S. K. [in Teilen]), Versuchsdesign (G. W., A. S., S. K. [in Teilen]), Datenerhebung (A. S., S. K. [mehrheitlich]), Datenauswertung (A. S., F. d. I. C., S. K. [in Teilen]), Ergebnisdiskussion (G. W., A. S., K.-J.

B., S. K. [in Teilen]), Erstellen und Revision des Manuskripts (G. W., A. S., K.-J. B., S. K. [in Teilen]).

Nr. 4 - Towards response success prediction: An integrative approach using high-resolution fMRI and autonomic indices.

Konzeption (S. K. [vollständig]), Literaturrecherche (S. K. [vollständig]), Versuchsdesign (A. S., S. K. [mehrheitlich]), Datenerhebung (S. K. [vollständig]), Datenauswertung (A. S., F. d. I. C., S. K. [mehrheitlich]), Ergebnisdiskussion (G. W., K.-J. B., A. S., S. K. [mehrheitlich]), Erstellen und Revision des Manuskripts (G. W., K.-J. B., A. S., S. K. [mehrheitlich]).

Bestätigung des Anteils der Mitautoren:

Ich bestätige die Richtigkeit der Angaben von Frau Stefanie Köhler sowie die aufgeführte Aufteilung.

Karl-Jürgen Bär

APPENDIX C

Eigenständigkeitserklärung

Ich versichere, dass mir die geltende Promotionsordnung mit dem aktuellen Stand bekannt ist.

Ich versichere, dass ich die Dissertationsschrift selbst angefertigt habe, dass keine Textabschnitte eines Dritten oder eigener Prüfungsarbeiten ohne Kennzeichnung übernommen habe und dass ich alle von mir benutzten Hilfsmittel, persönliche Mitteilungen und Quellen in meiner Arbeit angegeben habe.

Ich erkläre zudem, dass ich nicht die Hilfe eines Promotionsberaters in Anspruch genommen habe. Auch haben Dritte weder mittelbar noch unmittelbar geldwerte Leistungen von mir für Arbeiten erhalten, die im Zusammenhang mit dem Inhalt der vorliegenden Dissertation stehen.

Die Dissertation wurde nicht als Prüfungsarbeit für eine staatliche oder eine andere wissenschaftliche Prüfung eingereicht. Es wurde keine gleiche, eine in wesentlichen Teilen ähnliche oder eine andere Abhandlung bei einer anderen Hochschule bzw. anderen Fakultät als Dissertation eingereicht.

Jena, den 08.10.2018

Stefanie Köhler